

BULLETIN OF THE ASTRONOMICAL INSTITUTES OF THE NETHERLANDS

1955 FEBRUARY 12

VOLUME XII

NUMBER 459

COMMUNICATION FROM THE OBSERVATORY AT LEIDEN

THE PULSATIONS OF AI VELORUM, SX PHOENICIS AND RR LYRAE

BY TH. WALRAVEN

The short-period RR Lyrae-type variable AI Velorum has been observed on every clear night during three months in 1952 and during five months in 1953 with a photoelectric photometer, which directly records the light-curve. The photometer was attached to the 16" telescope of the Leiden Station in Johannesburg. The closely similar variable SX Phoenicis (HD 223065) has been observed with the same instrument on 21 nights in 1952.

By comparing the new observations of AI Velorum with those obtained in 1951 and also with the photographic observations of 1934-36 discussed by ZAGAR and VAN HOOFF the periods were corrected. They were found to be more constant than the period of RR Lyrae.

In a systematic analysis the light-variations caused by the two strong components of pulsation, P_0 and P_1 , were freed from the disturbing effect of the other weak oscillations observed in the light-curves of AI Velorum. This precaution was not required for SX Phoenicis as this star does not show such weak oscillations.

It is found that the corrected curves of AI Velorum and the observed light-curves of SX Phoenicis can be described with high accuracy as a distorted image of a curve $u = a \sin 2\pi\varphi_0 + b \sin 2\pi\varphi_1$ where φ_0 and φ_1 are the phases of the pulsations P_0 and P_1 . The distortion is a function of u only, and consists of two components. The first component displaces the points of the two-sine curve in time by an amount proportional to u . By this effect the curves become skew. A subsequent distortion displaces the points of the skew curve in height by an amount which is a smooth continuous function of u . It has been found by GRATTON that the radial-velocity curves of AI Velorum can be derived from the same two-sine function as the light-curves by applying the distortion in time only. Besides the strong pulsations P_0 and P_1 the light-curves of AI Velorum show a wave with an amplitude of about $0^m.02$ and with an average period P_2 of $0^d.0444019$. This oscillation varies in strength and phase with a period equal to the fundamental period P_0 . This effect can be described as a beat phenomenon of the oscillation P_2 with a weaker and shorter oscillation P_3 of which the frequency is the sum of the frequencies of P_2 and P_0 . Furthermore, an oscillation is present with an amplitude of the order of $0^m.01$ and a period nearly equal to P_1 ; the frequency of this wave is equal to the difference of the frequencies of P_2 and P_1 . A study of the photoelectric light-curves of RR Lyrae obtained by the author in 1947 shows that these are subject to a distortion of the same type as the light-curves of AI Velorum and SX Phoenicis. The same relation exists between the light-curves and the radial-velocity curves of RR Lyrae as in the case of AI Velorum.

In the light-curves and radial-velocity curves of RR Lyrae an oscillation is found, the frequency of which is the sum of the frequencies of the fundamental pulsation and the pulsation which causes the 72 cycle beat phenomenon. This oscillation is identified with the pulsation in higher mode which, according to the coupling theory of WOLTJER, produces the beat phenomenon, but which had not been observed at that time.

The well-known hump in the minimum of RR Lyrae appears to be part of a continuous wave superimposed on the entire light-curve, and having a period of exactly one fourth of the fundamental period.

The possibility is considered that the effect of coupling between different modes is not restricted to near commensurability of periods, as in WOLTJER's theory, but might be responsible also for the phenomenon observed in AI Velorum and SX Phoenicis.

Part I. AI VELORUM.

Introduction.

This star has been the subject of photoelectric observations with the 16" refractor of the Leiden Southern Station at Johannesburg during 1951. Some conclusions drawn from these observations have been published¹⁾.

The light-curve appeared to be that of an RR Lyrae-type variable with extremely short beat period, only $3^{1/2}$ times the primary period²⁾. Moreover the

variation in phase and amplitude appeared to be abnormally intense.

This phenomenon led to the discovery of a distortion effect, which is responsible for the transformation of simple harmonic curves into the peculiar skew and peaked light-curves. The transformation could be described as the sum of two transformations. The harmonic curves are first steepened, made skew, i.e. the crests come earlier and the valleys come later in phase, the phase-shift being approximately proportional to magnitude. We denote this effect by S-distortion.

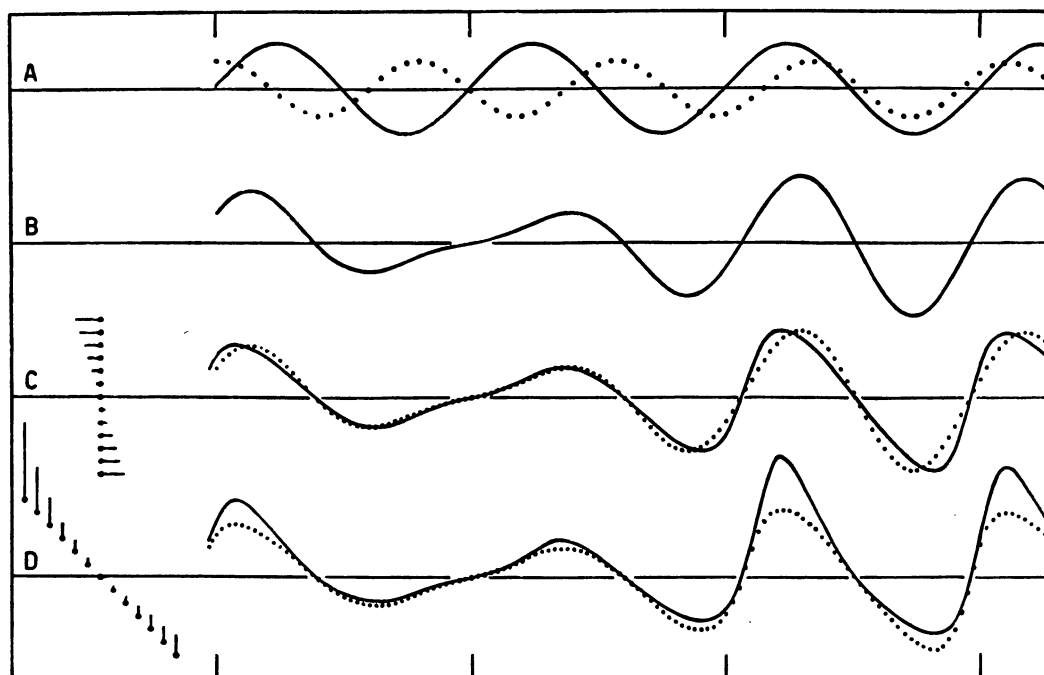
Then the curves are subject to another transformation, this time in magnitude, such that the crests are lifted up strongly, the valleys lifted up less, and the points with medium brightness are not affected. This effect we denote by M-distortion. GRATTON³⁾ has

¹⁾ TH. WALRAVEN, *B.A.N.* No 434, 1952.

²⁾ Often the designation secondary period has been used for the period in which the light-curves vary in intensity and position. To avoid confusion we shall denote in the present paper this period by beat period, while the period of the pulsation which by interference with the primary or principal pulsation causes the phenomenon is called secondary period.

³⁾ L. GRATTON, *B.A.N.* No 444, 1953.

FIGURE 1



Construction of radial-velocity curve and light-curve from two harmonic pulsations.

A: harmonic curves; — $a \sin 2\pi\phi_0$, ... $b \sin 2\pi\phi_1$

B: sum of curves in A.

C: curve B shown as dotted line is transformed into radial-velocity curve by displacement in time proportional to height (S-distortion); the way in which the displacement varies with height is shown on the left.

D: curve C shown as dotted line transformed into light-curve by M-distortion; the vertical lines in the left-hand corner show how the M-displacement varies with height.

shown that the radial-velocity curves of AI Velorum can be described by applying to the same harmonic curves the S-distortion but not the M-distortion. This is extremely important, as it makes certain that both the S- and M-distortion represent real physical processes in the star and are not meaningless manipulations. Figure 1 illustrates how the light-curves and radial-velocity curves of AI Velorum can be reconstructed from two sine-curves. It has been suggested that the sine-curves represent the two pulsations P_0 and P_1 of the main body of the star somewhere in the interior, and that the distortion in wave-shape takes place while the pulsations are propagated into the observed layers of the atmosphere of the star.

In the observations of 1951 the properties of the distortion and the characteristics of the harmonic components could not be determined precisely, due to the presence of weak oscillations with short periods, which in their turn escaped exact control because they were not observed continuously. The photoelectric observations of the light-curves were therefore continued in 1952 and 1953. A new automatic wedge-photometer had been constructed, based on the same

principle as the previous instrument, but much improved.

The principles of this instrument have been described¹⁾. A more detailed description will be published in the *B.A.N.* With this instrument, which uses the light of the variable star during nearly the whole time of observation, we hoped to get maximum efficiency and weight of the light-curve. Likewise for economy of time we observed only with the blue filter (BG 1, 2 mm + GG 13, 2 mm). As was found in 1951, the yellow light-curves, after multiplication of the magnitude-scale by a suitable factor, show hardly any difference from the blue light-curves.

During three months in 1952 and five months in 1953, the star was observed every clear moment, even between passing clouds. Unfortunately, at this time of the year, the climate of Johannesburg is not favourable. In 1952 we succeeded in obtaining a short, but homogeneous, series of light-curves. In 1953 the total observing time was greatest, but the quality of the sky

¹⁾ "Astronomical Photoelectric Photometry", *Am. Ass. Adv. of Science*, 1953. See also *M. N. Astr. Soc. of South Africa* 11, No 4, 1952.

in general was not good, and no regular series of long clear nights occurred.

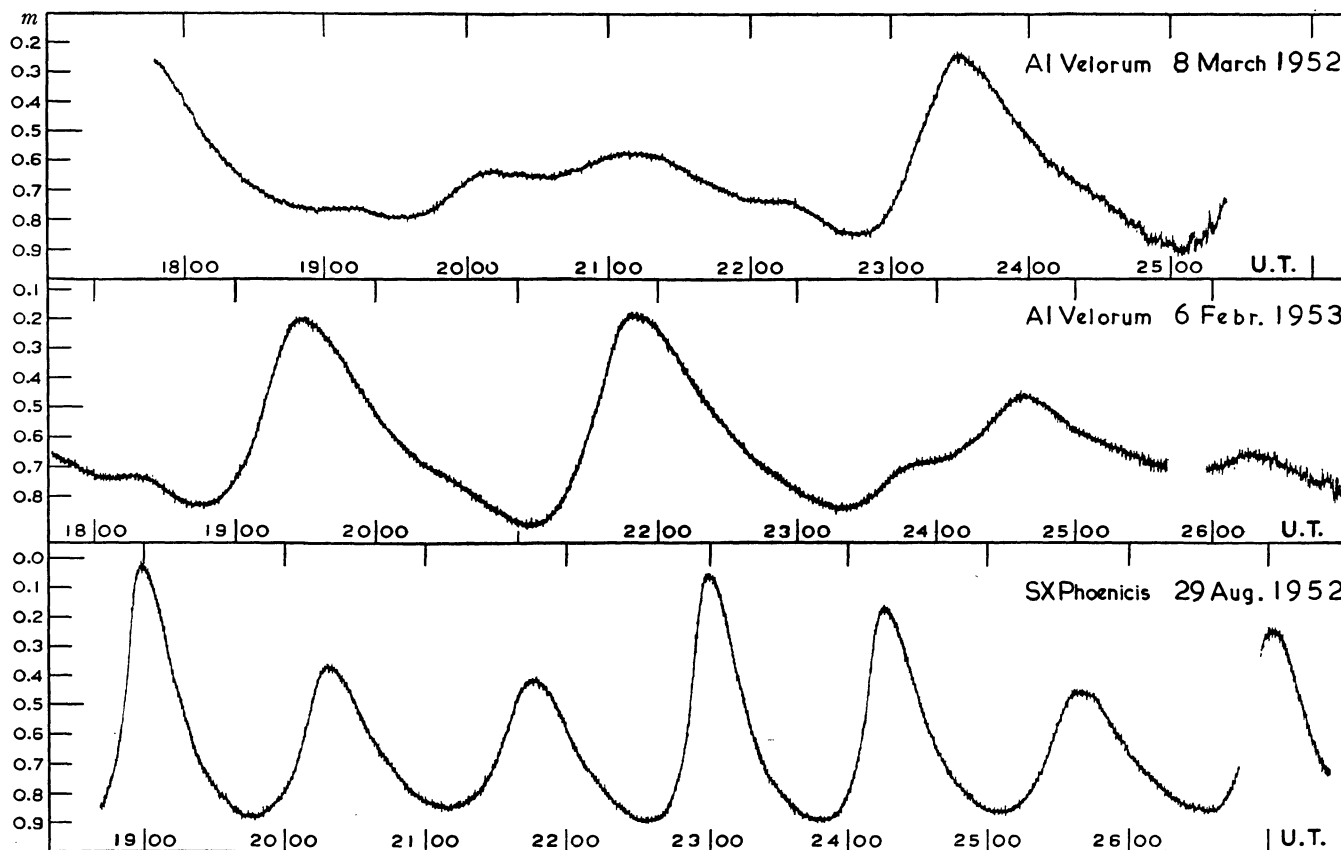
The reduction of the observations.

The light-curves were registered by the instrument on a sheet of graphical paper, divided in millimetres. The time scale, which has a reduction factor of one millimetre per minute, was controlled by making marks in the light-curves from time signals supplied

by the time service of the Union Observatory. The magnitude scale of the records is one millimetre per 0.00780 magnitudes. The linearity and scale factor were checked several times and found satisfactorily stable. On each sheet a reference line was recorded by a fixed pen, the position of which corresponds to one of the end positions of the optical wedge. Some records are shown in Figure 2.

The small irregularities in the curves are caused by

FIGURE 2



Sample records of light-curves. The roughness is caused by seeing, it increases when the star approaches the horizon.

seeing. This effect may vary strongly, even during a night; furthermore it depends systematically on the zenith-distance of the stars. Passing clouds cause increased irregularities depending on the transparency of the clouds.

With reasonable certainty smooth lines could be drawn through the records. This was done such that the line is as smooth as possible while points separated by 4 minutes are still independent.

A plan for a systematic analysis of the light-curves was set up as follows. The magnitudes must be found for definite phases φ_0 of the primary period. Then for each of these phases the magnitude is plotted as a function of the phase φ_1 of the secondary period. The components in the light-curves which are not a peri-

odic function of φ_0 and φ_1 cause a scatter in the plots. By smoothing out the scatter a system of curves is obtained, forming what we may call the mean light-surface, and which describes the magnitude as a function of φ_0 and φ_1 only.

The degree to which this surface deviates from the real surface depends on how numerous the observations are; how well the phases of the oscillations, not included in the surface, are distributed at random; and depends on the correctness of the assumption that the deviations corresponding to these free oscillations are as much positive as negative.

By now the analysis is split up into two parts. The principal oscillations P_0 and P_1 can be studied in pure form in the mean light-surface and all other oscilla-

tions are found in the residual curves obtained by subtracting from the observed magnitudes the magnitudes as given by the mean light-surface.

Since it was found from a preliminary inspection of the light-curves that the characteristics of P_0 and P_1 had changed from one year to another, it was decided to apply the described method to each season of observations separately. This has, moreover, the advantage that, if some effect is found repeatedly in each analysis, we can be reasonably sure of its reality.

The discussion in *B.A.N.* No 434 was based on the yellow light-curves of 1951. It was decided to subject the blue light-curves of 1951, obtained with the same colour filter as the new observations, together with these new observations, to one general discussion.

In order to perform the analysis of the observations of the three seasons in a fixed system of phases, the periods P_0 and P_1 should be known with increased accuracy. It is possible to obtain this knowledge directly from the recordings by reading the magnitudes and approximate positions of the maxima and minima, and, after estimating the median magnitude, reading the moments when the ascending and descending branches cross the median magnitude.

The periods P_0 and P_1 .

It is necessary to find the beat period first. In Table 1 (see page 238) the maxima and minima shown by the light-curves, are collected. Those found in the photographic measurements by ZAGAR and VAN HOOFF¹⁾ on plates taken in 1934–1936 are included.

The phase ψ of the beat period is computed with

$$\psi = (\text{J.D.} - 2430000) \times 2.637256. \quad (1)$$

For each group of observations a pair of envelopes was obtained by plotting magnitude of maximum and of minimum, respectively, versus phase ψ (Figure 3). The centres of symmetry of the curves were estimated as follows:

TABLE 2

group	phase of centre and estimated error	mean cycle number	phase shift with new period
1934–'36	0.20 ± 0.05	— 6050	0.198
1951	0.455 ± 0.004	9940	0.455
1952	0.467 ± 0.005	10770	0.468
1953	0.484 ± 0.004	11610	0.482

From the values in Table 2 a new beat period is found

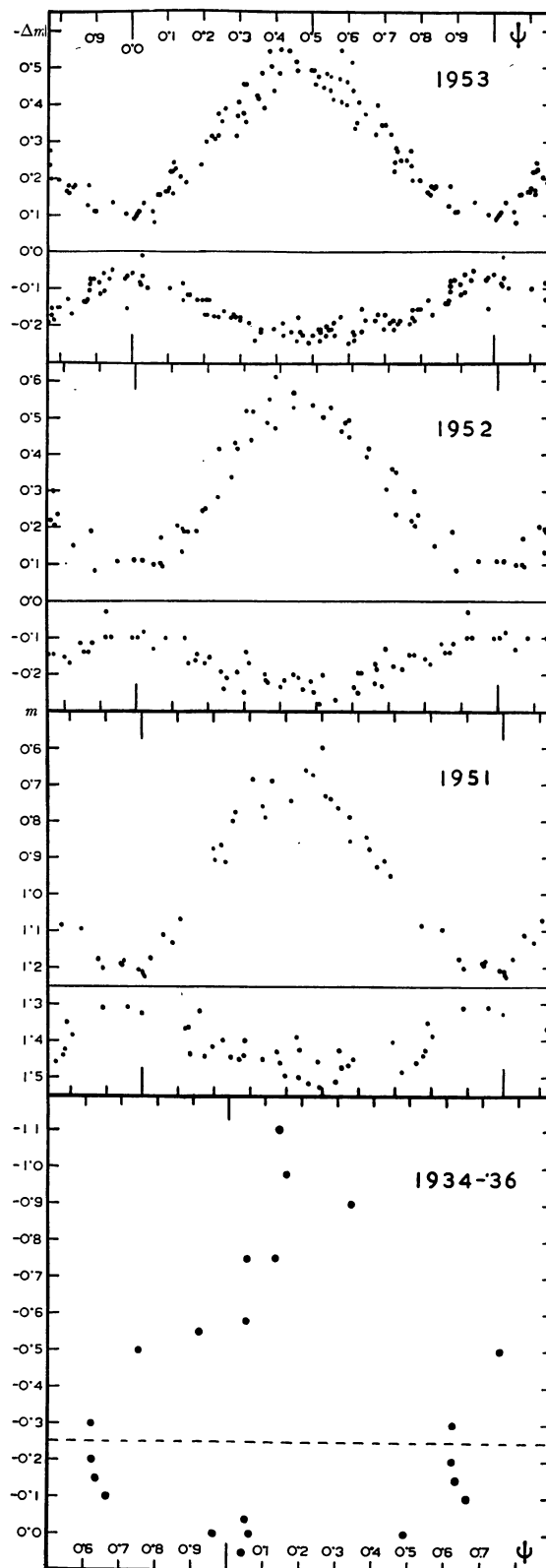
$$P_b = 0^d.379188 \pm 0^d.000001 \text{ (m.e.)}.$$

This period represents satisfactorily the entire interval from 1934 to 1953, as may be seen from the last column of Table 2 and from Figure 3.

¹⁾ F. ZAGAR, *B.A.N.* No 300, 169, 1937.

A. VAN HOOFF, *B.A.N.* No 300, 172, 1937.

FIGURE 3



Magnitude of maxima and minima as a function of the phase of the beat period. The ψ -scales refer to the preliminary elements of formula (1), whereas the curves are shifted into corresponding positions according to the improved elements of formula (3).

For the determination of the primary period the epochs of the ascending branches were found at the median magnitude. The low light-curves were excluded because they give uncertain results. The epochs are compiled in Table 3 (see page 240—241).

The phase is computed with HERTZSPRUNG's formula ¹⁾

$$J.D. = 2426142.190 + 0^d.111574E.$$

The phase of the beat period is found from

$$\psi = (J.D. - 2430000) 2.637214 + 0.7178. \quad (3)$$

Since only epochs on high light-curves were used, a practically linear relation exists between the phase-deviation from the primary cycles and the phase of the beat period (see Figure 3 in *B.A.N.* No 434). For each group of observations a linear function was fitted to the observed phases. The values of these functions at $\psi = 0$ are given in Table 4. From them the fundamental period can be found.

TABLE 4

group	mean cycle number E	mean phase at $\psi = 0$
(HERTZSPRUNG)	0	0.00 \pm 0.03 (m.e.)
1934-'36	13520	0.00 \pm 0.02 „
1951	68350	-0.014 \pm 0.003 „
1952	71180	-0.021 \pm 0.003 „
1953	74020	-0.027 \pm 0.002 „

The data of Table 4 show that in the interval of our photoelectric observations the primary period has been slightly shorter than on the average. The most probable period in this interval is

$$P_o = 0^d.11157375 \pm 0^d.00000005 \text{ (m.e.)}.$$

With this period and the new P_b we can derive $P_1 = 0^d.08620767$ for the secondary period.

However, in the same interval also the amplitude of the oscillations has changed, as will be demonstrated further on in this paper. Presuming that the effects on period and on amplitude are related, the way in which the amplitudes have changed suggests that we should not expect much bigger deviations in phase than observed up to now.

We then arrive at two curious conclusions. In the first place it follows that AI Velorum is a more regular variable, in spite of its strongly varying light-curve, than, for example, RR Lyrae, for which the deviations in phase are not counted in hundredths but in tenths of a cycle.

Secondly, it is surprising to note the accuracy of HERTZSPRUNG's elements, which were obtained by eye estimates. HERTZSPRUNG gives for the period $P_o = 0^d.111574 \pm 0^d.000002$. The average period found

¹⁾ E. HERTZSPRUNG, *B.A.N.* No 224, 147, 1931.

by comparing old with new observations, neglecting the change in phase during the photoelectric observations, is $P_o = 0^d.11157396 \pm 0^d.00000003$.

The mean light-curves.

For reading the light-curves we used the period which fits best the photoelectric observations.

With the formula

$$J.D. = 2433617.65005 + \phi_o \times 0^d.11157375 \quad (4)$$

the Julian Day was computed for values of ϕ_o of which the decimal fraction is a multiple of 0.025. At these moments the magnitude was found from the curves. The magnitudes found in this way had an arbitrary zero point. There was no reason to suspect a change in zero point during a season. However, a change of a few hundredths of a magnitude was found by comparing the observations of 1952 with those of 1953, which is not surprising as the optical parts of the photometer have been re-adjusted several times between the two series of observations. For each season a zero point was determined as the magnitude in the records at which the average distance between the ascending branch and descending branch of a light-curve is equal to one half of the primary period.

The difference between the magnitude read off the recordings and this median magnitude is used in the further discussion, and is given in the magnitude tables at the end of the paper; it is denoted by Δm .

For each reading the phase ϕ_1 of the second period was found from the Julian Day by means of the formula

$$\phi_1 = (J.D. - 2430000) 11.59989563 + 0.8722. \quad (5)$$

This formula is found from formulae (3) and (4) by the relation $\phi_1 = \psi + \phi_o$.

Then, for each season separately, the magnitudes were plotted against ϕ_1 for a fixed value of ϕ_o . Per season, forty graphs were thus obtained. The curves, represented by the bands of scattered points vary tremendously in shape in such a peculiar way that no analytical curves could be fitted in. They were smoothed, therefore, by determining centres of gravity of groups of points lying in narrow strips of ϕ_1 and connecting these points by a smooth curve.

A second smoothing was applied to the values of the curves at fixed ϕ_1 and different values of ϕ_o . After this two-dimensional smoothing the magnitudes of neighbouring phases are no longer independent. No loss of details occurs therefore if only twenty curves are read off at twenty points. Such readings are given in Tables 5^{a, b, c} (see page 241—242).

These tables are supposed to represent the mean light-surface, i.e. the magnitude as a function of ϕ_o and ϕ_1 only, freed from the disturbing effect of the other oscillations. They form the base for a study of the exact properties of the S- and M-distortion.

As follows from the results in *B.A.N.* No 434 the problem is to find a transformation, such that if it is applied to the function

$$u = a \sin 2\pi\varphi_0 + b \sin 2\pi\varphi_1 \quad (6)$$

we can find values of a , b , and the zero points of the phases for which the transformed function is identical with the observed mean light-curves. This transformation of co-ordinates then represents the S-M-distortion, and the values of a and b are the amplitudes of the basic oscillations.

To avoid confusion we shall denote, in the following discussion, cross sections of the mean light-surface as m -curves and those of the surface determined by (6) as u -curves. The cross sections of the mean light-surface, parallel to the direction of time, we denote as mean light-curves.

For fixed values of φ_0 the u -curves are all identical and have only different positions in vertical direction

$$u(\varphi_1) = \text{const.} + b \sin 2\pi\varphi_1. \quad (6a)$$

The attempt, however, to compare these curves with the corresponding $m(\varphi_1)$ -curves such as given in Tables 5^{a,b,c} fails completely, because the latter curves, instead of having all the same shape, differ enormously in amplitude, skewness and so on. The transformation required to reduce an $m(\varphi_1)$ -curve to the corresponding $u(\varphi_1)$ -curve is different for each curve. The reason for this can be understood if we think of the surface (6) as of a three-dimensional

model. It looks like a regular mountain landscape of which the peaks are situated at regular intervals on mountain-ridges which themselves lie parallel with regular intervals.

The mean light-surface has a similar appearance, except that all peaks are skew and stretched upward.

An impression of this surface is given in Figure 4, which shows iso-magnitude curves in the (φ_0, φ_1) -plane of AI Velorum in 1953. The peak (maximum brightness) is in the lower left-hand corner of the square, and the valley in the diagonally opposite corner. The direction of time, i.e. $\varphi_1 P_1 - \varphi_0 P_0 = \text{constant}$, is indicated by the straight line. Cross sections through the surface in this direction show the actual mean light-curves.

The curves $m(\varphi_1)$ are cross cuts through this model in the direction $\varphi_0 = \text{constant}$, which is entirely different from the direction of the light-curves, so that the distortion has lost completely its original character.

Obviously it is better to study cross sections in diagonal direction: $\varphi_1 - \varphi_0 = \text{constant}$. These curves show much resemblance to the light-curves as far as the distortion is concerned and yet the corresponding u -curves are simple mathematical functions. These curves are functions of $\chi = \frac{1}{2}(\varphi_1 + \varphi_0)$ with $\psi = \varphi_1 - \varphi_0$ constant. From (6) we derive

$$u(\chi) = A \sin 2\pi(\chi - \Delta\chi), \quad (7)$$

where

$$A = (a^2 + 2ab \cos 2\pi\psi + b^2)^{1/2} \quad (7a)$$

and

$$\tan 2\pi\Delta\chi = \frac{a-b}{a+b} \tan \pi\psi, \quad (7b)$$

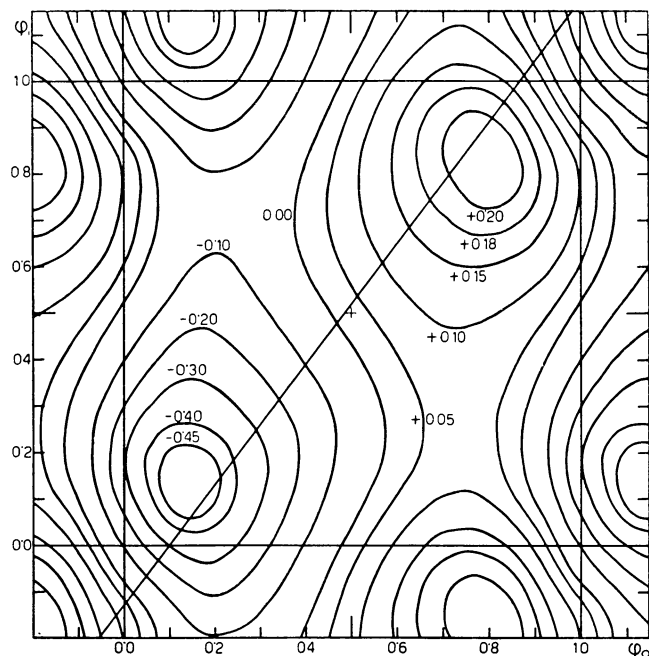
which shows that the $u(\chi)$ -curves are also sine-curves, which, however, are shifted in phase by the amount $\Delta\chi$ and have a varying amplitude A , depending on ψ .

The $m(\chi)$ -curves can be taken directly from the Tables 5^{a,b,c} by plotting the numbers standing parallel to the diagonal of the table against χ . Each table gives twenty curves. The curves are distinguished by their ψ . From these curves the S-M-distortion was derived as follows.

After estimating approximate values for a , b and the zero point of ψ the $u(\chi)$ -curves can be computed from (7). In each $m(\chi)$ -curve we now determined the magnitudes, Δm , at which the difference of the phases χ on the ascending and descending portions of the curve is respectively 0 , $\frac{1}{8}$, $\frac{2}{8}$... $\frac{7}{8}$ and 1 .

In the $u(\chi)$ -curves the corresponding values of u could be found. By plotting the Δm 's against the corresponding u 's a curve is obtained which represents the M-distortion. The plotted points are scattered, but it appeared that related points, e.g. all the points of the maxima, are placed in loops. A study of these loops gives an indication in which sense the values of

FIGURE 4



Iso-magnitude curves of AI Velorum (1953) giving an impression of the mean light-surface. The numbers near the curves denote Δm . Cross cuts through the surface parallel to the inserted line yield mean light-curves.

a , b , and the zeropoint of ψ can be improved in order to reduce the scattering of the points.

In a similar way the S-distortion could be found. The phase χ which is the mean of the phases on ascending and descending branches for a certain Δm is plotted against Δm and the median or curve of symmetry is obtained. The medians for the different curves $m(\chi)$ have more or less the same shape but are displaced parallel to each other in the direction of χ . They are shifted together and then a mean curve can be traced through them. This curve has the same character as the M-distortion curve and, consequently, if its Δm -scale is transformed into a u -scale by means of the M-distortion curve, it becomes a practically straight line. This represents the S-distortion.

It was found that the accuracy in the procedure is so high that the error introduced by the use of the $m(\chi)$ -curves instead of the real mean light-curves, is clearly perceptible. A correction was applied as follows.

The S-distortion can be represented by a vector in the (φ_0, φ_1) -plane. By studying the centres of symmetry of the iso-magnitude curves, as shown in Figure 4, it could be verified that the direction of the vectors is strictly parallel to the time direction. This demonstrates in a direct way that the S-distortion affects the sum of the oscillations and has no preference for one of them.

In the procedure described the component of the vector perpendicular to the χ -axis has been neglected. As a consequence the M-distortion differs somewhat from the real distortion. For example, the $m(\chi)$ -curve which has the highest maximum does not show the deepest minimum, as it should do.

From the Tables 5^{a, b, c} the $m(\psi)$ -curves were taken, i.e. the cross sections of the mean light-surface perpendicular to the $m(\chi)$ -curves. In these curves the error in Δm caused by the neglected component of the S-distortion can be directly determined. With sufficient accuracy the provisional values of the S-distortion can be used for this, since its effect has to be reduced by the factor

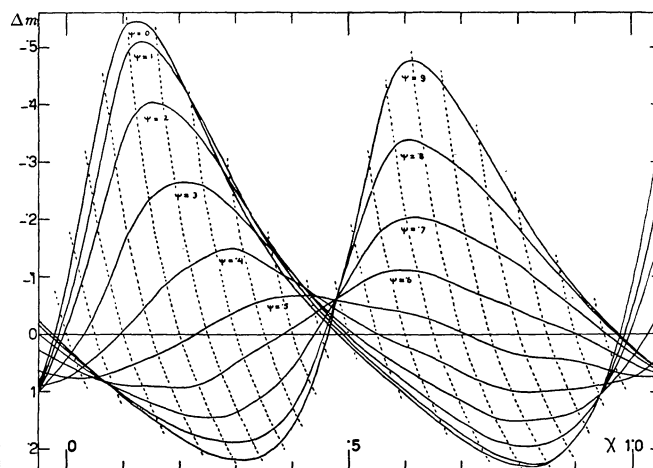
$$\frac{d\psi}{d\chi} = 2 \frac{P_0 - P_1}{P_0 + P_1} = 0.256.$$

The corrections, which can amount to some hundredths of a magnitude, were applied to the Δm 's and new $m(\chi)$ -curves were constructed which could be used for the final determination of the S-M-distortion. A set of $m(\chi)$ -curves is shown in Figure 5.

For 1953 the M-distortion curve is shown in Figure 6. The curve of 1952 is exactly the same, but that of 1951 deviates in shape, as can be seen in Table 6, it has a stronger curvature.

It should be remarked that the process of finding the M-distortion curve leaves the scale factor of u arbitrary.

FIGURE 5

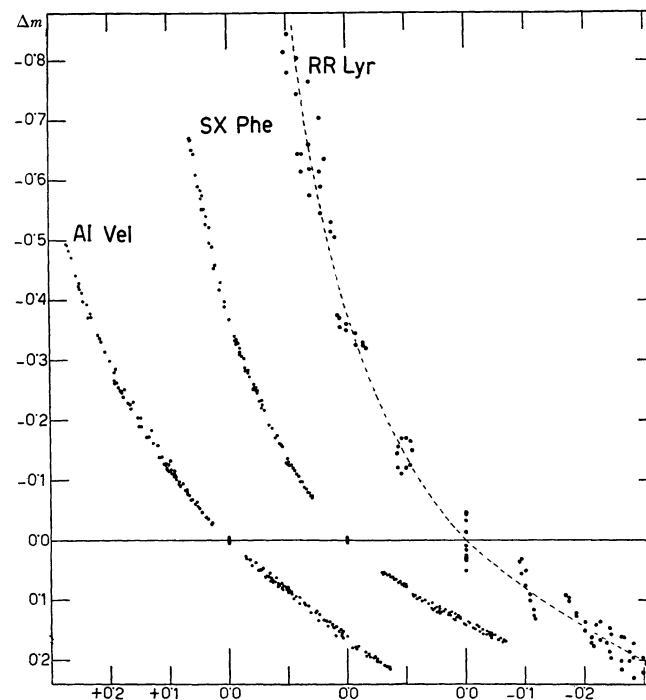


Set of curves as used for determination of S- and M-distortion. They show the magnitude as a function of χ for fixed values of ψ . By reading the curves at the dashed lines the effect of S-distortion is eliminated.

It can be fixed afterwards by the conditions that, at $\Delta m = 0$, $\frac{du}{d\Delta m} = -1$; which is equivalent to the assumption that weak oscillations are not distorted.

The S-distortion cannot be determined with the same smoothness as the M-distortion, which is under-

FIGURE 6



M-distortion curves, showing the relation between observed magnitudes Δm and the magnitudes u computed from the two-sine model.

TABLE 6
M-distortion

u	Δm 1951	Δm 1952-53	u	Δm 1951	Δm 1952-53
+0.28	-.588	-.525	-0.02	+.019	+.020
+0.26	-.508	-.456	-0.04	+.036	+.037
+0.24	-.438	-.394	-0.06	+.054	+.055
+0.22	-.376	-.340	-0.08	+.069	+.071
+0.20	-.320	-.294	-0.10	+.084	+.087
+0.18	-.273	-.252	-0.12	+.098	+.103
+0.16	-.231	-.216	-0.14	+.112	+.119
+0.14	-.192	-.182	-0.16	+.126	+.134
+0.12	-.157	-.150	-0.18	+.138	+.149
+0.10	-.125	-.121	-0.20	+.150	+.164
+0.08	-.095	-.093	-0.22	+.161	+.178
+0.06	-.068	-.066	-0.24	+.172	+.193
+0.04	-.044	-.042	-0.26	+.182	+.207
+0.02	-.021	-.020	-0.28	+.190	+.219
0.00	.000	.000			

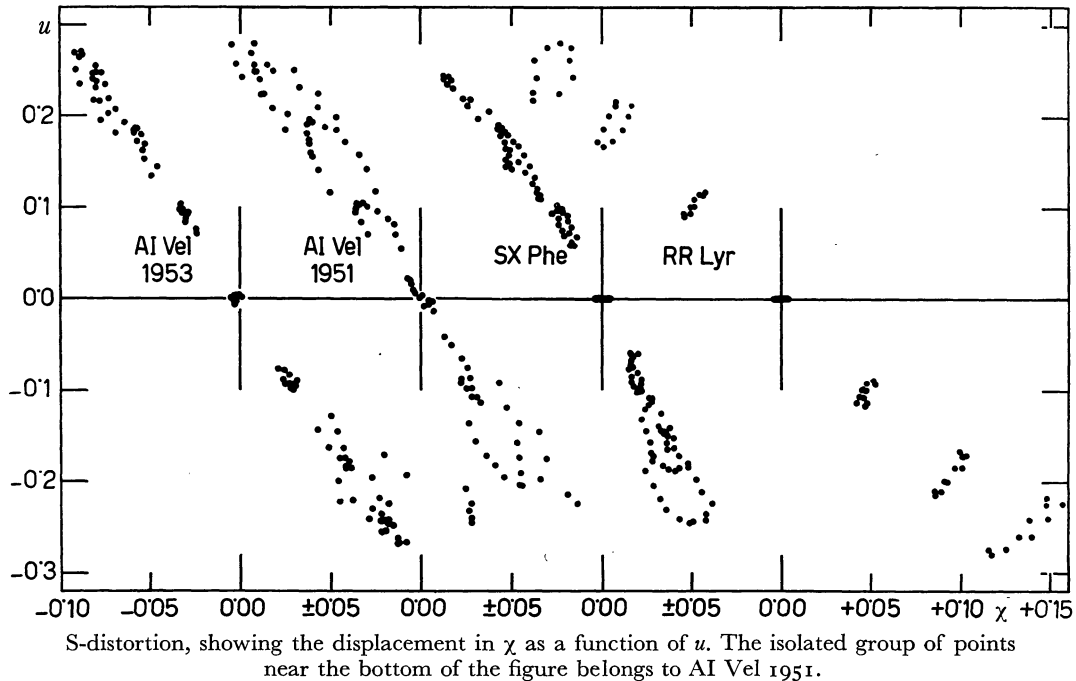
standable, since its effect on the light-curve is weaker. Especially in the low portions of the light-curves and in the flat light-curves small irregularities can give rise to strong deviations in phase. To all practical purposes the S-distortion could be represented by a straight line with a slope

$$\frac{d\chi}{du} = -0.32 \text{ cycle/magn.}$$

Figure 7 shows how the S-distortion was obtained. The flat light-curves and the minima of 1951 were not used.

Now that the S- and M-distortions have been determined we can reduce the $m(\chi)$ -curves and see how accurately they agree with the u -curves given by (7). In order to facilitate the computations this reduction was done graphically by drawing at regular intervals ordinate lines curved according to S-M-distortion

FIGURE 7



S-distortion, showing the displacement in χ as a function of u . The isolated group of points near the bottom of the figure belongs to AI Vel 1951.

(see Figure 5) and reading Δm at these lines. By means of Table 6 the Δm 's are converted into u 's.

It should be noted that the symbol u is used also for reduced observed magnitudes. A sine-curve was fitted to each of the u -curves thus obtained. In Table 7 the amplitudes A_{obs} , in Table 8 the phase-shifts $\Delta\chi_{obs}$, and in Table 9 the mean height \bar{u} of the fitted sine-curves are given.

A least-squares solution of equations of the type (7a) gave the most probable values of a , b and the phase ψ of the zero point. They are given in Table 10.

The computed amplitudes A_{com} agree perfectly with the A_{obs} , as can be seen in Table 7 and in Figure

8, where the full-drawn line represents the computed amplitude and the dots are observed (upper part of figure). In so far as the amplitude variation is concerned, the two-sine model gives a completely satisfactory description of the phenomena.

Less satisfactory is the agreement for the phase shift $\Delta\chi_{obs}$, for which it appeared impossible to obtain a good fit with equation (7b). Therefore, instead of trying to find the best values of the parameters we directly computed the phase shifts with (7b), using the elements of Table 10. The differences $\Delta\chi_{obs}$ minus $\Delta\chi_{comp}$ are shown also in Figure 8.

At the bottom of the figure is shown how the phase

TABLE 7

ψ	1951			1952			1953			ψ
	A_{obs}	A_{com}	$O-C$ ($0^m.0001$)	A_{obs}	A_{com}	$O-C$ ($0^m.0001$)	A_{obs}	A_{com}	$O-C$ ($0^m.0001$)	
.00	m 0.2749	m 0.2762	-13	m 0.2791	m 0.2798	-7	m 0.2678	m 0.2707	-29	.00
.05	0.2748	0.2749	-1	0.2778	0.2787	-9	0.2661	0.2696	-35	.05
.10	0.2690	0.2669	+21	0.2714	0.2711	+3	0.2601	0.2624	-23	.10
.15	0.2515	0.2525	-10	0.2584	0.2572	+12	0.2503	0.2492	+11	.15
.20	0.2340	0.2320	+20	0.2393	0.2375	+18	0.2339	0.2305	+34	.20
.25	0.2086	0.2061	+25	0.2133	0.2126	+7	0.2095	0.2070	+25	.25
.30	0.1782	0.1753	+29	0.1839	0.1833	+6	0.1821	0.1794	+27	.30
.35	0.1427	0.1408	+19	0.1501	0.1509	-8	0.1493	0.1491	+2	.35
.40	0.1047	0.1037	+10	0.1166	0.1173	-7	0.1177	0.1181	-4	.40
.45	0.0667	0.0668	-1	0.0817	0.0864	-47	0.0896	0.0903	-7	.45
.50	0.0373	0.0392	-19	0.0697	0.0669	+28	0.0736	0.0736	0	.50
.55	0.0439	0.0477	-38	0.0740	0.0714	+26	0.0788	0.0775	+13	.55
.60	0.0824	0.0812	+12	0.0963	0.0964	-1	0.0994	0.0992	+2	.60
.65	0.1242	0.1187	+55	0.1263	0.1289	-26	0.1302	0.1288	+14	.65
.70	0.1606	0.1549	+57	0.1605	0.1624	-19	0.1604	0.1598	+6	.70
.75	0.1926	0.1881	+45	0.1937	0.1938	-1	0.1913	0.1894	+19	.75
.80	0.2176	0.2170	+6	0.2237	0.2217	+20	0.2166	0.2157	+9	.80
.85	0.2374	0.2409	-35	0.2458	0.2449	+9	0.2379	0.2376	+3	.85
.90	0.2525	0.2590	-65	0.2622	0.2627	-5	0.2537	0.2544	-7	.90
.95	0.2649	0.2709	-60	0.2735	0.2744	-9	0.2644	0.2656	-12	.95

TABLE 8

ψ	1951			1952			1953			ψ
	$\Delta\chi_{obs}$	$\Delta\chi_{com}$	$O-C$	$\Delta\chi_{obs}$	$\Delta\chi_{com}$	$O-C$	$\Delta\chi_{obs}$	$\Delta\chi_{com}$	$O-C$	
.00	-.0327	-.0011	-.0316	-.0249	-.0019	-.0230	-.0273	-.0022	-.0251	.00
.05	-.0327	+.0023	-.0350	-.0201	+.0039	-.0240	-.0221	+.0045	-.0266	.05
.10	-.0281	+.0058	-.0339	-.0156	+.0099	-.0255	-.0157	+.0114	-.0271	.10
.15	-.0249	+.0095	-.0344	-.0120	+.0165	-.0285	-.0101	+.0188	-.0289	.15
.20	-.0176	+.0138	-.0314	-.0067	+.0240	-.0307	-.0014	+.0274	-.0288	.20
.25	-.0079	+.0192	-.0271	+.0042	+.0330	-.0288	+.0102	+.0376	-.0274	.25
.30	+.0052	+.0262	-.0210	+.0192	+.0447	-.0255	+.0258	+.0508	-.0250	.30
.35	+.0200	+.0363	-.0163	+.0409	+.0612	-.0203	+.0480	+.0690	-.0210	.35
.40	+.0381	+.0535	-.0154	+.0786	+.0870	-.0084	+.0817	+.0968	-.0151	.40
.45	+.0756	+.0896	-.0140	+.1329	+.1325	+.0004	+.1346	+.1431	-.0085	.45
.50	+.1813	+.1908	-.0095	+.2174	+.2149	+.0025	+.2144	+.2192	-.0048	.50
.55	+.3545	+.3558	-.0013	+.3169	+.3173	-.0004	+.3044	+.3096	-.0052	.55
.60	+.4264	+.4260	+.0004	+.3827	+.3858	-.0031	+.3660	+.3751	-.0091	.60
.65	+.4507	+.4534	-.0027	+.4232	+.4231	+.0001	+.4036	+.4139	-.0104	.65
.70	+.4624	+.4676	-.0052	+.4428	+.4451	-.0023	+.4253	+.4378	-.0125	.70
.75	+.4692	+.4764	-.0072	+.4555	+.4596	-.0041	+.4420	+.4541	-.0121	.75
.80	+.4724	+.4828	-.0104	+.4612	+.4702	-.0090	+.4530	+.4660	-.0130	.80
.85	+.4736	+.4877	-.0141	+.4651	+.4787	-.0136	+.4600	+.4756	-.0156	.85
.90	+.4720	+.4918	-.0198	+.4670	+.4858	-.0188	+.4646	+.4837	-.0191	.90
.95	+.4686	+.4955	-.0269	+.4710	+.4921	-.0211	+.4684	+.4910	-.0226	.95

TABLE 9

ψ	1951	1952	1953	ψ	1951	1952	1953
	\bar{u}	\bar{u}	\bar{u}		\bar{u}	\bar{u}	\bar{u}
.00	+ .0008	-.0019	+ .0007	.50	-.0035	-.0065	-.0022
.05	-.0008	-.0031	.0000	.55	-.0009	-.0045	-.0014
.10	-.0022	-.0024	-.0007	.60	+ .0025	-.0031	-.0007
.15	-.0041	-.0007	-.0009	.65	+ .0070	-.0015	+ .0005
.20	-.0073	+ .0012	-.0010	.70	+ .0101	-.0024	+ .0007
.25	-.0088	-.0010	-.0015	.75	+ .0107	-.0012	-.0002
.30	-.0104	-.0034	-.0012	.80	+ .0093	.0000	+ .0002
.35	-.0079	-.0071	-.0024	.85	+ .0063	+ .0003	-.0003
.40	-.0068	-.0081	-.0022	.90	+ .0051	+ .0014	+ .0010
.45	-.0047	-.0095	-.0021	.95	+ .0032	+ .0005	+ .0015

TABLE 10

season	a	b	ψ of zero point	$a + b$	$\frac{a+b}{a-b}$
1951	m 0.1568 ± 0.0014 m.e.	m 0.1197 ± 0.0016 m.e.	$+ 5^{\circ}25'$ $\pm 0^{\circ}33'$ m.e.	m 0.276	7.45
1952	0.1728 ± 0.0007 m.e.	0.1074 ± 0.0007 m.e.	$+ 5^{\circ}54'$ $\pm 0^{\circ}18'$ m.e.	0.280	4.28
1953	0.1717 ± 0.0008 m.e.	0.0993 ± 0.0008 m.e.	$+ 5^{\circ}52'$ $\pm 0^{\circ}20'$ m.e.	0.271	3.74

shift is affected by a change in $\frac{a+b}{a-b}$, from 4.0 to 5.0, and by a change of the zero point of ψ of 0.01.

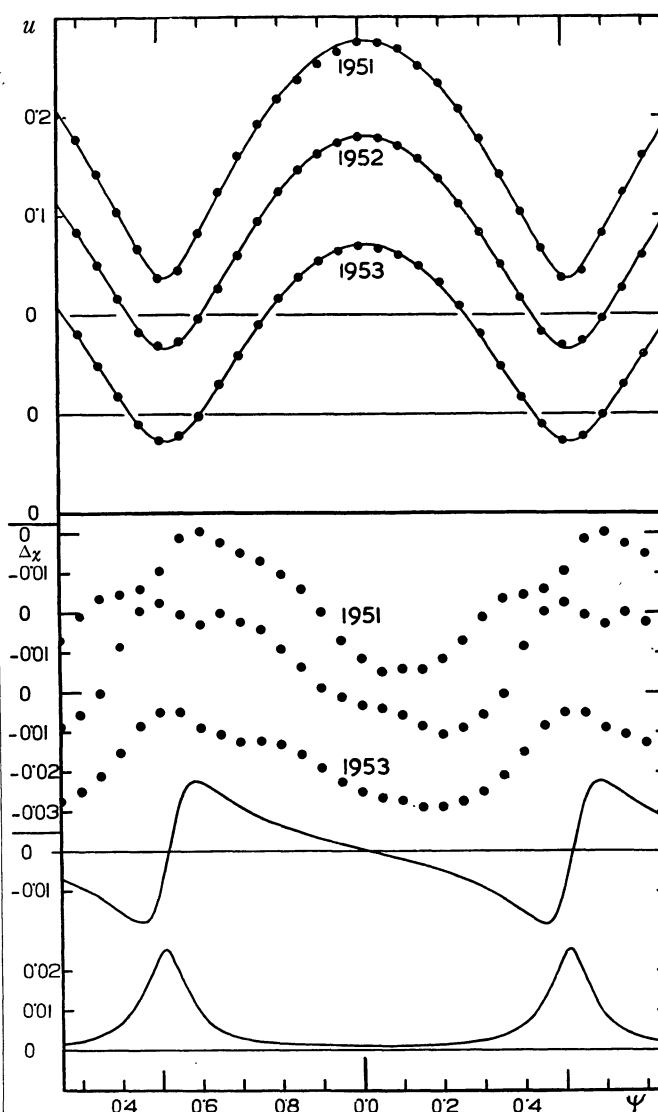
By comparing these effects with the observed residuals it is clear that a relatively small change in the parameters would produce sharp irregularities in the residuals and make them more irregular than they are now. Each season shows more or less the same run of deviations in phase (which will be found also in SX Phoenicis); we must conclude therefore that it is a real effect and presents a deviation from our two-sine model.

But then, apart from this systematic effect, the variation in phase is in perfect agreement with the variation in amplitude, for the variations in $\frac{a+b}{a-b}$, found from the amplitudes, are strictly confirmed by the phases.

As can be seen in Table 9 the mean level of the reduced curves shows hardly any variation. One might perhaps conclude that the variations suggest the existence of a wave with a length equal to the beat period, but this is not worth considering seriously.

The same can be said about the residuals of the reduced u -curves with respect to the (fitted-in) sine-curves. These residuals also suggest waves which fit twice and four times, respectively, in one cycle of χ , but, if they are real, the amplitudes are not more than some thousandths of a magnitude. The average deviations from the sine-curves are about $\pm 0^m.005$ for 1952 and 1953, and somewhat more for 1951.

FIGURE 8



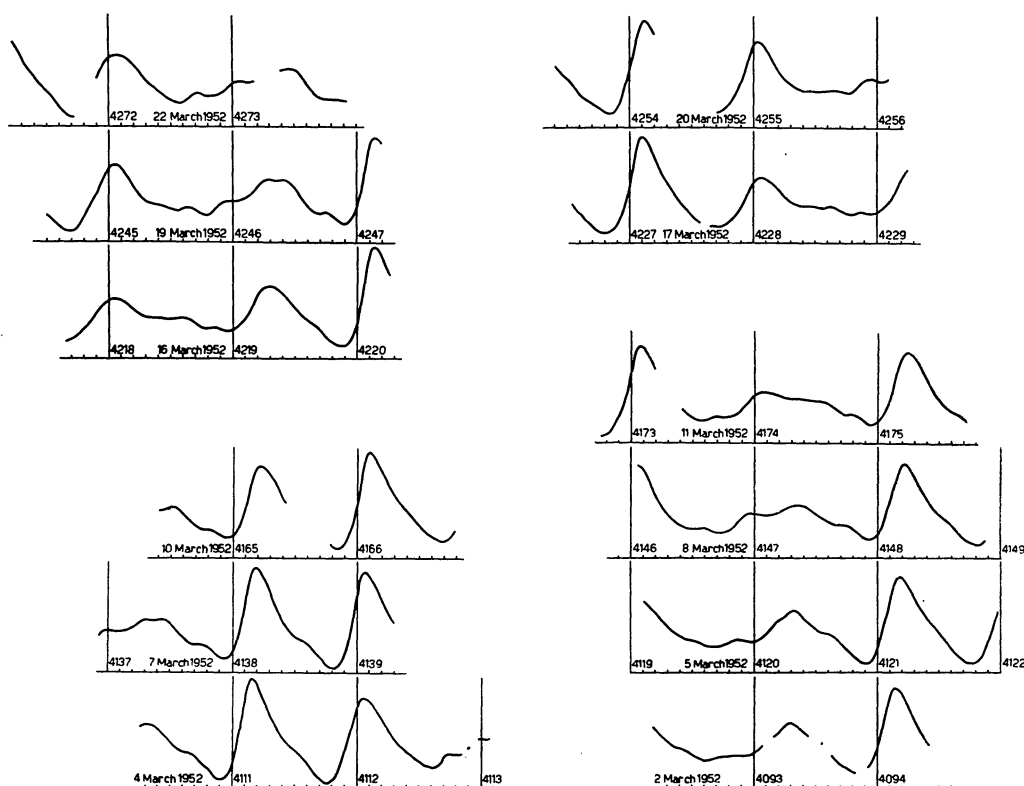
Above: variation of amplitude with phase ψ of beat period, the dots are observed values and the full-drawn lines are computed functions of the form $A = (a^2 + 2ab \cos 2\pi\psi + b^2)^{1/2}$. Under: deviations in phase χ of the light-curves with respect to the two-sine model; the effect of changes in the parameters of the model is shown by the lines at the bottom.

The results of the study of the mean light-curves can be summarized as follows.

The mean light-curve of AI Velorum, in all its peculiar shapes, can be represented as a distortion of the sum of two sine-curves; no other sine waves with an amplitude of more than a few thousandths of a magnitude are present. Apart from the phase shift of the high light-curves with respect to the low ones, of the order of two hundredths of a cycle, the distortion is a smooth function of magnitude valid for the whole curve.

The difference of the amplitudes of the two sine waves has decreased during the observations; rapidly

FIGURE 9



Some observed light-curves of AI Velorum.
The vertical lines indicate zero points of the primary phase and the numbers are cycle-numbers according to formula (4). The absence of March 13 and 14 and the gaps in the curves are due to clouds.

from 1951 to 1952, much less, but well perceptibly, from 1952 to 1953. The sum of the amplitudes remained practically constant. Probably, the distortion is not a fixed function but can vary slightly, together with the difference of the two amplitudes.

The residual curves.

From the observed magnitudes the mean magnitude, found from the mean $m(\varphi_1)$ -curves corresponding to Table 5, is subtracted. The residuals, plotted against time, were used to study the characteristics of the short waves. The most pronounced wave has an average length of one hour and an amplitude of some hundredths of a magnitude. This wave has been studied in our light-curves of 1951, where it was necessary to superpose two sine-curves in order to interpret the observed shapes. These waves were called P_2 and P_3 . It was found furthermore that this model could not describe the observations of all nights; often strong deviations occur. We hoped to get a better insight into the phenomenon from the more extensive observations obtained in 1952 and 1953. This hope has not been fulfilled completely. The waves P_2 and P_3 could be followed throughout all observations; but, as in 1951, many deviations from these waves occur. Al-

though we succeeded in recognizing some other waves with reasonable certainty we could not interpret all residual curves down to the limit of the accuracy of the observations. As a consequence the study of the residual curves could not reach a higher level than that of estimating the amplitudes and phases of the observed humps.

Before discussing the phenomena in the residual curves we shall make some remarks about the appearance of the short waves in the observed light-curves. In Figure 9 a series of light-curves is shown.

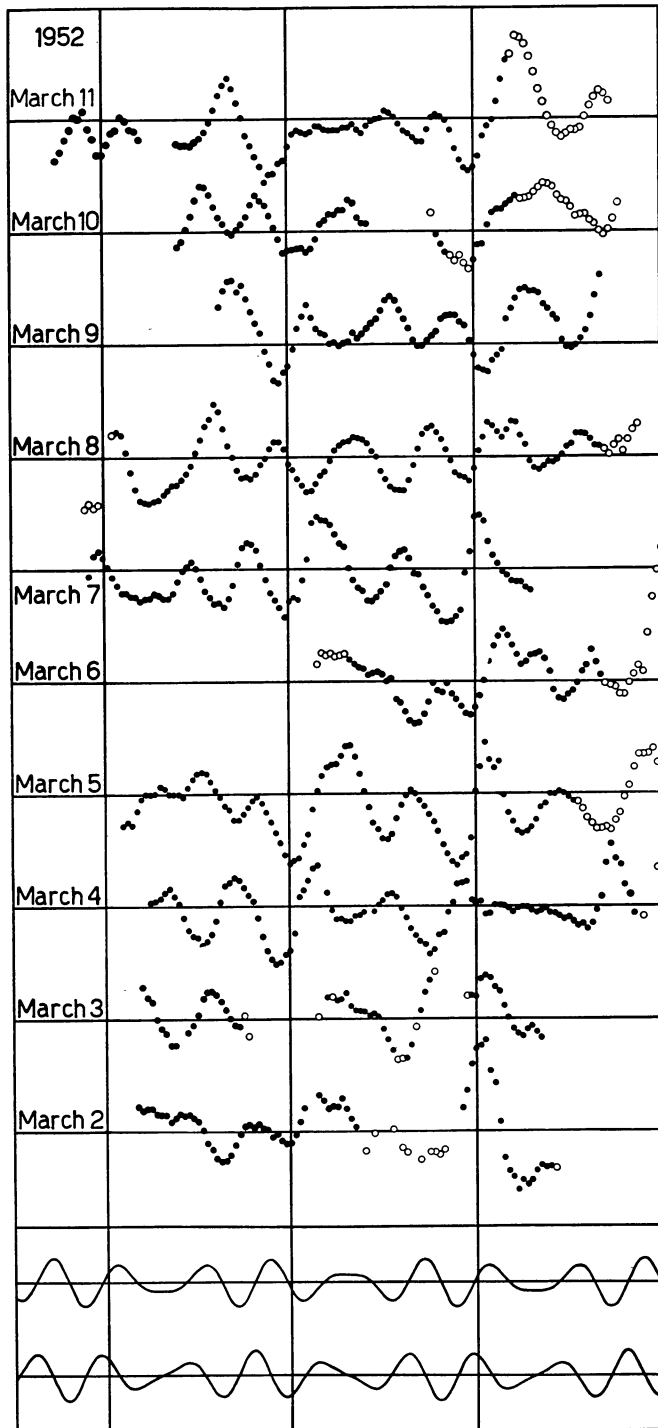
In these curves the small oscillations can easily be distinguished. Their influence can be judged also by comparing the curves of March 5 and 7 with the synthetic curve of Figure 1.

The vertical lines mark the zero points of the primary phase φ_0 , computed from (4). The curves are placed such that intervals of 27 cycles of P_0 are shown one above the other. This interval contains 34.945 cycles P_1 , and therefore only a slow change takes place in the shape of the mean light-curve.

The sequence from 2 to 20 March shows how the light-curve creeps through the narrow bottle-neck of the pair of envelopes. It is curious to see how the maximum shown in the central interval at φ_0 about

0.3 on March 2 and 5 gradually sinks down and disappears and how a new maximum rises at φ_0 about zero. This impression of discontinuity in the place of the

FIGURE 10



Residual curves obtained by subtracting mean light-curves, which are functions of φ_0 and φ_1 only, from the observed light-curves.

The vertical lines indicate zero points of φ_0 .

The separation of the horizontal zero lines corresponds to 0.12 magnitude. At the bottom synthetic $P_2 + P_3$ curves are shown for comparison. Open circles indicate poor observations.

maximum, which we remarked in many such sequences, is probably only apparent and caused by the waves P_2 and P_3 , which in the sequence gradually shift to the right; but the possibility that the effect is real should be kept in mind.

The displacement of the humps of P_2 and P_3 to a later phase φ_0 can be found in all 27-cycle comparisons that can be made. Besides the 27-cycle interval several other interesting intervals have been found.

Each observed pair of a certain interval reveals the same change in shape, typical for that interval. From this simple inspection of the light-curves it may be concluded that the waves superposed on the light-curves consist of a number of components with at least approximately regular periods, and that no real irregular phenomena occur. However in comparing light-curves of different seasons the correspondence had a less permanent character. This seems to indicate that the strengths or the periods of some of the components are subject to gradual changes. Among the comparisons, that of the 17-cycle interval should be specially mentioned. This interval contains 22.002 cycles P_1 and, consequently, the mean light-curve should repeat itself almost exactly. As can be seen in Figure 9, where light-curves differing by this interval are placed side by side, the actual light-curves differ considerably. This proves, in a direct way, that other oscillations than P_0 and P_1 exist independently and that the observed humps are not produced by some complicated interaction of P_0 and P_1 .

In Figure 10 a sequence of residual curves is shown. The open circles represent doubtful observations. The curves are placed such that intervals of 9 cycles P_0 are shown one above the other. The long vertical lines indicate again the zero-points of φ_0 .

The oscillation P_2 is clearly distinguishable in most of the curves. Because the average length of the observed light-curves is greater than in 1951 a better estimate could be made of the mean period of P_2 . It appeared that the period $P_2 = 0^d.046460$, given in *B.A.N.* No 434, is too long, but this period can be corrected immediately by adding the reciprocal of a sidereal day to the reciprocal of the period. In other words, one more cycle is fitted in a day. The value found in this way is $P_2 = 0^d.0443919$.

The curious fact emerged that now the ratios $\frac{P_0}{P_3} = 3.5132$ and $\frac{P_0}{P_2} = 2.5134$ differ very nearly by one unit.

This fact escaped our attention in 1951. It means that the beat period of P_2 and P_3 is very nearly equal to P_0 .

From the elements given in *B.A.N.* No 434 we can derive that P_2 and P_3 reach the same phase at $\varphi_0 = 0.80$. (It should be noted that the epochs given in Table 8 and formula (35) in *B.A.N.* No 434 refer by mistake to maxima instead of, as was intended, to

phase zero.) Consequently the wave has been strong in the second half of each cycle P_0 , where P_2 and P_3 are in phase, and weak and stretched in the first half of the primary cycle. The new observations show the same behaviour, and there is no doubt that the beat period of P_2 and P_3 is exactly equal to P_0 .

In this case it seems more natural to assume that, instead of two waves, only one wave is present which is periodically distorted by the fundamental oscillation of the star. This is probably the real effect. The superposition of the two waves P_2 and P_3 is only a description of it.

It is not immediately clear which of the waves P_2 and P_3 has the original period, in other words, which would be observed if the periodic distortion did not exist. If it is P_2 , then the distortion makes it stronger and shorter in the second half of the primary cycle. If it is P_3 , then the distortion makes it stronger and longer in the same region. The answer to this question seems of extreme importance.

A very remarkable aspect of the phenomenon is that it depends on the fundamental oscillation P_0 and not on the combined effect of P_0 and P_1 together, as is the case with the S-M-distortion. We can be rather certain of this. In the first place the effect can be most clearly distinguished in the flat light-curves. It is shown in the results of the discussion of 1951 where P_2 and P_3 were found from flat light-curves while we were unaware of the new interpretation.

The flat light-curves exhibit a variety of shapes with maxima and minima at rather different phases φ_0 . The points at which P_2 and P_3 are in phase fall within a narrow region of phase near $\varphi_0 = 0.80$, so that the distortion is obviously not connected with the shape of the light-curve.

In order to make sure of this we made an analysis of P_2 and P_3 in the most homogeneous series of observations, i.e. the 19 nights of March 1952. The nights of March 15 and 16 were excluded, as these did not show the waves P_2 and P_3 . In the remainder the primary cycles were selected in groups. For one group at $\varphi_0 = 0$ the phase φ_1 lies between 0.25 and 0.65; these are low light-curves. The others we considered as high light-curves. In both groups four subgroups were selected depending on the phase of P_2 at $\varphi_0 = 0$. Then the mean residual curve was found from all cycles belonging to the same subgroup. The mean was found after shifting the residual curves slightly in phase such as to bring the phase of P_2 in accordance with that of the centre of the group. In this way eight mean residual curves were obtained, each one primary cycle long. Such a curve is the mean of between 2 and 7 original curves.

The exact analysis of the mean curves gave the results shown in Table 11.

In the table the phase of P_2 denotes the computed

TABLE 11

	low light-curves		high light-curves	
	P_2	P_3	P_2	P_3
amplitude	^m 0.0180	^m 0.0076	^m 0.0191	^m 0.0061
m.e.	± 0.0004	± 0.0011	± 0.0006	± 0.0009
phase	-0.100	0.685	-0.048	0.775
m.e.	± 0.004	± 0.023	± 0.005	± 0.023
difference	0.785		0.823	

phase φ_2 , with the elements (8), of the real zero point of the observed wave. Similarly, the phase of P_3 denotes the computed phase $\varphi_2 + \varphi_0$ of the observed zero point of P_3 . It follows that the two waves are in phase at $\varphi_0 = 0.804$, as in 1951.

It can be seen in the table that no difference exists between the distortion on the high and on the low light-curves, and we can conclude that the wave P_2 (or P_3) is distorted by P_0 such that apparently the wave P_3 (or P_2) is added. In this process the oscillation P_1 has no effect.

We could not detect a pronounced influence of the S-M-distortion on the wave $P_2 + P_3$. With regard to M-distortion this conclusion could have been made directly by inspecting Figure 3 and Figure 6. According to the M-distortion curve a certain change in the undistorted light-curve would result in a change in the distorted light-curve, which is four times bigger in the maxima than in the minima. But in Figure 3 the scatter of the maxima is of the same order of magnitude as that of the minima. Furthermore, if the inverse S-M-transformation is applied to the observed light-curves, with the humps included, the resulting curves have a rather irregular, queer appearance with very steep humps. We may conclude, therefore, that the oscillations P_2 and P_3 do not participate in the general M-distortion.

With regard to S-distortion we are not certain. In many of the deep minima the $(P_2 + P_3)$ -wave seems to be stretched in phase, as compared to the waves in the flat light-curves. Furthermore, on many of the ascending branches of high light-curves the $(P_2 + P_3)$ -wave looks shortened and exaggerated in height. Such effects might be caused by S-distortion but, since the effects are not clearly more pronounced than the general irregularities, the interpretation is doubtful.

The determination of the exact values of the periods of P_2 and P_3 is by the foregoing discussion reduced to one period only.

We made a survey through the residual curves of 1952 and 1953 by comparing them with a set of model curves, which were obtained by adding two sine-curves representing P_2 and P_3 respectively, with different phase-combinations. Two such model curves are shown in Figure 10. The amplitudes used are ^m0.018 for P_2 and ^m0.009 for P_3 ; the sine-curves are in phase at $\varphi_0 = 0.80$.

TABLE 12

date	cycle-number	$O-C$	amplitude	date	cycle-number	$O-C$	amplitude	date	cycle-number	$O-C$	amplitude
1952	m	φ_0	$0^m.001$	1952	m	φ_0	$0^m.001$	1953	m	φ_0	$0^m.001$
17 Feb	9972	-.05	16	7 Apr	11096	-.04	34	16 Jan	—	—	—
22 Feb	10083	-.01	20	13 Apr	11229	-.02:	14:	17 Jan	17515	-.05	10
2 Mar	10286	-.06	21					18 Jan	17538	-.02	15
3 Mar	10309	-.02	22					19 Jan	17560	-.01	15
4 Mar	10332	.00	29					20 Jan	17582	-.01:	20:
5 Mar	10354	-.03	28					22 Jan	17628	-.02	25
6 Mar	10379	-.02	28					23 Jan	17653	+.02	20
7 Mar	10400	+.00	33	21 Nov	16234	+.04:	30:	26 Jan	17720	+.04	15
8 Mar	10422	+.00	30	5 Dec	16548	+.04:	25:	28 Jan	17764	+.03	10
9 Mar	10445	-.01	26	6 Dec	16571	+.04:	30:	29 Jan	—	—	—
10 Mar	10465	+.01	25	20 Dec	16886	-.02	20	30 Jan	17809	-.01	10
11 Mar	10490	+.01	19	21 Dec	16909	-.02	25	5 Feb	17944	+.01	25
15 Mar	10578	-.10:	9:	22 Dec	16934	+.09:	20:	6 Feb	17965	+.04	25
16 Mar	10601	-.05:	10:	23 Dec	16954	+.02	15	7 Feb	17987	+.06	20
17 Mar	10623	-.04	16	26 Dec	17019	+.06:	10:	16 Feb	18192	-.05:	10:
18 Mar	10646	-.07	22	29 Dec	—	—	—	18 Feb	18236	-.02	10
19 Mar	10668	-.06	29	8 Jan	17312	+.01	25	27 Feb	18439	+.01	15
20 Mar	10694	-.04	22	9 Jan	17335	+.03	15	28 Feb	18461	+.04	10
21 Mar	10714	-.04	26	10 Jan	17357	+.13:	10:	4 Mar	18552	+.01	5
22 Mar	10736	-.03	32	11 Jan	—	—	—	5 Mar	18574	+.04	10
				15 Jan	17473	+.02:	10:				

From the comparison the phase of P_2 could be estimated in each primary cycle. Also the amplitude of the waves in the second half of the primary cycle was estimated. Since the mean level of the waves swings up and down considerably, the amplitude of the $P_2 + P_3$ wave was not referred to the zero-line, but was found as half the difference between maxima and minima.

The results of the survey are given in Table 12, showing the observed zero points of the phase of P_2 , expressed in φ_0 .

From the interval 1952 to 1953, and especially in the long interval of 1953, the exact period of P_2 has been found as $P_2 = 0^d.0444019$, or $P_2 = 0^p.397960$. The computed phase for which $\varphi_2 = 0$ has been found from

$$\varphi_0 = 0.133 + m \times 0.397960. \quad (8)$$

The waves of 1951 come on the average $0.03 P_0$ too late with respect to the elements (8); the waves of 1952 are too early by the same amount, and those of 1953 fit in the formula (8) directly.

The amplitude of the wave $P_2 + P_3$ has gradually diminished during the period of observation. For the yellow light-curves of 1951 we found for the sum of the amplitudes $0^m.033$. In 1952 the strongest waves had an average amplitude of $0^m.030$, and in 1953 it was $0^m.025$.

Besides the continuous decrease in strength a periodic variation is observed. About every two weeks some nights' observations show hardly the $P_2 + P_3$ waves, they become weak and short. What happens

exactly can not be distinguished. The variation in strength is accompanied by a variation in phase; the two effects are such as if an interfering wave is present, which is slightly longer than P_2 , and which produces a beat phenomenon with a period of about 144 cycles P_0 . The presence of a wave somewhat shorter than P_2 and a corresponding beat period of 9.5 cycles P_0 would give the same picture.

In 1953 the agreement between residual curves and model curves was not as good as in 1952. On many nights the waves $P_2 + P_3$ could not be recognized. Nevertheless there was also a considerable number of nights where the agreement was satisfactory and the phases found from these nights fitted the elements. Furthermore the above mentioned comparisons of fixed intervals showed the same characteristic changes as in the other years. The light-curves of February 16 and 18 threw some light on the mystery. The residual curves of these nights showed no $P_2 + P_3$ wave, but instead a wave with a length of one half of a primary cycle. It appeared then that in most of the puzzling residual curves this wave was responsible for the poor agreement with the model curves.

By the fact that P_2 and P_3 fit approximately $2^{1/2}$, respectively $3^{1/2}$, times into one primary cycle, and the disturbing wave fits twice it, we were able to distinguish the different waves by either adding or subtracting the residual curves of two successive primary cycles. The waves of $P_2 + P_3$ obtained in this way were well represented by the elements, as can be seen in Table 12. The other wave behaved rather peculiar-

ly. It was found to maintain its position with respect to φ_0 , the phase of the fundamental oscillation, for about a month, then it disappeared and returned again at another position in the primary cycle. This was repeated several times. The best fitting period of the wave is $0^{\text{P}}.49961$.

The average amplitude is of the order of one hundredth of a magnitude, although it may reach, as on February 16th, three hundredths of a magnitude.

Several circumstances, such as the extreme complexity of the phenomena superimposed upon each other in the residual curves, for, as will be shown, still other oscillations can be found in the residual curves, the irregular distribution of the observations and the generally bad atmospheric conditions in 1953 prevent a more accurate discussion of the wave. The fact that this wave is not perceptible in the observations of 1952 could perhaps be explained by the shortness of the interval of observations. If during March 1952 the wave has maintained a fixed position in the primary cycle it is absorbed in the mean light-curves.

Besides the short waves also longer waves can be recognized in the residual curves of 1952 and 1953. By comparison with the model curves the wave $P_2 + P_3$ appears to be superimposed on a waving curve. Like the short waves, these longer waves were rather puzzling at first. Sometimes they oscillate up and down intensely, at other places they are vague and irregular. The average length is about $4/5$ th of a primary cycle.

It appeared possible to represent the complete set of observed curves by two interfering waves. Although often for individual waves this representation is only approximate, the overall agreement was consistently reasonable, especially for the strong waves.

Strong discrepancies between the shapes of the observed wave and the two-sine model occur in general near or on the ascending branches of the light-curves, which indicates that the waves are subject to distortions. This can be seen in Figure 10 by comparing with Figure 9, e.g. in cycle No 4094 of March 2. The period of the strongest component was found to be of about the same length as P_1 . We therefore called this wave P'_1 . The phase φ_0 of the moments when φ'_1 is zero is given by

$$\varphi_0 = 4093.06 + p \times 0^{\text{P}}.82065. \quad (9)$$

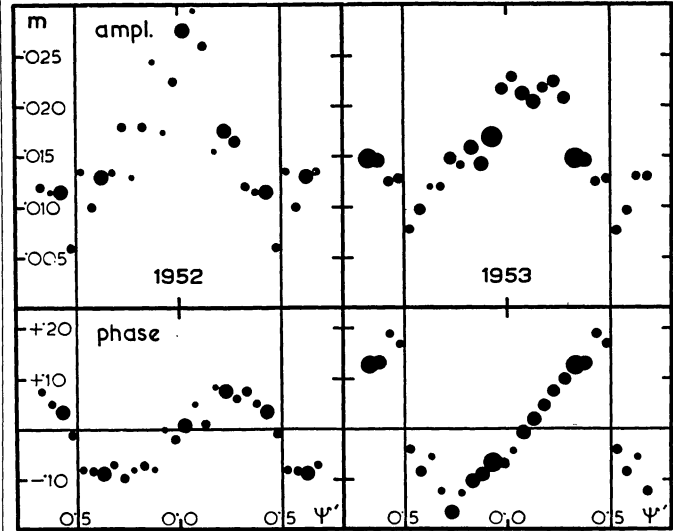
With less, although reasonable, certainty it could be established that the phase and amplitude of the wave oscillate with a period of nearly five primary cycles. If this is correct the interfering wave has a period which is nearly equal to the primary period. It was named P'_0 .

The zero point of the phase ψ' of the beat period of P'_0 and P'_1 can be computed from

$$\varphi_0 = 4094.86 + q \times 5^{\text{P}}.0145. \quad (10)$$

The amplitudes of all waves were plotted against ψ' , computed by (10). The mean of the amplitudes, which were plotted inside narrow strips of ψ' , was computed and plotted in Figure 11.

FIGURE 11



Amplitude and deviation in phase of the oscillation P'_1 as functions of ψ' , the phase of the beat period of P'_1 and P'_0 .

The same was done with the residuals, observed phase φ_0 minus phase computed from (9). For the residuals in phase the result is shown in the lower part of Figure 11. The size of the dots indicates the number of waves from which the average was formed. The average number is four in 1952, six in 1953. As can be seen in Figure 11 the variations in phase and in amplitude agree well, and leave little doubt about the reality of the waves.

The variation in phase indicates that the wave P'_0 had a somewhat smaller amplitude than P'_1 during 1952 and that the amplitudes were nearly equal in 1953. This seems to be contradicted by the amplitude, which is still considerable at $\psi' = 0.5$. But this can almost certainly be interpreted as due to the effect of erratic deviations. Such deviations, distributed at random, do not affect the mean amplitude of the strong waves near $\psi' = 0$, but at $\psi' = 0.5$ they may introduce false maxima and minima, which increases systematically the estimated amplitude.

From the curves of Figure 11 it can be estimated that the amplitude of P'_1 was $0^{\text{m}}.015$ in 1952 and $0^{\text{m}}.010$ in 1953, while that of P'_0 was $0^{\text{m}}.010$ in 1952 and about the same in 1953.

The period of P'_1 is interesting. The ratio $\frac{P'_0}{P'_1}$ is equal to 1.218546. It was found earlier that $\frac{P'_0}{P_2}$ is

TABLE I
Maxima and minima of the light-curves of AI Velorum

1934-'36

$$\psi = (\text{J.D.} - 2430000) 2.637256$$

J.D. -2420000	ψ	m^*	J.D. -2430000	ψ	m	J.D. -2430000	ψ	m
7443.415	-6742.369	-0.15	3763.219	9924.572	1.467	3792.195	10000.989	1.205
			3763.263	9924.688	0.952	3792.250	10001.134	1.436
7445.470	-6736.950	-0.04	3763.340	9924.891	1.309	3792.287	10001.232	0.913
7445.510	-6736.844	-0.98.	3763.403	9925.057	1.112		10003.718	1.484
						3793.230	10003.832	1.096
7465.420	-6684.336	-0.10	3764.248	9927.286	1.402			
			3764.277	9927.362	0.691			
7494.350	-6608.040	0.00	3764.347	9927.547	1.425	1952	ψ	Δm
7494.385	-6607.948	-0.75.	3764.376	9927.623	0.844	4060.299	10708.048	-0.102
						4060.370	10708.235	+0.195
7495.255	-6605.654	-0.90.	3766.239	9932.536	1.510	4060.397	10708.306	-0.518
7495.310	-6605.509	0.00	3766.275	9932.631	0.878	4060.465	10708.486	+0.218
7495.360	-6605.377	-0.30.	3766.331	9932.779	1.439	4060.497	10708.570	-0.463
			3766.373	9932.890	1.201	4060.561	10708.739	+0.187
7496.280	-6602.950	-0.58.	3766.416	9933.003	1.217	4060.613	10708.876	-0.189
7529.265	-6515.961	+0.05	3767.259	9935.226	1.449	4065.272	10721.163	+0.163
7529.300	-6515.868	-0.75.	3767.358	9935.487	1.455	4065.310	10721.263	-0.338
			3767.392	9935.577	0.857	4065.376	10721.437	+0.203
8235.255	-4654.084	-0.55.				4065.408	10721.522	-0.502
8235.310	-4653.939	0.00	3768.229	9937.784	1.425	4065.472	10721.690	+0.132
8235.340	-4653.860	-1.10.	3768.289	9937.943	1.190			
			3768.312	9938.003	1.213	4074.279	10744.917	+0.101
8236.280	-4651.381	-0.20				4074.354	10745.114	-0.205
8236.330	-4651.249	-0.50.	3769.186	9940.308	0.684	4074.417	10745.281	+0.195
			3769.256	9940.493	1.526	4074.450	10745.368	-0.486
			3769.287	9940.575	0.789			
						4075.298	10747.604	+0.234
			3770.209	9943.006	1.224	4075.332	10747.694	-0.306
			3770.273	9943.175	1.443	4075.393	10747.855	+0.140
			3770.305	9943.259	0.775	4075.473	10748.066	-0.103
			3770.371	9943.434	1.498			
			3770.405	9943.523	0.738	4076.256	10750.130	-0.197
						4076.320	10750.299	+0.250
			3775.219	9956.219	0.866	4076.347	10750.370	-0.549
			3775.287	9956.398	1.494	4076.416	10750.552	+0.273
			3775.315	9956.472	0.674	4076.449	10750.640	-0.393
						4076.509	10750.798	+0.156
			3784.275	9980.102	1.130			
			3784.339	9980.271	1.450	4077.298	10752.879	+0.116
			3784.366	9980.342	0.789	4077.370	10753.068	-0.173
						4077.436	10753.242	+0.242
			3785.204	9982.552	1.473	4077.465	10753.319	-0.440
			3785.241	9982.650	0.927	4077.531	10753.493	+0.250
			3785.295	9982.792	1.352			
						4078.411	10755.814	+0.171
			3786.226	9985.247	1.444	4078.480	10755.996	-0.111
			3786.259	9985.334	0.758	4078.546	10756.170	+0.148
			3787.196	9987.805	1.386			
			3787.251	9987.950	1.181	4079.267	10758.071	-0.095
			3787.279	9988.024	1.176	4079.335	10758.251	+0.210
			3787.331	9988.161	1.320	4079.363	10758.324	-0.518
						4079.433	10758.509	+0.281
			3789.241	9993.198	1.418	4079.460	10758.580	-0.486
			3789.273	9993.283	0.868			
						4080.243	10760.645	-0.416
			3790.212	9995.759	1.459	4080.319	10760.846	+0.116
			3790.257	9995.878	1.177	4080.384	10761.017	-0.111
						4080.450	10761.191	+0.171
			3791.237	9998.462	1.516	4080.482	10761.276	-0.432
			3791.268	9998.544	0.765	4080.548	10761.450	+0.210

* dots indicate maxima.

1951

J.D. -2430000	ψ	m
3753.239	9898.252	0.800
3753.306	9898.429	1.389
3753.333	9898.500	0.599
3754.260	9900.945	1.193
3754.327	9901.121	1.368
3754.356	9901.198	0.877
3754.423	9901.374	1.431
3755.205	9903.437	1.427
3755.232	9903.508	0.782
3755.303	9903.695	1.403
3755.333	9903.774	1.085
3755.403	9903.959	1.308
3756.226	9906.130	1.363
3756.254	9906.203	0.908
3756.322	9906.383	1.461
3756.349	9906.454	0.662
3761.233	9919.334	1.449
3761.263	9919.413	0.744
3761.328	9919.585	1.448
3761.361	9919.672	0.962
3762.244	9922.000	1.328
3762.284	9922.106	1.068
3762.351	9922.283	1.441

TABLE I (continued)

J.D. -2430000	ψ	Δm	J.D. -2430000	ψ	Δm	J.D. -2430000	ψ	Δm
4081.332	10763.517	+0.203	4094.301	10797.720	-0.236	4382.355	11557.392	+0.208
4081.359	10763.588	-0.494	4094.357	10797.868	+0.140			
4081.428	10763.770	+0.148	4094.456	10798.129	-0.134	4386.293	11567.778	-0.197
4081.495	10763.947	-0.111				4386.348	11567.922	+0.107
			4110.212	10839.681	+0.234	4386.386	11568.023	+0.091
4082.301	10766.073	-0.095	4110.250	10839.781	-0.236	4386.424	11568.123	-0.228
4082.350	10766.202	+0.156	4110.334	10840.003	+0.101	4386.486	11568.287	+0.177
4082.380	10766.281	-0.416	4110.397	10840.169	-0.189	4386.526	11568.392	-0.438
4082.449	10766.463	+0.242						
4082.478	10766.540	-0.526						
4082.544	10766.714	+0.179						
			1953	ψ	Δm	4387.271	11570.357	+0.216
			4338.430	11441.550	-0.438	4387.302	11570.438	-0.547
			4338.487	11441.700	+0.169	4387.369	11570.615	+0.239
4083.256	10768.591	-0.447				4387.408	11570.718	-0.322
4083.319	10768.758	+0.148	4339.450	11444.240	-0.376	4387.466	11570.871	+0.138
4083.367	10768.884	-0.087				4387.544	11571.077	-0.158
4083.466	10769.145	+0.171				4387.594	11571.209	+0.169
4083.498	10769.230	-0.416	4352.383	11478.348	-0.423			
			4352.454	11478.535	+0.224	4388.325	11573.136	-0.205
4087.254	10779.135	+0.101	4352.482	11478.609	-0.516	4388.387	11573.300	+0.177
4087.289	10779.227	-0.283	4352.551	11478.791	+0.154	4388.420	11573.387	-0.501
4087.359	10779.412	+0.218				4388.486	11573.561	+0.224
4087.388	10779.488	-0.533	4353.412	11481.062	-0.080	4388.518	11573.645	-0.376
4087.454	10779.662	+0.171	4353.447	11481.154	+0.115			
4087.492	10779.763	-0.220	4353.501	11481.297	-0.407	4389.265	11575.615	+0.224
						4389.298	11575.702	-0.345
4088.274	10781.825	-0.150	4354.345	11483.522	+0.216	4389.360	11575.866	+0.138
4088.372	10782.084	+0.101	4354.379	11483.612	-0.438	4389.440	11576.077	-0.158
4088.413	10782.192	-0.252				4389.507	11576.254	+0.161
4088.479	10782.366	+0.226	4367.412	11517.984	+0.068			
4088.506	10782.437	-0.565	4367.457	11518.102	-0.174	4393.277	11586.196	+0.130
			4367.523	11518.276	+0.177	4393.336	11586.352	-0.415
			4367.558	11518.368	-0.392	4393.400	11586.520	+0.239
4089.250	10784.399	+0.234				4393.429	11586.597	-0.462
4089.284	10784.489	-0.533	4368.306	11520.341	+0.239	4393.496	11586.774	+0.177
4089.352	10784.668	+0.187	4368.334	11520.415	-0.547	4393.543	11586.898	-0.111
4089.392	10784.774	-0.205	4368.405	11520.602	+0.247			
4089.486	10785.021	+0.085	4368.439	11520.692	-0.345	4394.277	11588.833	+0.169
			4368.526	11520.921	+0.060	4394.353	11589.034	-0.135
4090.255	10787.050	+0.132	4368.578	11521.058	-0.111	4394.419	11589.208	+0.130
4090.306	10787.184	-0.244				4394.452	11589.295	-0.368
4090.372	10787.358	+0.203	4369.358	11523.116	-0.158	4394.517	11589.466	+0.216
4090.402	10787.437	-0.565				4394.549	11589.551	-0.477
4090.473	10787.624	+0.195						
4090.510	10787.722	-0.353	4370.304	11525.610	+0.216			
			4370.331	11525.682	-0.399	4395.296	11591.521	+0.208
4091.246	10789.663	+0.226	4370.404	11525.874	+0.130	4395.326	11591.600	-0.407
4091.287	10789.771	-0.299				4395.395	11591.782	+0.185
4091.370	10789.990	+0.101	4370.460	11526.021	-0.111	4395.431	11591.877	-0.127
4091.428	10790.143	-0.189	4370.538	11526.228	+0.169	4395.531	11592.140	+0.084
4091.492	10790.312	+0.171	4370.569	11526.309	-0.454	4395.569	11592.241	-0.314
4091.521	10790.388	-0.612						
			4372.353	11531.014	-0.103	4396.317	11594.213	+0.130
4092.268	10792.358	+0.218				4396.353	11594.308	-0.376
4092.298	10792.437	-0.526	4373.313	11533.546	+0.208	4396.415	11594.472	+0.224
4092.366	10792.617	+0.195	4373.344	11533.628	-0.407	4396.438	11594.532	-0.446
4092.401	10792.709	-0.361	4373.417	11533.820	+0.130	4396.511	11594.725	+0.208
4092.480	10792.917	+0.030	4373.490	11534.013	-0.096	4396.554	11594.838	-0.174
4093.243	10794.930	+0.101	4376.329	11541.500	+0.224	4397.288	11596.774	+0.154
4093.320	10795.133	-0.189	4376.360	11541.582	-0.547	4397.368	11596.985	-0.103
4093.386	10795.307	+0.140	4376.558	11542.104	+0.099	4397.434	11597.159	+0.115
4093.416	10795.386	-0.471				4397.468	11597.249	-0.353
			4381.379	11554.818	-0.166	4397.533	11597.420	+0.224
						4397.564	11597.502	-0.493
4094.261	10797.614	+0.250	4382.291	11557.223	-0.314			

TABLE I (continued)

J.D. -2430000	ψ	Δm	J.D. -2430000	ψ	Δm	J.D. -2430000	ψ	Δm
4398.251	11599.314	-0.353	4408.507	11626.362	-0.485	4436.247	11699.519	+0.208
4398.306	11599.459	+0.177	4408.574	11626.538	+0.200	4436.276	11699.595	-0.399
4398.344	11599.559	-0.415	4408.604	11626.617	-0.337	4436.341	11699.767	+0.193
4398.410	11599.733	+0.193				4436.390	11699.896	-0.111
4398.445	11599.825	-0.158	4414.265	11641.547	+0.208	4436.483	11700.141	+0.130
			4414.294	11641.623	-0.353	4436.516	11700.228	-0.306
4400.302	11604.723	+0.185	4414.360	11641.797	+0.154			
4400.342	11604.828	-0.181	4414.417	11641.948	-0.135	4437.264	11702.201	+0.169
4400.423	11605.042	+0.099	4414.431	11641.985	+0.154	4437.298	11702.291	-0.314
4400.485	11605.205	-0.298	4414.535	11642.259	-0.392	4437.361	11702.457	+0.239
						4437.393	11702.541	-0.485
4401.359	11607.510	-0.454	4415.284	11644.234	+0.177	4437.458	11702.713	+0.193
4401.423	11607.679	+0.169	4415.315	11644.316	-0.454	4437.507	11702.842	-0.181
4401.454	11607.761	-0.251	4415.381	11644.490	+0.247			
4401.537	11607.980	+0.076	4415.414	11644.577	-0.470	4441.366	11713.019	+0.084
			4415.476	11644.740	+0.185	4441.432	11713.193	-0.236
4404.373	11615.459	-0.493	4415.530	11644.883	-0.181	4441.494	11713.357	+0.208
4404.475	11615.728	-0.244						
4404.544	11615.910	+0.115	4416.336	11647.009	-0.096	4442.275	11715.416	+0.193
			4416.401	11647.180	+0.130	4442.306	11715.498	-0.493
4406.268	11620.457	-0.516				4442.372	11715.672	+0.185
4406.336	11620.636	+0.216	4425.295	11670.636	+0.154	4442.410	11715.772	-0.236
4406.372	11620.731	-0.283	4425.329	11670.725	-0.220	4442.472	11715.936	+0.076
4406.429	11620.881	+0.107	4425.398	11670.907	+0.084			
4406.512	11621.100	-0.166	4425.443	11671.026	+0.068	4461.244	11765.442	+0.216
			4425.478	11671.118	-0.244	4461.273	11765.519	-0.477
4407.289	11623.149	-0.189	4425.547	11671.300	+0.185	4461.341	11765.698	+0.208
4407.355	11623.323	+0.193				4461.379	11765.798	-0.197
4407.387	11623.408	-0.485	4427.243	11675.773	-0.275	4461.434	11765.944	+0.052
4407.452	11623.579	+0.177	4427.288	11675.892	+0.076			
4407.488	11623.674	-0.322	4427.330	11676.003	+0.060	4466.250	11778.645	+0.185
			4427.372	11676.113	-0.220	4466.288	11778.745	-0.251
4408.269	11625.734	-0.275	4427.444	11676.303	+0.185	4466.340	11778.882	+0.076
4408.325	11625.882	+0.091	4427.473	11676.380	-0.547	4466.395	11779.027	+0.013
4408.406	11626.095	-0.166	4427.541	11676.559	+0.193	4466.426	11779.109	-0.220
4408.477	11626.282	+0.169						

TABLE 3

Epochs of ascending branches of AI Velorum

1st column: observed epoch2^d column: E computed from $J.D. = 2426142.190 + 0^d.111574 E$ 3^d column: $\psi = (J.D. - 2430000) 2.637214 + 0.7178$

J.D. -2430000	E	ψ	J.D. -2430000	E	ψ	J.D. -2430000	E	ψ
	1951						1952	
			3766.2555:	68331.919	.140			
			3767.2749	68341.056	.828			
3753.2192	68215.079	.760	3767.3756:	68341.958	.093	4060.3820	70968.075	.814
3753.3186	68215.970	.022	3769.2720	68358.955	.095	4060.4808	70968.961	.075
3754.3376	68225.103	.709	3770.2882	68368.063	.775	4065.2890	71012.055	.755
3754.4363	68225.988	.970	3770.3908	68368.982	.045	4065.3926	71012.984	.028
3755.2167	68232.982	.028	3775.2017:	68412.101	.733	4074.4324	71094.004	.868
3756.2364	68242.121	.717	3775.3001	68412.983	.992	4076.3327	71111.036	.879
3756.3351	68243.006	.977	3784.3494	68494.088	.857	4076.4308	71111.915	.138
3761.2466	68287.026	.930	3785.2224	68501.913	.159	4077.4490	71121.041	.823
3761.3442	68287.901	.187	3786.2404	68511.037	.844	4077.5486	71121.934	.086
3763.2419	68304.909	.192	3789.2546	68538.052	.793	4079.3479	71138.060	.831
3764.2598	68314.032	.876	3791.2528	68555.961	.003	4079.4473	71138.951	.093
3764.3605:	68314.935	.142	3792.2694	68565.073	.744	4080.4638	71148.062	.774

AI Velorum, 1953

TABLE 5^c

φ_1	.00	.05	.10	.15	.20	.25	.30	.35	.40	.45	.50	.55	.60	.65	.70	.75	.80	.85	.90	.95	φ_1
φ_0																					φ_0
.00	+112	+178	+243	+286	+283	+243	+193	+141	+095	+053	+015	-019	-049	-072	-087	-095	-097	-078	-025	+041	.00
.05	+220	+306	+374	+404	+399	+352	+288	+221	+167	+116	+071	+035	+006	-016	-028	-031	-027	-006	+052	+130	.05
.10	+310	+411	+470	+479	+453	+403	+345	+288	+230	+176	+126	+087	+058	+036	+026	+026	+038	+068	+129	+212	.10
.15	+355	+437	+493	+493	+460	+409	+357	+306	+256	+210	+167	+131	+100	+075	+063	+065	+084	+127	+192	+273	.15
.20	+352	+413	+457	+465	+437	+389	+337	+289	+245	+205	+168	+139	+112	+091	+079	+080	+097	+146	+212	+283	.20
.25	+303	+353	+390	+396	+382	+342	+298	+254	+213	+177	+146	+119	+099	+082	+075	+076	+091	+133	+188	+246	.25
.30	+236	+277	+310	+324	+316	+287	+247	+211	+175	+142	+113	+087	+068	+054	+050	+054	+069	+099	+141	+190	.30
.35	+166	+201	+230	+248	+247	+229	+198	+167	+134	+103	+077	+051	+034	+021	+018	+021	+033	+057	+088	+127	.35
.40	+096	+129	+156	+175	+179	+170	+150	+122	+093	+064	+038	+017	000	-012	-016	-015	-007	+011	+035	+065	.40
.45	+033	+063	+090	+107	+118	+115	+102	+078	+051	+025	+002	-019	-033	-044	-050	-051	-047	-034	-017	+005	.45
.50	-022	+007	+033	+053	+065	+064	+055	+036	+015	-009	-029	-048	-063	-075	-083	-087	-087	-079	-066	-047	.50
.55	-067	-039	-015	+005	+018	+019	+011	-003	-020	-040	-057	-075	-090	-104	-115	-122	-123	-121	-109	-091	.55
.60	-107	-077	-053	-032	-021	-019	-025	-035	-048	-064	-079	-097	-113	-128	-142	-151	-156	-157	-148	-132	.60
.65	-141	-110	-083	-060	-050	-047	-049	-059	-070	-084	-099	-115	-132	-150	-163	-173	-180	-183	-179	-165	.65
.70	-163	-133	-103	-079	-065	-062	-064	-071	-082	-094	-109	-126	-145	-162	-177	-189	-199	-200	-197	-185	.70
.75	-169	-138	-107	-086	-070	-066	-067	-072	-082	-094	-110	-129	-151	-172	-189	-201	-207	-209	-206	-194	.75
.80	-163	-127	-092	-072	-061	-058	-060	-065	-075	-088	-105	-125	-150	-173	-194	-206	-213	-213	-206	-191	.80
.85	-139	-097	-056	-034	-024	-026	-032	-046	-058	-074	-092	-115	-142	-167	-188	-201	-208	-205	-195	-175	.85
.90	-086	-038	+005	+033	+041	+036	+022	-002	-025	-048	-071	-098	-127	-151	-170	-183	-188	-180	-162	-130	.90
.95	+001	+056	+111	+141	+143	+129	+098	+063	+027	-004	-036	-067	-096	-119	-138	-148	-150	-135	-102	-052	.95

equal to 2.512815. The difference of the two numbers is 1.294269, which is practically identical with $\frac{P_0}{P_1} = 1.294244$.

Furthermore, using (4), (5), (8) and (9) and taking into account the systematic deviation in 1952 of the wave P_2 with respect to the elements (8), we find

$$\begin{aligned} \varphi'_1 &= \varphi_2 - \varphi_1 + 0.798 \quad (1952), \\ \varphi'_1 &= \varphi_2 - \varphi_1 + 0.810 \quad (1953). \end{aligned}$$

Hence it follows that between P'_1 , P_2 and P_1 the same relationship exists as we found earlier between P_2 , P_3 and P_0 .

Part II: SX PHOENICIS (HD 223065)

The variability of HD 223065 was discovered by EGGEN¹⁾. Because of the strong resemblance with AI Velorum Professor HERTZSPRUNG suggested to observe the light-curve. The same instrument was used as for AI Velorum in 1952, also with blue filter. An example of a recorded light-curve is shown in Figure 2.

A preliminary investigation of the records yielded the exact period P_0 and also the beat period, which, as in AI Velorum, is about $3^{1/2}$ times P_0 . These results have been published in *B.A.N.* No 446.

In the present paper we shall describe our investigation of the shape of the light-curves. Exactly the same procedure being followed as for AI Velorum the description can be brief.

The moments at which the phase of the primary period, φ_0 , is a multiple of 0.050 were computed from

$$J.D. = 2434200.0389 + \varphi_0 \times 0^d.0549642. \quad (11)$$

At these moments the magnitude was read off the

smooth curves drawn on the records. The readings give the magnitude with an arbitrary zero point.

In the discussion and in the table of observations at the end of the paper the magnitudes Δm refer to the mean magnitude, which is defined by the condition that the mean difference in phase between ascending and descending branches is 0.5.

For the moment at which the magnitudes have been found, the phase of the second period has been computed from

$$\varphi_1 = (J.D. - 2434200.0105) \times 23.37941. \quad (12)$$

The mean light-surface, i.e. the mean value of Δm as a function of φ_0 and φ_1 , was determined. This could be done more accurately than for AI Velorum, because the scatter of the Δm 's is much less. In Table 13 the mean light-surface is given.

Preliminary S- and M-distortion curves were derived from the diagonal curves, the $m(\chi)$ -curves. New $m(\chi)$ -curves were found after correcting ψ for S-distortion in the $m(\psi)$ -curves. The final M-distortion curve is given in Table 14 and Figure 6.

The S-distortion curve is shown in Figure 7. In SX Phoenicis the S-distortion curve cannot be represented by a straight line, and in the reductions we used the function given in Table 15.

With the known distortion the $m(\chi)$ -curves were reduced, and sine-curves were fitted to the resulting curves.

In Table 16 the amplitude A_{obs} , the phase shifts $\Delta\chi_{obs}$ and the mean level \bar{u} of the sine-curves are given. The table contains also the values computed by a least-squares solution of equation (7a). The values of the parameters which followed from the solution are in Table 17.

¹⁾ O. J. EGGEN, *P.A.S.P.* 64, 31, 1952.

TABLE 13

SX Phoenicis

Magnitude ($-\Delta m$) as function of ϕ_0 and ϕ_1 . Unit is $0^m.001$.

$\phi_0 \backslash \phi_1$.00	.05	.10	.15	.20	.25	.30	.35	.40	.45	.50	.55	.60	.65	.70	.75	.80	.85	.90	.95	$\phi_1 \backslash \phi_0$
.00	+18	+54	+84	+106	+113	+100	+76	+52	+28	+7	-21	-25	-37	-45	-52	-56	-55	-47	-32	-9	.00
.05	+159	+229	+306	+340	+342	+321	+267	+209	+160	+121	+90	+64	+43	+29	+23	+23	+30	+49	+75	+110	.05
.10	+398	+516	+598	+619	+603	+542	+474	+401	+333	+255	+214	+178	+152	+133	+126	+129	+147	+180	+236	+306	.10
.15	+540	+614	+657	+673	+666	+629	+563	+496	+435	+369	+312	+266	+241	+226	+222	+224	+240	+285	+354	+447	.15
.20	+525	+580	+617	+640	+635	+599	+554	+508	+453	+404	+353	+310	+274	+256	+252	+259	+279	+314	+366	+432	.20
.25	+424	+486	+534	+548	+544	+517	+481	+438	+397	+360	+328	+294	+267	+245	+235	+241	+257	+280	+317	+366	.25
.30	+328	+367	+404	+432	+424	+398	+369	+340	+311	+284	+259	+237	+219	+206	+193	+198	+206	+224	+253	+292	.30
.35	+228	+258	+282	+297	+301	+290	+273	+250	+227	+205	+184	+164	+149	+141	+139	+139	+144	+157	+178	+205	.35
.40	+141	+163	+180	+195	+199	+195	+180	+163	+143	+123	+105	+93	+84	+77	+75	+78	+83	+90	+103	+120	.40
.45	+63	+83	+94	+107	+113	+112	+103	+87	+71	+52	+34	+24	+15	+11	+11	+14	+19	+27	+36	+48	.45
.50	+2	+15	+27	+38	+46	+44	+37	+27	+13	+1	-14	-25	-33	-39	-39	-39	-33	-26	-17	-8	.50
.55	-47	-36	-24	-13	-7	-7	-10	-14	-27	-36	-48	-58	-67	-74	-77	-79	-76	-62	-54	-55	.55
.60	-85	-74	-65	-55	-49	-49	-49	-52	-59	-68	-77	-85	-94	-101	-106	-111	-110	-106	-100	-93	.60
.65	-116	-105	-97	-90	-84	-82	-82	-83	-87	-93	-100	-109	-117	-124	-130	-135	-138	-136	-131	-124	.65
.70	-137	-127	-116	-112	-109	-106	-106	-106	-109	-113	-120	-127	-135	-144	-150	-153	-154	-154	-151	-145	.70
.75	-146	-137	-129	-123	-119	-116	-117	-119	-123	-128	-134	-140	-147	-155	-160	-164	-162	-164	-159	-154	.75
.80	-142	-136	-130	-124	-120	-118	-118	-121	-126	-133	-138	-145	-152	-158	-164	-169	-169	-167	-161	-154	.80
.85	-128	-119	-113	-110	-108	-107	-109	-113	-117	-124	-128	-138	-146	-155	-162	-167	-166	-162	-153	-141	.85
.90	-103	-90	-80	-75	-73	-74	-79	-86	-94	-102	-110	-117	-129	-139	-146	-150	-147	-144	-134	-118	.90
.95	-59	-40	-24	-9	-9	-18	-28	-38	-49	-62	-74	-83	-92	-99	-106	-112	-113	-105	-92	-75	.95

TABLE 14

M-distortion, SX Phoenicis

u	Δm	u	Δm	u	Δm
+0.26	-0.646	+0.08	-0.100	-0.10	+0.078
+0.24	-0.548	+0.06	-0.073	-0.12	+0.091
+0.22	-0.457	+0.04	-0.046	-0.14	+0.104
+0.20	-0.378	+0.02	-0.022	-0.16	+0.115
+0.18	-0.315	0.00	0.000	-0.18	+0.127
+0.16	-0.262	-0.02	+0.019	-0.20	+0.139
+0.14	-0.215	-0.04	+0.035	-0.22	+0.150
+0.12	-0.172	-0.06	+0.050	-0.24	+0.160
+0.10	-0.134	-0.08	+0.065	-0.26	+0.171

TABLE 15

S-distortion, SX Phoenicis

Δm	$\Delta \chi$	Δm	$\Delta \chi$	Δm	$\Delta \chi$
-0.65	-0.093	-0.35	-0.062	-0.05	-0.011
-0.60	-0.089	-0.30	-0.055	0.00	0.000
-0.55	-0.084	-0.25	-0.047	+0.05	+0.013
-0.50	-0.079	-0.20	-0.039	+0.10	+0.028
-0.45	-0.074	-0.15	-0.030	+0.15	+0.047
-0.40	-0.068	-0.10	-0.021		

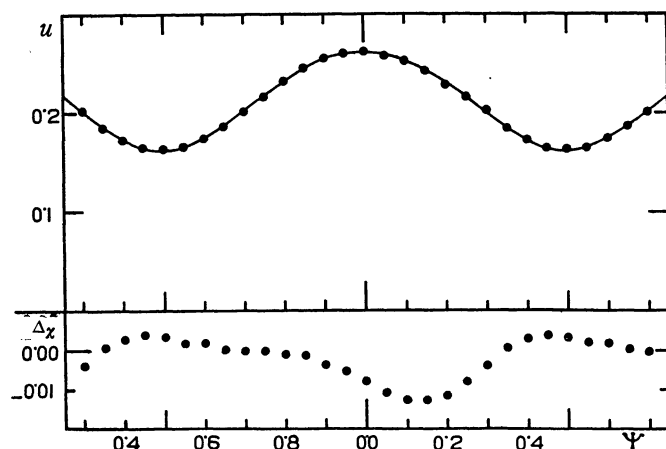
TABLE 16

ψ	A_{obs}	A_{com}	$O-C$ m 0.0001	$\Delta \chi_{obs}$	$\Delta \chi_{com}$	$O-C$	\bar{u}	ψ
	m	m					m	
.00	0.2605	0.2607	-2	-0.067	+0.0010	-0.0077	+0.0017	.00
.05	0.2571	0.2585	-14	+0.062	+0.0166	-0.0104	+0.0040	.05
.10	0.2524	0.2525	-1	+0.0207	+0.0328	-0.0121	+0.0041	.10
.15	0.2434	0.2429	+5	+0.0378	+0.0499	-0.0121	+0.0040	.15
.20	0.2291	0.2305	-14	+0.0579	+0.0688	-0.0109	+0.0054	.20
.25	0.2164	0.2159	+5	+0.0825	+0.0899	-0.0074	+0.0038	.25
.30	0.2018	0.2004	+14	+0.1108	+0.1142	-0.0034	+0.0008	.30
.35	0.1844	0.1855	-11	+0.1436	+0.1426	+0.0010	-0.0008	.35
.40	0.1718	0.1728	-10	+0.1788	+0.1756	+0.0032	-0.0020	.40
.45	0.1651	0.1643	+8	+0.2170	+0.2128	+0.0042	-0.0041	.45
.50	0.1636	0.1616	+20	+0.2560	+0.2526	+0.0034	-0.0044	.50
.55	0.1661	0.1651	+10	+0.2944	+0.2922	+0.0022	-0.0048	.55
.60	0.1746	0.1742	+4	+0.3310	+0.3290	+0.0020	-0.0034	.60
.65	0.1855	0.1873	-18	+0.3619	+0.3613	+0.0006	-0.0027	.65
.70	0.2012	0.2024	-12	+0.3891	+0.3891	0.0000	-0.0018	.70
.75	0.2161	0.2179	-18	+0.4129	+0.4130	-0.0001	-0.0012	.75
.80	0.2322	0.2322	0	+0.4330	+0.4338	-0.0008	0.0000	.80
.85	0.2456	0.2443	+13	+0.4513	+0.4524	-0.0011	-0.0004	.85
.90	0.2555	0.2534	+21	+0.4659	+0.4694	-0.0035	+0.0003	.90
.95	0.2592	0.2590	+2	+0.4804	+0.4854	-0.0050	+0.0013	.95

TABLE 17

a	b	ψ of zero point	$a + b$	$\frac{a + b}{a - b}$
^m 0.2112	^m 0.0496	$-1^{\circ}10'$	^m 0.261	1.161

FIGURE 12



Variation in amplitude and deviation in phase of the light-curves of SX Phoenicis during the beat period. The corresponding quantities for AI Velorum are shown in Figure 8.

The data of Table 16 are shown graphically in Figure 12. In the upper part of the figure the dots represent A_{obs} , the line is computed with the parameters of Table 17. In the lower part the residuals of the phase shift $\Delta\chi_{obs}$ minus $\Delta\chi_{comp}$ are shown. The agreement with the corresponding values for AI Velorum, in Figure 8, is remarkable.

As in AI Velorum the reduced $m(\chi)$ -curves show deviations from the sine-curves in which waves twice as short as a cycle of χ are present. However, these waves, having an amplitude of only some thousandths of a magnitude, are too weak to deserve consideration. Likewise the slow swinging up and down of the curves themselves during the beat period as shown by \bar{u} is smaller and reaches only five thousandths of a magnitude.

In the case of SX Phoenicis we are therefore also led to the conclusion that the mean light-curve can be represented with high accuracy as a distortion of the sum of two pure sine-curves.

The presence of short-period waves in SX Phoenicis has not been investigated. If present, they must be very weak.

Part III. RR LYRAE

In *B.A.N.* No 434 we have remarked that in the light-curve of RR Lyrae an M-distortion is present which is similar to that of AI Velorum. This strongly suggests that the M-distortion is a general property of Cepheids. It seemed worth while to investigate this in

detail. For this purpose we have used the light-curves published by the author in 1949¹⁾.

A complicating circumstance in the case of RR Lyrae is the presence of two secondary periods. Besides the well-known beat period of 72 cycles there exists another of 217 cycles, the influence of which is quite perceptible. The number of observations, however, is not adequate to study the latter beat phenomenon separately. We have therefore used the light-curves obtained by smoothing out the effects of this third period, such as given in Table 8 and Figure 8 of *B.A.N.* No 403¹⁾.

Because of the arbitrariness in the process of smoothing, these curves are less reliable than the original light-curves, but they have the advantage of giving a systematic and complete picture of the variations in the light-curve during the 72-cycle period. Another problem was presented by the humps on the light-curves, especially the secondary maximum observed around minimum. These humps do not participate in the general S-M-distortion, for, if the inverse S-M-transformation is applied to the light-curves the descending part of the curve, between the secondary maximum and the minimum, assumes an impossible slope; this becomes infinite, or, even worse, sometimes gives a multiple-valued function of the time. In order to find the correct S-M-transformation we must therefore first remove the humps. But, since in RR Lyrae the humps do not shift, as in the case of AI Velorum, but maintain a more or less fixed position in the light-curve, they cannot easily be smoothed out.

In the first attempt to estimate the shapes of the clean light-curves it was assumed that the hump in the minimum consisted of one full wave only, a maximum followed by a minimum. It appeared however that the curves obtained by reducing the smoothed light-curves with the determined S-M-distortion, as described in full detail for AI Velorum, showed on the descending branch ugly humps with a very steeply descending slope. To remove these it appeared to be necessary to consider the weak flexure on the descending branch of the light-curves as another wave, preceding that in the minimum and which had to be smoothed out also.

In the same way, in a further stage of the discussion, near the maximum of the light-curves a third wave presented itself. It seems highly probable, therefore, that the hump in the minimum and the occasionally visible hump on the ascending branch are only the best perceptible waves of a complete wave-train which is superposed on the smooth light-curve.

The clean light-curves were inserted in the ten mean light-curves of Table 8, *B.A.N.* No 403, by estimate, cutting off the waves on the middle of the

¹⁾ *B.A.N.* 11, 17, 1949.

descending branches, in the minima and on the ascending branch, if present; the maxima and the upper parts of the descending branches were followed exactly, as we were then unaware of the humps which appeared later.

From the estimated curves the S- and M-distortions were determined in the same way as described for AI Velorum and SX Phoenicis. Some details of the procedure should be mentioned.

The light-curves in Table 8 of the paper on RR Lyrae are given in terms of a reduced phase φ_1 , which is the normal phase of the fundamental period from which the phase deviation caused by the beat periods had been subtracted. This had been done in order not to smooth out the flexure on the ascending branch. For the present analysis, however, the curves must be brought in their original position, which was done by correcting the reduced phase φ_1 by an amount

$0.0183 \sin \frac{2\pi}{P_k} (t - 32.38)$, which is the phase shift connected with the beat period P_k of 72.37 cycles (see *B.A.N.* No 403, page 23).

Since, in the case of RR Lyrae, the two periods P_0 and P_1 have very nearly the same length, the phase $\chi = \frac{1}{2}(\varphi_0 + \varphi_1)$ can be replaced by the phase φ_0 itself, which has in fact already been done in Table 8.

The symbol χ of the present article should not be identified with that in the paper on RR Lyrae, where it denotes the phase of the second beat period; the symbol ψ is used for the same purpose in both cases.

As preliminary parameters we chose $b/\bar{a} = 1/8$ and the zero point at $\psi = 0.4$.

The resulting M-distortion curve is shown in Figure 6, the S-distortion curve in Figure 7. In both graphs considerable looping is present, which could not be removed by choosing other values of the parameters.

TABLE 18

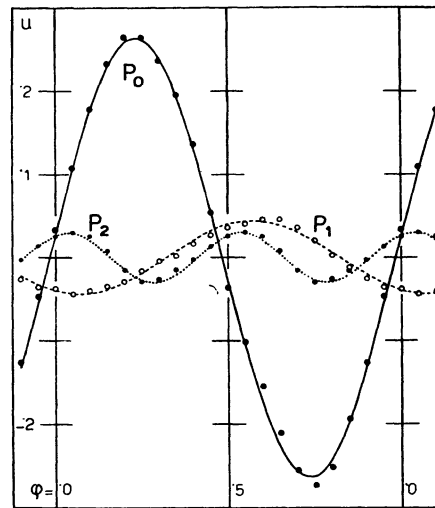
u	Δm	u	Δm
+0.28	-0.834	0.00	-0.056
+0.24	-0.594	-0.04	-0.021
+0.20	-0.435	-0.08	+0.010
+0.16	-0.316	-0.12	+0.038
+0.12	-0.227	-0.16	+0.063
+0.08	-0.157	-0.20	+0.087
+0.04	-0.100	-0.24	+0.110
0.00	-0.056	-0.28	+0.133

The M-distortion curve adopted is given in Table 18, and is shown as a dashed curve in Figure 6.

The S-distortion was represented by a straight line, with $\frac{d\varphi}{du} = -0.51$ cycle/mag.

By means of these functions the smoothed light-curves were transformed into curves which should resemble sine-curves.

FIGURE 13



The pulsations of RR Lyrae. P_0 is the principal pulsation. The waves P_1 and P_2 shift gradually to the left in the successive light-curves, P_1 about twice as fast as P_2 . After 72 cycles the relative positions of the three waves are the same again.

The mean of all ten transformed curves is given in Table 19 as P_0 , and is shown graphically in Figure 13. This represents the fundamental oscillation of RR Lyrae in undistorted state.

That it resembles fairly well a sine-curve does not mean much in this case; we only find again what we put into it. The beautiful check possible for AI Velorum and SX Phoenicis is lacking, because the amplitude of the light-curves varies not much. Only the fact that the S- and M-distortion curves are similar to those of the other stars suggests that there is sense in the transformation into a sine-curve.

More interesting are the residuals which are found by subtracting from each reduced light-curve the mean curve P_0 . These values are plotted as circles in Figure 14. They represent the wave which causes the periodic changes in shape and phase of the light-curve of RR Lyrae. The residuals reveal that besides the known oscillation P_1 with a period slightly shorter than that of the main oscillation, a strong wave is present with half the principal period. The latter will be called P_2 . The two waves are coupled, and both shift forward one full wave length relative to the main pulsation during the beat period.

By shifting each residual curve to the right by an amount ψ we bring the wave P_1 of all curves in the same position. By averaging P_2 is cancelled out, and the shape of P_1 is found. Similarly, P_2 can be isolated by shifting each residual curve by an amount $\frac{1}{2}\psi$. The results are given in Table 19 and plotted in Figure 13.

One more wave is included in the residual curves, manifesting itself in a periodic displacement of the

entire curve up and down during the 72-cycle period. This wave we denote by P_s .

All four waves can be well represented by sine-curves. These sine-curves, except P_s , are shown in Figure 13, and the numerical values are given in Table 19.

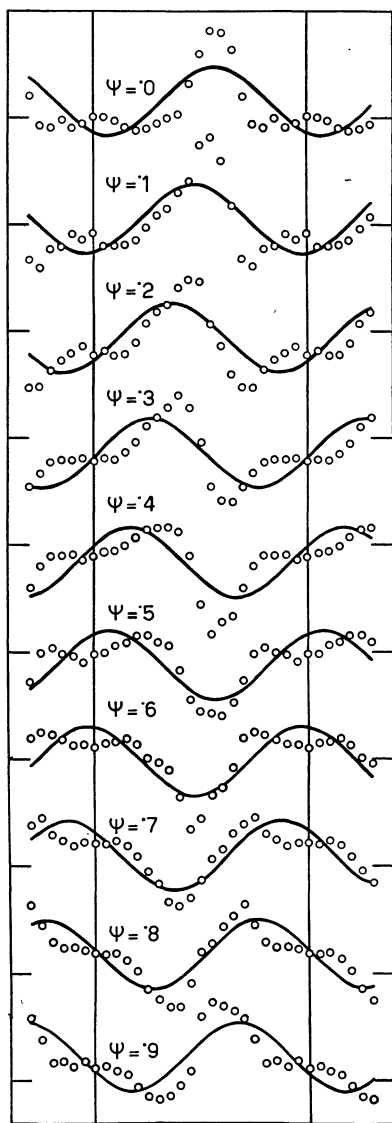
In order to show more clearly the wave P_2 the oscillations P_1 and P_s were inserted as regular sine waves in Figure 14. The whole picture is so regular

that there remains little doubt about the reality of the wave P_2 . At the same time this regularity indicates that for RR Lyrae as well as for AI Velorum and SX Phoenicis the inverse S-M-transformation leads to beautifully harmonic curves which probably represent the basic pulsations of the star.

We can summarize the results by the following formula

$$\Delta m = M. \left[S. \left\{ 0^m.264 \sin(2\pi\phi + 6^\circ) + 0^m.0429 \sin(2\pi\phi + 2\pi\psi - 116^\circ) + 0^m.0294 \sin(4\pi\phi + 2\pi\psi + 64^\circ) + 0^m.024 \sin(2\pi\psi + 132^\circ) \right\} \right]. \quad (13)$$

FIGURE 14



The circles show the deviations of the individual reduced light-curves from the mean curve. The full-drawn line represents the pulsation P_1 , which is inserted to show more clearly the effect of P_2 .

Here the four sine terms correspond to the four waves P_0 , P_1 , P_2 and P_s ; M and S refer to the distortions.

The light-curves computed by formula (13) are shown in Figure 15. The circles are reproduced from Table 8, *B.A.N.* No 403, and represent the observed light-curves.

The difference between the observed and the computed light-curves represents a wave of which sometimes three and sometimes four cycles are visible in one primary cycle. In several respects this wave bears a resemblance to the $P_2 + P_3$ wave in AI Velorum. As has been explained before the wave is not included in the M-distortion.

The influence of S-distortion which perhaps is present in the $P_2 + P_3$ wave in AI Velorum is unmistakably present in RR Lyrae. Especially in the minima of the light-curves we can see how the wave slides forward and backward in synchronism with the variation in magnitude of the mean light-curve.

The behaviour of the hump on the ascending branch of several of the light-curves might likewise be explained as an effect of S-distortion. Originally, the ascending branch contained one full cycle of the wave, which after distortion is compressed together with the ascending branch and eventually becomes completely invisible. Figure 15 shows clearly how the visibility of a wave on the ascending branch depends on the steepness. If this interpretation is correct it means that in RR Lyrae an oscillation is present which has a period of exactly one quarter of the fundamental period. It may be possible that this is some high mode of radial pulsation which by close commensurability is excited into resonance.

Finally we can make for RR Lyrae a comparison between light-curves and radial-velocity curve.

Observations of radial velocity were made, practically simultaneously with the photometric observations, by STRUVE and BLAAUW¹⁾ and independently by SANFORD²⁾. GRATTON³⁾ has found that the radial-velocity curves of AI Velorum correspond closely in

¹⁾ O. STRUVE and A. BLAAUW, *Ap. J.* **108**, 60, 1948.

²⁾ R. F. SANFORD, *Ap. J.* **109**, 208, 1949.

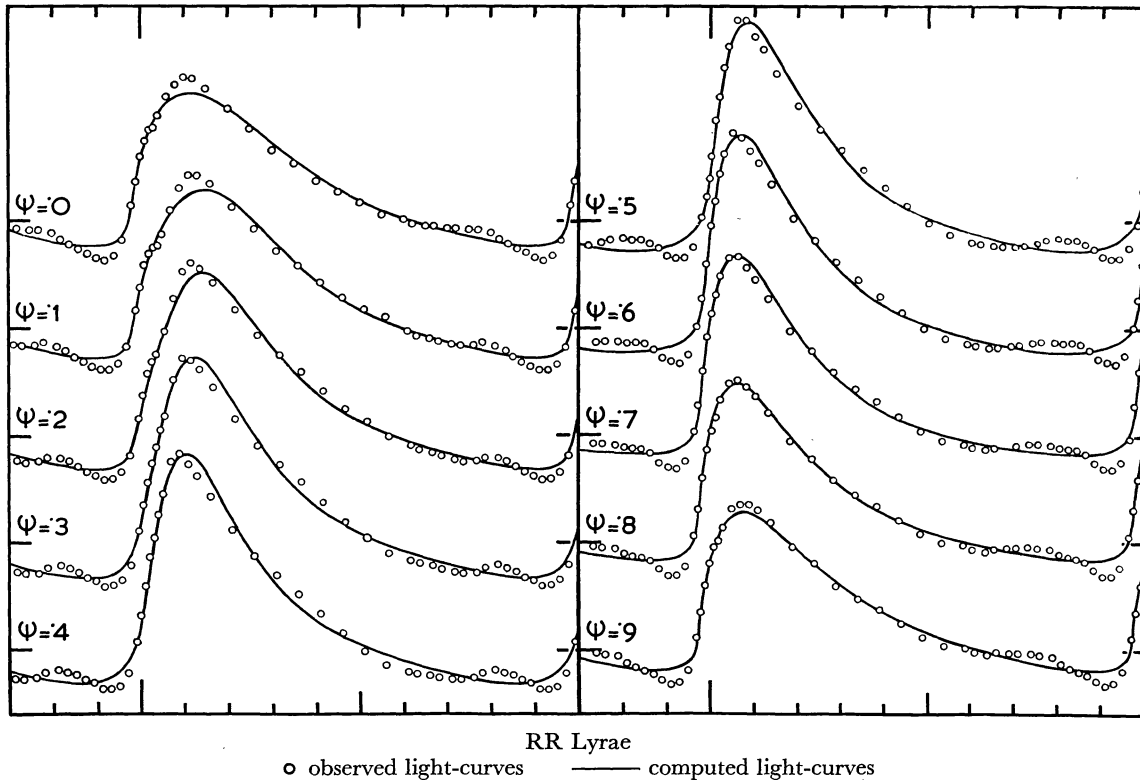
³⁾ L. GRATTON, *B.A.N.* No 444, 1953.

TABLE 19

φ	P_0 obs.	P_0 sine	P_1 obs.	P_1 sine	P_2 obs.	P_2 sine	ψ	P_s obs.	P_s sine
.00	+.033	+.027	-.035	-.039	+.025	+.026	.0	+.018	+.018
.05	+.110	+.107	-.041	-.043	+.030	+.029	.1	+.006	+.005
.10	+.179	+.176	-.038	-.042	+.025	+.020	.2	-.012	-.010
.15	+.234	+.229	-.033	-.038	+.008	+.004	.3	-.021	-.021
.20	+.266	+.258	-.027	-.030	-.015	-.014	.4	-.024	-.024
.25	+.266	+.263	-.014	-.019	-.029	-.026	.5	-.019	-.018
.30	+.238	+.241	-.003	-.006	-.026	-.029	.6	-.005	-.005
.35	+.196	+.196	+.004	+.008	-.015	-.020	.7	+.011	+.010
.40	+.136	+.132	+.018	+.020	-.003	-.004	.8	+.019	+.021
.45	+.054	+.055	+.029	+.031	+.013	+.014	.9	+.027	+.024
.50	-.038	-.027	+.038	+.039					
.55	-.102	-.107	+.042	+.043					
.60	-.155	-.176	+.047	+.042					
.65	-.211	-.229	+.047	+.038					
.70	-.257	-.258	+.037	+.030					
.75	-.274	-.263	+.021	+.019					
.80	-.253	-.241	+.004	+.006					
.85	-.195	-.196	-.010	-.008					
.90	-.127	-.132	-.024	-.020					
.95	-.048	-.055	-.034	-.031					

The values in the table are expressed in magnitudes. The waves P_1 and P_2 are given for the moment $\psi = 0$.

FIGURE 15



phase and amplitude to the curve obtained by adding two sine-curves P_0 and P_1 and subjecting the result to S-distortion but not to M-distortion. We make the same comparison for RR Lyrae. STRUVE and BLAAUW

observed the star during a complete secondary period and they divided the observations into six successive groups. For the phases ψ corresponding approximately to these groups we computed curves according to formula (13) but without applying the M-transformation.

By multiplying the magnitude scale by a factor 110 km/sec. magn. our curves were made comparable with the radial-velocity curves. They are shown in Figure 16, together with the velocity curves of the metal lines, reproduced from STRUVE and BLAAUW's paper.

There is a striking similarity between the two sets of curves, and it is clear that, as in AI Velorum, the M-distortion produces the difference in appearance between radial-velocity and light-curves. In fact there is only one small difference to be seen, the radial-velocity curves are systematically weakly curved as compared with the light-curves without M-distortion. Apart from this effect the agreement is remarkable. The fact that our curves show a greater variation in amplitude than STRUVE and BLAAUW's curves can be satisfactorily explained. Our curves show the effect of the 72-cycle beat period alone, whereas the observations of STRUVE and BLAAUW cover a cycle where the 72-cycle variation was opposed by the other beat effect (see Figure 2 in *B.A.N.* No 403). As a matter of fact SANFORD's radial-velocity curves, which happened to fall in cycles where the two secondary periods reinforced each other, show a greater difference in amplitude than our curves (Figure 1 E in SANFORD's paper).

Also the variations in shape are similar in both sets of curves. For example, group IV and phase $\psi = .8$ show both the most upward curved ascending parts.

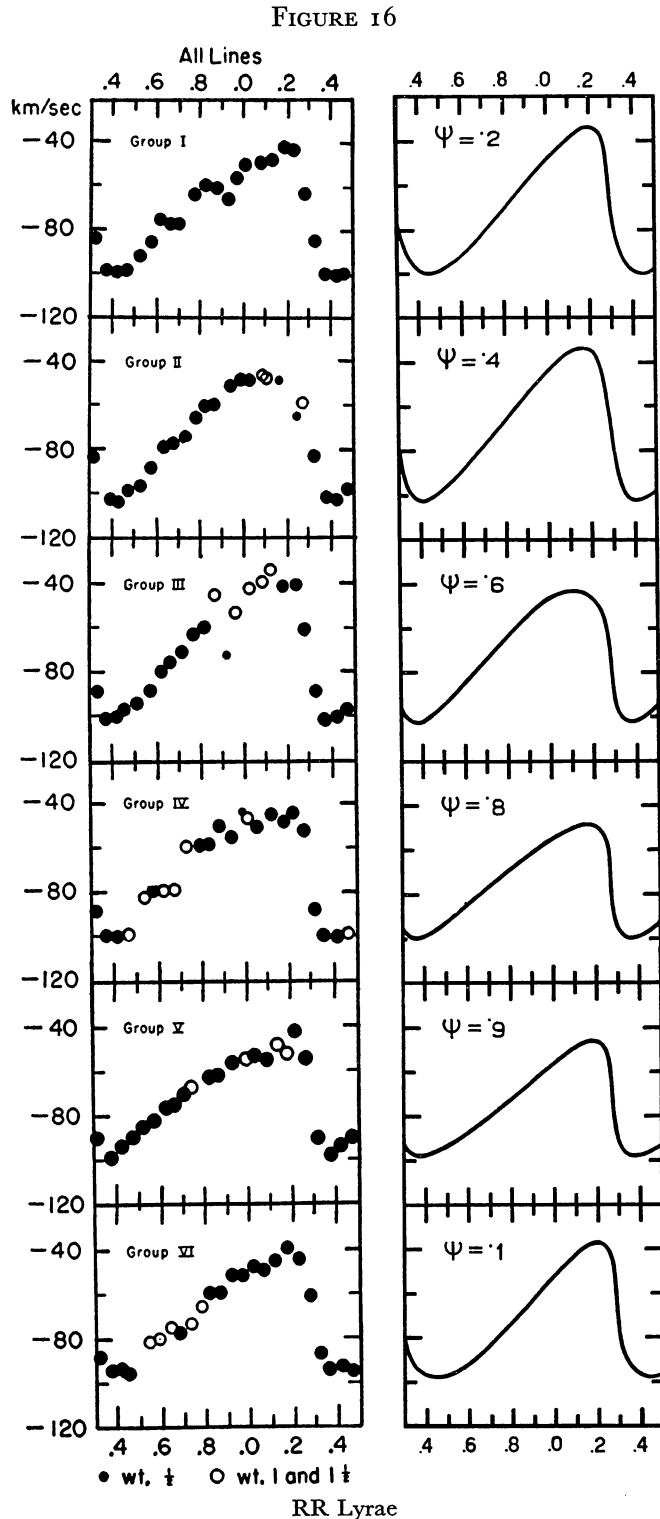
The strong difference in slope between the descending branches for $\psi = .4$ and $\psi = .9$ can be seen also in groups II and V. This effect may be observed more clearly in Figure 6 of STRUVE and BLAAUW's paper. It is also shown in SANFORD's curves.

It is interesting that the short wave which causes the hump in the minima of the light-curves seems to be absent in the velocity curves. The accuracy of STRUVE and BLAAUW's radial velocities is so great that one might expect the wave to be perceptible.

Finally it may be remarked that the fact that in the computed curves of Figure 16 the maximum varies more than three times as much in height as the minimum, is perhaps connected with STRUVE and BLAAUW's observation of a similar effect in the spectral type (Figure 8 of their paper).

Part IV. RECAPITULATION AND INTERPRETATION OF RESULTS.

In the foregoing discussions it appeared that the transformations required to reduce the light-curves



to simple harmonic curves have the same character for AI Velorum, SX Phoenicis and RR Lyrae. Furthermore, it appeared that the close relation between radial-velocity and light-curve found for AI Velorum exists also for RR Lyrae. The transformations are single-valued functions of the magnitude except for a small systematic displacement in phase of strong light-variations with respect to weak variations.

In AI Velorum two cases, and in RR Lyrae one case of coupling between waves have been found. Both in AI Velorum and RR Lyrae the short waves in the light-curves are not subject to M-distortion. These waves seem to be unobservable or absent in the radial-velocity curves.

We shall now consider some details of the phenomena.

The M-distortion curve is not exactly the same for different stars and it may vary even for one star, as was found for AI Velorum. The M-distortion curves which have been determined differ from each other mainly by their curvature, or, in other words, the increase in brightness of the maxima of the light-curves is affected in the same sense as the increase of brightness of the minima. Also the S-distortion curve may vary somewhat in shape from one case to the other. As can be seen in Figure 7 the S-distortion is not strictly proportional to u but increases more rapidly for the high maxima. This bending of the upper part of the S-distortion curve seems to increase with the curvature in the M-distortion. The behaviour of the lower part of the S-distortion curve is very uncertainly determined.

In *B.A.N.* No 434 we suggested that the steepening or skewness of the curves introduced by the S-distortion might be interpreted as the gradual change in wave shape shown by a running wave of appreciable amplitude. Depending on the amplitude of the pulsation this steepening might eventually produce a shock front responsible for the strong increase of brightness of the maxima, observed in the light-curves as M-distortion.

The new observations and their discussion provide us with a more accurate picture of the distortions, which however is not essentially different from the results given in the previous paper on AI Velorum. Some details of the new results should be considered as they may perhaps throw some light on the problem.

The most striking result is the regularity of the wave shapes and the accuracy with which they can be predicted from a simple model of two harmonic components. Neither in the shape nor in the amplitude of the light-curves a discontinuity or irregularity can be observed. This property of the light-curves seems to be contradictory to the idea of shock waves being generated from continuous waves when they reach a certain amplitude.

On the other hand it seems hardly possible to find another cause than something in the nature of shock waves which can explain the sharp rise of the maxima of the light-curves.

Perhaps the most important new result is the systematic deviation in phase of the light-curves as compared to the curves of the two-sine model. This effect is small, it had been detected already in the discussion in *B.A.N.* No 434, but then its reality was doubted. By now it is definitely established by the strict agreement between the three seasons of AI Velorum and by its presence in SX Phoenicis. The effect deserves careful consideration as it is the only significant deviation of the light-curves from the distorted two-sine model curves. We have not yet studied in detail the properties of the effect but some remarks can be made about it.

As can be seen in Figures 8 and 12 the deviation in phase of the mean light-curves shows a definite systematic variation with ψ . Roughly speaking the light-curves with big amplitude, near $\psi = 0$, arrive too early or otherwise, the light-curves with small amplitude, near $\psi = 0.5$, arrive too late. It is not known which is the right interpretation. In the second case the deviations, expressed in magnitudes, of the light-curves from the two-sine model are small, in the first case they become quite appreciable.

Let us suppose, as being more natural, that the low light-curves, which are the least distorted in shape, also are the least affected by phase shift. Then an interesting remark can be made. A phase shift of about two hundredths of a cycle of the high light-curves corresponds to an increase of brightness on the ascending branch which is of the order of a tenth of a magnitude and this amount is intermediary between the rise of the minimum and of the maximum of the light-curve which are introduced by the M-distortion. It may well be, therefore, that the phase shift is related to and merely an other aspect of the phenomenon of M-distortion. In that case the M-distortion consists of the addition of an excess of light which varies continuously over the light-curve and is small in the minimum, increases on the ascending branch, reaches a maximum somewhere on the upper part of the ascending branch and decreases again. Near the middle of the descending branch of the light-curve the excess is slightly negative.

This variation of light-excess resembles the reversed displacement curve and it suggests therefore the presence of density variations due to an increase of amplitude and of skewness of the wave while it is propagated outward.

It would be interesting to see whether the phase displacement exhibits itself in the radial-velocity curves. Unfortunately, the observations of GRATTON are not sufficiently numerous and accurate to be used for this test.

In the light-curves of RR Lyrae the effect has not been noted. It is probably small in this case, because there is not much difference in amplitude between the high and the low curves. However, the radial-velocity curves of STRUVE and BLAAUW come systematically later than the light-curves by about a hundredth of a cycle.

Finally it might be remarked that SCHWARZSCHILD's study¹⁾ of the light-curve of δ Cephei reveals an effect of the same type.

Although at the moment the observations do not permit a more definite conclusion it seems possible that the effect observed as phase deviation, when better investigated may give important information about the mechanism of the pulsations. It is clear that strictly simultaneous observations of light-curves and radial-velocity curves of RR Lyrae stars and cepheids are very important.

An interesting phenomenon in AI Velorum is the gradual change in the ratio of the amplitudes a and b of the principal pulsations. For 1951 we found for the blue light-curves the value $b/a = 0.763$, whereas in *B.A.N.* No 434 a practically identical value, $b/a = 0.748$, was shown by the yellow curves. The ratio decreased rapidly to 0.621 in 1952, and more slowly to 0.578 in 1953. From the radial-velocity curves of January 1950 GRATTON derived $b/a = 0.76$. Finally, the photographic observations of 1934-'36 indicate that at that time the behaviour of AI Velorum was not very different from what it is now. It may well be, therefore, that the variation in b/a is of a cyclical nature, with a period of some years.

It may be noted that the amplitude of P_2 and that of its coupling oscillation P'_1 have decreased in the same sense as b/a during our observations.

The coupling between the oscillations P_2 and P_3 such that the beat period is equal to P_0 , is one of the most interesting phenomena in AI Velorum. The most probable explanation is that one of the two is the original wave, which is periodically distorted by the fundamental oscillation. It is extremely curious that, whereas in all phenomena such as light-curve, distortions, radial velocity, colour, spectrum, it is always the same combination of the oscillations P_0 and P_1 which is observed, the P_2, P_3 coupling depends only on P_0 . The oscillation P_1 has its own effect on P_2 , as shown by the wave P'_1 . The coupling observed in RR Lyrae seems to be of the same nature. Here the phase of the fundamental period at which the distorted wave shows the biggest amplitude is 0.6, instead of 0.8 as found in AI Velorum, which is not a serious discrepancy.

The question arises why, if the coupling is such a common phenomenon, no such coupling is observed

between the strongest oscillations P_0 and P_1 in AI Velorum and SX Phoenicis.

Other problems are the following. The coupling of P_2 with P_1 in AI Velorum suggests that P_2 is the original oscillation, and P_3 is generated by the action of P_0 on P_2 . But why is the generated frequency in this case equal to the sum of the frequencies of the interacting oscillations, whereas in the other cases it is the difference?

An answer to these questions may perhaps be found in a generalization of WOLTJER's¹⁾ hypothesis that the beat phenomenon observed in RR Lyrae stars is due to a coupling between the pulsations of the fundamental mode and a higher mode. According to this theory the interaction may give rise to a new oscillation of which the frequency is the difference of the frequencies of the interacting modes. When the higher mode has a frequency of nearly twice the frequency of the fundamental mode the excited oscillation may reach an appreciable amplitude by resonance, and its frequency is nearly equal to that of the fundamental pulsation, so that a slow beat phenomenon takes place. At the time when WOLTJER suggested this hypothesis the higher mode of about twice the fundamental frequency had not been observed. The results of our discussion in part III of the present paper show that the higher mode and the excited oscillation are indeed observable in both light-curve and radial-velocity curve; they are the waves P_2 and P_1 . It is found that the amplitude of the excited oscillation P_1 is greater than that of the exciting oscillation P_2 . These results undoubtedly support the coupling hypothesis.

It seems very doubtful whether the same idea can be applied to AI Velorum and SX Phoenicis, since there is no commensurability and therefore, no resonance. Moreover, no trace has been detected of the exciting mode, although we have looked carefully for it. But, on the other hand we do not see a satisfactory alternative explanation. The difficulty of interpreting the observed secondary pulsation P_1 itself as a higher mode, for example as the first overtone, has already been discussed by ROSSELAND²⁾ for δ Scuti. The observed ratio of the periods P_1/P_0 is about 0.812 according to FATH³⁾, and is higher than any of the values computed by SCHWARZSCHILD for the standard model. ROSSELAND therefore concluded that "if the periods are really correctly determined as they stand, they are difficult to interpret, and the constitution of the star had to differ markedly from conventional models". The same conclusion holds for AI Velorum, SX Phoenicis and VZ Cancri⁴⁾, as follows from Table

¹⁾ *M.N.* **95**, 260, 1935; cf. also H. A. KLUYVER, *B.A.N.* **7**, 313, 1936.

²⁾ S. ROSSELAND, "The Pulsation Theory of Variable Stars", p. 47.

³⁾ FATH, *Lick Obs. Bull.* No 501, 1940.

⁴⁾ L. DETRE, *I.A.U. Circular* No 1442, 1954.

¹⁾ M. SCHWARZSCHILD, *Harvard Circular* No 431, 1938.

20, where the ratios of observed periods are given.

The possibility of other models has been considered by Dr LEDOUX¹⁾, who pointed out that P_1/P_0 for stellar models with high mass concentration, such as those studied by EPSTEIN²⁾, is close to the values observed for AI Velorum and SX Phoenicis. However, it would

TABLE 20

star	P_0	P_1/P_0
	d	
SX Phoenicis	0.055	0.778
AI Velorum	0.112	0.773
VZ Cancri	0.178	0.801
δ Scuti	0.194	0.812
RR Lyrae stars	0.5	0.98

seem difficult to extend this explanation to VZ Cancri and δ Scuti. We will therefore consider the possibility that the coupling hypothesis holds also for AI Velorum, and investigate whether reasonable periods are found in that case. We must suppose then that the observed pulsation P_1 is excited by a higher mode of which the frequency is the sum of the frequencies of P_0 and P_1 . Assuming that the same type of coupling exists between all modes we arrive at the following scheme.

TABLE 21

fund. mode	1.00000 (P_0)	} 1.29425 (P_1) } } 1.21856 (P_1') }	} 2.51281 (P_2) }
1st overtone	2.29425 ?		
2d overtone	3.51281 (P_3)		

The numbers in the table are frequencies expressed in that of P_0 as unit. In this scheme we have considered P_3 as an original pulsation and P_2 as an excited wave.

A similar scheme can be set up for RR Lyrae:

TABLE 22

fund. mode	1.00000 (P_0)	} 1.01382 (P_1) } } 1.00921 }	} (2.02303) }
1st overtone	2.01382 (P_2)		
2d overtone	(3.02303)		

In this scheme the wave P_1 is excited by coupling of P_2 with P_0 . It produces with P_0 the well-known beat period of 72 cycles. The observed beat phenomenon of 217 cycles, assumed in the table to correspond to the effect of a wave frequency 1.00921, has been interpreted tentatively as the coupling effect between the first and second overtones. The frequency of the second overtone and of its coupling terms with P_0 have been put in parentheses. More continuous and com-

plete photometric observations are needed to check the presence of these waves in the light-curves.

The schemes in Tables 21 and 22 place all the well-observed oscillations in the two stars in a logical order of frequency and strength. The observed waves not indicated in the schemes are also the most doubtful in the observations.

We have compared the frequencies in Tables 21 and 22 with the ratios of periods computed by SCHWARZSCHILD for the standard model³⁾. These computations were performed for discrete values of the ratio of specific heats, γ , and give P_i/P_0 for $i = 1, 2, 3$ and 4. We found that the interpolation formula

$$(P_i/P_0)^2 = p_i + q_i/\alpha, \quad (14)$$

where $\alpha = 3 - 4/\gamma$, gave a satisfactory representation of the computed ratios. The values of the parameters p_i and q_i obtained are given in Table 23.

TABLE 23

i	p_i	q_i
1	0.9795	0.4557
2	1.3522	0.9672
3	1.8310	1.6241
4	2.4311	2.4274

Table 24 shows the values of γ computed from (14) with the data of Tables 21, 22 and 23.

TABLE 24

	AI Vel	RR Lyrae
1st overtone	$\gamma = 1.382$	$\gamma = 1.403$
2d overtone	1.374	1.391

The values of γ for different modes deviate considerably from each other, but the agreement can be very much improved by a systematic change in the values of the parameters, for example by interpolating in Table 23. This suggests the possibility that by choosing other star models the theoretical frequencies can be brought into agreement with the observed ones.

An argument in favour of this idea may perhaps be found in the following. It was found by BALAZS and DETRE⁴⁾ that in several other stars besides RR Lyrae the beat phenomenon is accompanied by a three times longer period. These stars are RW Cancri, RW Draconis and RZ Lyrae. MULLER⁵⁾ observed the same ratio in XZ Cygni. In scheme 22 we interpreted the phenomenon as an interference of the coupling waves of the first and second overtones.

In order to make the 1 : 3 ratio in the beat phenomena a general property of RR Lyrae stars a certain change in frequency of the first overtone, expressed in P_0 as unit, must be accompanied by a change in

¹⁾ Private communication.

²⁾ I. EPSTEIN, *Ap. J.* **112**, 6, 1950.

³⁾ M. SCHWARZSCHILD, *Ap. J.* **94**, 245, 1941.

⁴⁾ J. BALAZS and L. DETRE, *Mitt. Budapest* No 27, 1952.

⁵⁾ A. B. MULLER, *B.A.N.* **12**, 11, 1953.

frequency of the second overtone which is $5/3$ times larger. This condition is exactly fulfilled by the parameters p_i and q_i which are needed to bring the γ -values of Table 24 for different modes into agreement.

We are well aware that the hypothesis discussed in the foregoing is highly speculative. The complete absence of the oscillation which should represent the first overtone in AI Velorum and SX Phoenicis, as well as the low values of γ are difficult to explain. The regularity in the values of γ in Table 24 may be accidental.

The mechanism responsible for the coupling is not known. We cannot present WOLTJER's theory as a support, because the condition of resonance is not fulfilled in AI Velorum. The only justification for its discussion in this paper is that so far there is no alternative explanation. Without this hypothesis every observed oscillation in AI Velorum becomes a problem of its own. No regularity can then be found in the arrangement of frequencies, in the properties of the coupling, nor in the comparison with RR Lyrae.

Finally, a remark may be made about EGGEN's discovery that SX Phoenicis has a low luminosity ($M = +4$). This is definitely established by the trigonometric parallax, an exceptionally large proper motion and KUIPER's classification of the star as a subdwarf.

The question arises whether AI Velorum and VZ Cancri¹⁾, which photometrically show such striking resemblance to SX Phoenicis, might likewise be subdwarfs. As regards AI Velorum this seems unlikely because it has a small proper motion ($0''.034$ per

¹⁾ L. DETRE, private communication to Prof. OORT.

annum). Those that are subdwarfs may belong to an important new group of pulsating stars of which only one or two bright members have been discovered. It seems possible that such a group has hitherto escaped attention because the chances of discovery are small, due to the short period and the character of the light-curve.

I am much obliged to Dr P. LEDOUX for the many valuable discussions we had during his stay at the Leiden Observatory.

Also I wish to express my appreciation to my wife and to Miss N. SPLINTER for their assistance in the reductions.

Part V. TABLES OF OBSERVATIONS

The following tables contain the magnitudes read off the recordings of the light-curves. The readings were made at predetermined places corresponding to round values of the phase φ_0 of the primary period.

The curves of AI Velorum were read at forty points per primary cycle, those of SX Phoenicis at twenty points per cycle.

For AI Velorum the relation between heliocentric Julian Day and φ_0 is

$$J.D. \text{ h.c.} = 2433617.65005 + \varphi_0 \times 0^d.11157375.$$

For SX Phoenicis the relation is

$$J.D. \text{ h.c.} = 2434200.0389 + \varphi_0 \times 0^d.0549642.$$

The magnitudes are given as $-\Delta m$, i.e. the difference between a fixed median magnitude and the observed magnitude.

Uncertain readings, due to clouds, are marked by a colon.

Table of observations. AI Velorum 1952

φ_0	$-\Delta m$	φ_0	$-\Delta m$	φ_0	$-\Delta m$	φ_0	$-\Delta m$	φ_0	$-\Delta m$	φ_0	$-\Delta m$	φ_0	$-\Delta m$
3950.80	—		—0.032	.95	—0.039		—0.088	.60	—0.092		—0.024	4011.60	—
	—0.033	.65	—0.056		—0.025	.80	—0.105		—0.100	.45	—0.049		+0.003
.85	—0.058		—0.076	3967.00	—0.014		—0.126	.65	—0.126		—0.075	.65	—0.021
	—0.083	.70	—		—0.007	.85	—0.146		—0.147	.50	—0.101		—0.043
.90	—0.105		—0.127	.05	+0.003		—0.161	.70	—0.169		—0.122	.70	—0.066
	—0.118	.75	—0.143		+0.014	.90	—0.173		—0.190	.55	—0.141		—0.083
.95	—0.118		—0.154	.10	+0.018		—0.186	.75	—0.206		—0.159	.75	—0.105
	—0.104	.80	—0.152		+0.027	.95	—0.195		—0.217	.60	—0.169		—0.123
3951.00	—0.072		—0.140	.15	+0.043		—0.186	.80	—0.219		—0.175	.80	—0.132
	—0.013	.85	—		+0.051	3968.00	—0.155		—	.65	—0.179		—0.146
.05	+0.054		—0.090	.20	+0.068		—0.116	.85	—0.222		—0.184	.85	—0.155
	+0.121	.90	—		+0.079	.05	—0.054		—0.200	.70	—0.177		—0.159
.10	+0.187		+0.062	.25	+0.087		+0.033	.90	—0.157		—	.90	—0.156
	+0.289	.95	+0.141		+0.097	.10	+0.145		—0.094	.75	—0.116		—0.154
.15	+0.383		+0.228	.30	+0.102		+0.282	.95	—0.07		—0.080	.95	—0.143
	+0.458	3952.00	+0.334		+0.102	.15	+0.399		+0.107	.80	—0.045		—0.119
.20	+0.495		+0.446	.35	+0.098		+0.492	3969.00	+0.209		—0.013	4012.00	—0.091
	+0.492	.05	+0.509		+0.098	.20	+0.523		+0.333	.85	+0.005		—0.046
.25	+0.474		+0.540	.40	+0.103		+0.518	.05	+0.416		+0.024	.05	+0.007
	+0.446	.10	+0.554		+0.100	.25	+0.486		—	.90	+0.038		+0.051
.30	+0.398		—	.45	+0.096		+0.427	.10	+0.462		+0.063	.10	+0.105
	+0.348		—		+0.080	.30	+0.372		+0.450	.95	+0.085		+0.160
.35	+0.303		—	.50	+0.061		+0.304	.15	+0.420		+0.099	.15	+0.236
	+0.256		—		+0.051	.35	+0.250		+0.381	3970.00	+0.113		+0.295
.40	+0.214		—	.55	+0.046		+0.186	.20	+0.334		+0.134	.20	+0.331
	+0.171	3966.75	—		+0.025	.40	+0.130		+0.282		—	.40	+0.340
.45	+0.136		—0.117	.60	—0.005		+0.088	.25	+0.244		+0.166	.25	+0.338
	+0.105	.80	—0.119		—0.032	.45	+0.037		+0.209	.10	+0.182		+0.325
.50	+0.078		—0.119	.65	—0.052		+0.011	.30	+0.167		+0.191	.30	+0.294
	+0.044	.85	—0.107		—0.062	.50	—0.003		+0.127		—	.50	+0.268
.55	+0.016		—0.086	.70	—0.071		—0.026	.35	+0.087		—	.35	+0.246
	—0.001	.90	—0.068		—0.080	.55	—0.049		+0.044		—	.55	+0.213
.60	—0.013		—0.052	.75	—0.083		—0.072	.40	+0.009		—	.40	+0.175

AI Velorum 1952

φ_0	$-\Delta m$	φ_0	$-\Delta m$	φ_0	$-\Delta m$	φ_0	$-\Delta m$	φ_0	$-\Delta m$	φ_0	$-\Delta m$	φ_0	$-\Delta m$
.45	+ .143	.90	-.063	.85	-.170:	.75	-.114	.10	—	.35	+ .230	.70	-.064:
	+ .113		-.063		—		-.138				+ .193		-.063:
	+ .082	.95	-.060	.90	-.064:	.80	-.159	.80	-.159	.40	+ .155	.75	-.097:
.50	+ .042		-.053	.90	—		-.189	.85	-.218		+ .121	.80	-.119:
	+ .009	4093.00	-.042		—		-.218		-.238	4119.10	+ .088	.80	-.129:
.55	-.022		-.022	.95	+ .153:	.90	-.247		-.242		+ .058	.85	-.127:
	-.053	.05	.000		—	.95	-.242	.15	+ .209	.50	+ .026	.85	-.127:
.60	-.072		+ .025	4102.00	—		-.224	.15	+ .184	.50	-.007	.90	-.136:
	-.104	.10	—		—	.95	-.224		+ .184		-.037	.90	-.136:
.65	-.126		—	.05	+ .315:		-.187	.20	+ .162	.55	-.065:		-.098:
	-.144	.15	+ .087		—	4111.00	-.119		+ .135		-.066:	.95	-.054:
.70	-.160		+ .105	.10	—		-.012	.25	+ .104	.60	-.128:		-.010:
	-.169	.20	+ .127		—	.05	+ .120		+ .074		-.159:	4131.00	+ .025:
.75	-.182		+ .150	.15	+ .245:		+ .254	.30	+ .053	.65	-.187:		
	-.190	.25	+ .183		—	.10	+ .400		+ .026		-.207:		
.80	-.195		+ .206	.20	+ .191		+ .506	.35	+ .001	.70	-.226:		
	-.199	.30	+ .200		+ .158:	.15	+ .559:		-.018		-.243:		
.85	-.192		+ .191	.25	+ .125		—	.40	-.032	.75	-.249:	4136.90	—
	-.178	.35	+ .175		+ .095	.20	+ .496		-.046		-.249:		-.033
.90	-.159		—	.30	+ .069		+ .436	.45	-.050	.80	-.237:	.95	-.003
	-.124	.40	+ .132		+ .036	.25	+ .373		-.054		-.216:		+ .012
.95	-.067		—	.35	+ .011		+ .316	.50	-.059	.85	-.180:	4137.00	+ .013
	+ .001	.45	+ .093		-.009	.30	+ .257		-.068		-.128:		+ .011
4013.00	+ .091		—	.40	-.025		-.022	.55	-.080	.90	-.073:	.05	+ .010
	+ .218	.50	—		-.040	.35	+ .160		-.092		+ .001:		+ .006
.05	+ .359		—	.45	-.051:		+ .120	.60	-.101	.95	+ .084:	.10	+ .006
	+ .460	.55	+ .038		-.070	.40	+ .085		-.106		+ .175:		+ .011
.10	+ .502		—	.50	-.093		+ .051	.65	-.112	4122.00	+ .291:	.15	+ .019
	+ .502	.60	—		-.114	.45	+ .023		-.112		—	.20	+ .027
.15	+ .463		-.053	.55	-.135:		.000	.70	-.112		—		+ .038
	+ .410	.65	-.080		-.148:	.50	-.020		-.109		—		+ .055
.20	+ .353		—	.60	-.149		-.040	.75	-.101		—	.25	+ .074
	+ .301	.70	-.125		-.147	.55	-.093		-.090	4129.15	+ .322:		+ .091
.25	+ .246		—	.65	-.127		-.092	.80	-.077		+ .294:	.30	+ .098
	+ .201	.75	-.155		-.102:	.60	-.126		-.066	.20	+ .250:		+ .100
.30	+ .158		-.171	.70	-.077		-.158	.85	-.059		+ .207:	.35	+ .099
	+ .116	.80	-.188		-.052	.65	-.192		-.057	.25	+ .167:		+ .098
.35	+ .080		-.195	.75	-.039		-.218	.90	-.063		+ .132:	.40	+ .102
	+ .045	.85	—		-.026:	.70	-.242		-.066	.30	+ .102:	.45	+ .105
.40	+ .016		—	.80	-.025:		-.260	.95	-.070		+ .066	.45	+ .105
	-.010	.90	—		—	.75	-.277		-.072	.35	+ .032	.50	+ .096
.45	-.036		-.155	.85	—		-.275	4120.00	-.072		+ .005:	.60	+ .076
	-.057	.95	-.123		—	.80	-.257		-.062	.40	-.016		+ .050
.50	-.073		-.065	.90	—		-.231	.05	-.050		-.038	.55	+ .021
	-.090	4094.00	+ .016		—	.85	-.172		-.030	.45	-.054		-.009
.55	-.105		+ .103	.95	+ .008:		-.105	.10	-.010		-.068	.60	-.036
	-.113	.05	+ .213		+ .020	.90	-.021		+ .020	.50	-.087		-.056
.60	-.121		+ .300	4103.00	+ .037		+ .056	.15	+ .051		-.107	.65	-.081
	-.126	.10	+ .417		+ .054	.95	+ .144		+ .076	.55	-.125:		-.090
.65	-.131		+ .474	.05	+ .067		+ .238	.20	+ .098		-.145	.70	-.095
	-.131	.15	+ .487		+ .069	4112.00	+ .324		+ .117	.60	-.156		-.092
.70	-.131		+ .467	.10	+ .069		+ .383	.25	+ .136		-.168	.75	-.090
	-.127	.20	+ .433		+ .067	.05	+ .395		+ .156	.65	-.172		-.098
.75	—		+ .378	.15	+ .061		+ .388	.30	+ .174		-.168	.80	-.113
	—	.25	+ .334		+ .057	.10	+ .373		+ .180	.70	-.156:		-.133
.80	—		+ .276	.20	+ .059		+ .342	.35	+ .168		+ .168	.85	-.157
	—	.30	+ .221		+ .069	.15	+ .308		+ .145	.75	-.116		-.180
.85	—		+ .177	.25	+ .084		+ .264	.40	+ .116		-.086	.90	-.196
	-.028	.35	+ .134		+ .104	.20	+ .219		+ .092	.80	-.062		-.207
.90	—		+ .093	.30	+ .113		+ .179	.45	+ .069		-.046	.95	-.205
	—	.40	+ .055		+ .112	.25	+ .142		+ .049	.85	-.036		-.191
	—	.45	+ .021	.35	+ .106		+ .107	.50	+ .029		-.032	4138.00	-.151
	—		—		—	.30	+ .069		+ .021	.90	-.025		-.089
	—	.50	—	.40	—		+ .036	.55	+ .001		-.018	.05	-.006
4092.15	—		—		—	.35	+ .011		-.005	.95	-.014		+ .109
	+ .170		—	.45	—		-.010	.60	-.011		-.002	.10	+ .246
.20	+ .148		—		—	.40	-.033		-.020	4130.00	+ .015		+ .380
	+ .124	.50	—		—	.45	-.051	.65	-.036		+ .033	.15	+ .483
.25	+ .100		—	.55	—		-.072		-.059	.05	+ .056		+ .522
	+ .069	4101.20	+ .493	.55	+ .069:		-.091	.70	-.084		+ .082	.20	+ .518
.30	+ .050		+ .427		—	.50	-.105		-.111	.10	+ .102		+ .488
	+ .029	.25	+ .359		—	.55	-.122	.75	-.134		+ .109	.25	+ .442
.35	+ .008		+ .285		—		-.140		-.156	.15	+ .116		+ .389
	.000	.30	+ .217		—		-.144	.80	-.180		+ .109	.30	+ .332
.40	-.005		+ .156	4110.25	+ .163	.60	-.156		-.205	.20	+ .102		+ .258
	-.013	.35	+ .108		+ .178		-.154	.85	-.224		-.224	.35	+ .195
.45	-.022		+ .069	.30	+ .186	.65	-.137		-.239	.25	+ .087		+ .143
	-.036	.40	—		+ .192		-.115	.90	-.246		+ .096	.40	+ .097
.50	-.052		—	.35	+ .186		-.068		-.240	.30	+ .105		+ .054
	-.068	.45	-.011		+ .174	.70	-.047	.95	-.227		+ .112	.45	+ .021
.55	-.085		-.032	.40	+ .156		-.044	.75	-.187	.35	+ .114		-.006
	-.095	.50	-.043		+ .131		-.050		-.116	4121.00	+ .104	.50	-.029
.60	-.102		-.051	.45	+ .105	.80	-.050		-.031	.40	+ .084		-.047
	-.102	.55	-.067		+ .077		-.047	.05	+ .071		+ .059	.55	-.035
.65	-.098		-.090	.50	+ .052	.85	-.044		+ .152	.45	+ .042		-.067
	-.090	.60	-.116		+ .042		—	.10	+ .258		+ .030	.60	-.086
.70	-.080		-.144	.55	-.001	.90	-.013:		+ .361	.50	+ .032		-.108
	-.071	.65	-.173		-.017		—	.15	+ .422		+ .029	.65	-.138
.75	-.067		-.199	.60	-.027		—		+ .447	.55	+ .029		-.169
	-.068	.70	-.219		-.033		+ .077:	.20	+ .438		+ .029	.70	-.197
.80	-.067		-.228	.65	-.036	4113.00	+ .081:		+ .401:	.60	+ .022		-.225
	-.062	.75	-.217:		-.051		+ .077:	.25	+ .362		+ .014	.75	-.250
.85	-.061		-.230:	.70	-.065		+ .073:		+ .322	.65	-.009		-.268
	-.060	.80	—		-.088		+ .077:	.30	+ .275		-.037	.80	-.279

AI Velorum 1952

φ_0	$-\Delta m$	φ_0	$-\Delta m$	φ_0	$-\Delta m$	φ_0	$-\Delta m$	φ_0	$-\Delta m$	φ_0	$-\Delta m$	φ_0	$-\Delta m$
.85	-.280	.65	-.054	.55	-.077	.50	—	.70	-.109	.80	-.081	.15	+ .193 :
	-.264		-.054		-.094		—		-.107		-.076		+ .187 :
	-.224	.70	-.054	.60	-.116		—		-.112	.15	-.080		+ .170 :
.90	-.162		-.055		-.132	.55	—	.75	-.116	.85	-.077	.20	+ .154 :
	-.083	.75	-.061	.65	-.140		—		-.115		-.076		+ .135 :
.95	+ .036		-.072		-.149	.60	—	.80	-.108	.90	-.081	.25	+ .122 :
	+ .164	.80	-.090	.70	-.146		—		-.101		-.090		+ .097 :
4139.00	+ .314		-.109		-.134	.65	—	.85	-.090	.95	-.097	.30	+ .072 :
	+ .433	.85	-.128	.75	-.115		—		-.072		-.098		+ .048 :
.05	+ .486		-.148		-.090	.70	—	.90	-.043	4209.00	-.086	.35	—
	+ .488	.90	-.165	.80	-.066		—		-.019		-.059		
.10	+ .458		-.172		-.034	.75	—	.95	+ .008		-.018		
	+ .417	.95	-.167	.85	-.004		-.197 :		+ .036	.05	-.018		
.15	+ .373		-.155		+ .026	.80	-.228	4174.00	+ .061	.10	+ .086		
	+ .319	4148.00	-.130	.90	+ .048		-.242		+ .080		+ .127	4217.65	-.182
.20	+ .268		-.083		+ .064	.85	-.242	.05	+ .087	.15	+ .181		-.177
	+ .217	.05	-.014	.95	+ .076		-.222 :		+ .087		+ .237	.70	-.166
.25	+ .167		+ .068		+ .084	.90	-.189 :	.10	+ .086	.20	+ .272		-.152
	+ .123 :	.10	+ .151	4157.00	+ .080		-.134 :		+ .082		+ .288	.75	-.131
.30	+ .083 :		+ .234		+ .075	.95	-.068 :	.15	+ .076	.25	+ .283		-.113
		.15	+ .321	.05	+ .073		+ .021 :		+ .068		+ .274	.80	-.084
			+ .395		+ .073	4166.00	+ .141	.20	+ .058	.30	+ .263		-.057
		.20	+ .432	.10	+ .086		+ .286		+ .049		+ .253	.85	-.025
4145.90	-.093 :		+ .432		+ .084	.05	+ .420	.25	+ .042	.35	+ .241		+ .003
	-.009 :	.25	+ .406	.15	+ .091		+ .507		+ .038		+ .223	.90	+ .038
.95	+ .076 :		+ .370		+ .102	.10	+ .528		+ .036	.40	+ .191		+ .070
	+ .185 :	.30	+ .322	.20	+ .108		+ .504		+ .036		+ .160	.95	+ .102
4146.00	—		+ .272		+ .111	.15	+ .464	.35	+ .040	.45	+ .127		+ .125
		.35	+ .225	.25	+ .111		+ .417		+ .034		+ .096	4218.00	+ .143
			+ .188		+ .110	.20	+ .370	.40	+ .026	.50	+ .066		+ .151
.05	+ .420 :	.40	+ .150	.30	+ .101		+ .321		+ .025		+ .037	.05	+ .152
	+ .416		+ .110		+ .099	.25	+ .266 :	.45	+ .023	.55	+ .006		+ .145
.10	+ .389		+ .077	.35	+ .097		+ .219 :		+ .018		-.019	.10	+ .138
	+ .340	.45	+ .052		+ .088	.30	+ .177 :	.50	+ .015	.60	-.046		+ .124
.15	+ .284		+ .031	.40	+ .078		+ .144 :		+ .014		-.070	.15	+ .105
	+ .228	.50	+ .009		+ .062	.35	+ .112 :	.55	+ .011	.65	-.086		+ .086
.20	+ .174		-.010	.45	+ .049		+ .087 :		+ .004		-.102	.20	+ .066
	+ .127	.55	-.035		+ .022	.40	+ .058 :	.60	-.009	.70	-.119		+ .045
.25	+ .088		-.059	.50	+ .008		+ .027 :		-.025		-.138	.25	+ .025
	+ .056	.60	-.086		+ .001	.45	-.004 :	.65	-.041	.75	-.160		+ .013
.30	+ .026	.65	-.115	.55	-.000		-.030 :		-.060		-.181	.30	+ .003
	.000		-.139		+ .006	.50	-.054 :	.70	-.078	.80	-.200		.000
.35	-.022	.70	-.162 :	.60	+ .011		-.081 :		-.090		-.213	.35	+ .001
	-.041		-.186 :		+ .017	.55	-.110 :	.75	-.090	.85	-.218		+ .001
.40	-.058		-.192 :	.65	+ .026		-.126 :		-.087		-.207	.40	-.001
	-.069	.80	-.199 :		+ .034	.60	-.140 :	.80	-.091	.90	-.187		-.003
.45	-.080		-.219 :	.70	—		-.159 :		-.099		-.141	.45	-.007
	-.086		-.211 :			.65	-.170 :	.85	-.112	.95	-.079		-.009
.50	-.089	.85	-.192 :				-.179 :		-.132		.000	.50	-.008
	-.086		-.165 :			.70	-.177 :	.90	-.152	4210.00	+ .096		-.007
.55	-.085	.90	—				-.163 :		-.168		+ .221	.55	-.004
	-.084			4164.40	+ .060	.75	-.140 :	.95	-.170		+ .366		-.001
.60	-.076				+ .060		-.097 :		-.162	4175.00	-.148	.60	.000
	-.086				+ .065	.45			-.148		+ .485		-.003
.65	-.100				+ .072				-.118	.10	+ .521	.65	-.014
	-.108			.50	+ .084			.05	-.071		+ .486		-.030
.70	-.112	4155.60	—		+ .090				-.021	.15	+ .430	.70	-.047
	-.116		-.089	.55	+ .081 :	4172.75	-.267	.10	+ .041	.20	+ .380		-.065
.75	-.116	.65	-.094		+ .060		-.264		+ .126		+ .325	.75	-.080
	-.105		-.107	.60	+ .033	.80	-.255	.15	+ .218	.25	+ .250		-.085
.80	-.094	.70	-.124		+ .006 :		-.235		+ .314		+ .194	.80	-.084
	-.077		-.141	.65	-.020	.85	-.202	.20	+ .369	.30	+ .154		-.082
.85	-.047	.75	-.161		-.045		-.159		+ .401 :		+ .120	.85	-.080
	-.022		-.180	.70	-.065	.90	-.101	.25	+ .407 :	.35	+ .080		-.083
.90	+ .001	.80	-.199		-.077		-.043		+ .393 :		+ .048	.90	-.090
	+ .024		-.202	.75	-.084	.95	+ .025	.30	+ .367 :	.40	+ .023		-.101
.95	+ .034	.85	-.193		-.090		+ .117		+ .330 :		.000	.95	-.107
	+ .039		-.172	.80	-.088	4173.00	+ .229	.35	+ .282 :	.45	-.016		-.103
4147.00	+ .033	.90	-.130		-.090		+ .349		+ .238 :		-.030	4219.00	-.094
	+ .033		-.075	.85	-.104	.05	+ .428	.40	+ .185 :	.50	-.044		-.079
.05	+ .030	.95	.000		-.117		+ .449		+ .138 :		-.064	.05	-.054
	+ .026		+ .095	.90	-.132	.10	+ .438	.45	+ .093 :	.55	-.083		-.029
.10	+ .025	4156.00	+ .239		-.148		+ .405		+ .057 :		-.108	.10	-.004
	+ .025		+ .371	.95	-.153	.15	+ .360	.50	+ .031 :	.60	-.130		+ .034
.15	+ .031		+ .461		-.152		+ .308		+ .005 :		-.151	.15	+ .080
	+ .040	.05	+ .494	4165.00	-.138	.20	+ .253	.55	-.023 :	.65	-.166		+ .134
.20	+ .047		+ .480		-.109		—		-.046 :		-.174	.20	+ .182
	+ .062	.10	+ .437		-.053	.25	—	.60	-.059 :	.70	-.174		+ .221
.25	+ .077		+ .388	.05	+ .016		—		-.070 :		-.165	.25	+ .243
	+ .087	.15	+ .336		+ .102	.30	—	.65	-.082 :	.75	-.159		+ .250
.30	+ .096	.20	+ .286		+ .196		—		-.098 :		-.147	.30	+ .249
	+ .102		+ .229	.15	+ .297	.35	—	.70	-.121 :	.80	-.132		+ .243
.35	+ .105	.25	+ .182		+ .378		—		-.147 :		-.106	.35	+ .236
	+ .102		+ .138	.20	+ .412	.40	-.041	.85	-.064		-.064		+ .211
.40	+ .094	.30	+ .104		+ .419		-.065		-.013	.40	-.013		+ .192
	+ .085		+ .073	.25	+ .403	.45	-.084		+ .036		+ .076	.45	+ .165
.45	+ .067	.35	+ .048		+ .381		-.103	4208.60	-.001	.95	+ .130 :		+ .138
	+ .051		+ .016	.30	+ .349	.50	-.119		-.009		+ .170 :	.50	+ .107
.50	+ .032	.40	-.003		+ .316		-.132		-.020		+ .196 :		+ .082
	+ .016		-.019	.35	+ .268	.55	-.140	.65	-.032	4211.00	+ .210 :	.55	+ .055
.55	.000	.45	-.034		+ .211		-.143		-.032		+ .222 :		+ .024
	-.016		-.047	.40	+ .164	.60	-.141	.70	-.050	.05	+ .222 :		-.004
.60	-.030	.50	-.058		+ .123		-.132		-.069		+ .215 :	.60	-.026
	-.046		-.064	.45	—	.65	-.119	.75	-.077	.10	+ .202 :		-.031

AI Velorum 1952

φ_0	$-\Delta m$	φ_0	$-\Delta m$	φ_0	$-\Delta m$	φ_0	$-\Delta m$	φ_0	$-\Delta m$	φ_0	$-\Delta m$	φ_0	$-\Delta m$
.65	-.056	.10	+.192		+.116	.05	+.292		+.091		-.007	4271.20	—
	-.076		+.177	.50	+.075		+.286	.50	—	.85	+.020		+.363
.70	-.094	.15	+.153		+.034	.10	+.264		+.043		+.048	.25	+.320
	-.123		+.133	.55	-.004		+.231	.55	+.018	.90	+.065		+.273
.75	-.150	.20	+.106		-.043	.15	+.194		-.017		+.072	.30	+.223
	-.173		+.081	.60	-.076		+.154	.60	-.050	.95	+.076		+.177
.80	-.192	.25	+.053		-.108	.20	+.116		-.077		+.072	.35	+.138
	-.205		+.026	.65	-.134		+.082	.65	-.094	4256.00	+.056		+.106
.85	-.221	.30	+.008		-.157	.25	+.049		-.111		+.049	.40	+.073
	-.224		-.004	.70	-.178		+.022	.70	-.131		+.051		+.036
.90	-.225	.35	-.016		-.179	.30	+.001		-.144		+.062	.45	+.012
	-.213		-.025	.75	-.182		-.009	.75	-.159	.10	+.072		-.014
.95	-.180	.40	-.023		-.185	.35	-.018		-.174		—	.50	-.040
	-.124		-.025	.80	-.187		-.022	.80	-.192		—		-.066
4220.00	-.033	.45	-.027		-.194	.40	-.025		-.203		—	.55	-.097
	+.088		-.028	.85	-.201		-.031	.85	-.210		—		-.130
.05	+.229	.50	-.028		-.202	.45	-.036		-.200	4262.35	+.039	.60	-.162
	+.386		-.035	.90	-.190		-.050	.90	-.167		+.033		-.193
.10	+.502	.55	-.041		-.161	.50	-.060		-.120	.40	+.022	.65	-.217
	+.559		-.037	.95	-.130		-.068	.95	-.036		+.005	.20	-.240
.15	+.562	.60	-.028		-.055	.55	-.073		+.048	.45	-.021	.70	-.250
	+.530		-.026	4237.00	+.034		-.066	4254.00	+.148		-.046		-.250
.20	+.486	.65	-.034		+.142	.60	-.056		+.260	.50	-.066	.75	—
	+.426		-.047	.05	+.291		-.046	.05	+.379		-.079		—
.25	+.369	.70	-.063		+.448	.65	-.046		+.469	.55	-.091	.80	—
	+.323		-.077	.10	+.544		-.053	.10	+.526		-.101		—
	—	.75	-.086		+.570	.70	-.071		+.538	.60	-.097	.85	—
	—		-.089	.15	+.547		-.087	.15	+.514		-.087		—
	—	.80	-.090		+.501	.75	-.097		+.471	.65	-.072	.90	+.054
	—		-.083	.20	+.448		-.104	.20	+.422		-.054		+.104
4226.50	—	.85	-.072		+.389	.80	-.108		—	.70	-.036	.95	+.151
	+.007		-.074	.25	+.331		-.095	.25	—		-.025		+.196
.55	-.027	.90	-.083		+.272	.85	-.071		—	.75	-.019	4272.00	+.223
	-.062		-.087	.30	+.217		-.046	.30	—		-.025		+.233
.60	-.087	.95	-.087		+.161	.90	-.021		—	.80	-.032	.05	+.239
	-.116		-.084	.35	+.110		-.002	.35	—		-.034		+.236
.65	-.144	4229.00	-.078		+.072	.95	+.007		+.077	.85	-.040	.10	+.231
	-.169		-.058	.40	+.032		+.007	.40	+.046		-.041		+.225
.70	-.192	.05	-.033		-.003	4246.00	+.008		+.017	.90	-.043	.15	+.206
	-.213		-.015	.45	-.033		+.007	.45	—		-.042		+.186
.75	-.229	.10	+.011		-.055	.05	+.012		—	.95	-.041	.20	+.156
	-.237		+.045	.50	-.079		+.018	.50	—		-.035		+.138
.80	-.241	.15	+.094		-.093	.10	+.028		—	4263.00	-.025	.25	+.108
	-.236		+.145	.55	-.101		+.041	.55	—		-.014		+.070
.85	-.222	.20	+.192		-.108	.15	+.060		—	.05	+.001	.30	+.040
	-.204		+.232	.60	-.120		+.087	.60	—		+.017		+.016
.90	-.171	.25	+.269		-.137	.20	+.118		—	.10	+.031	.35	-.003
	-.123		—	.65	-.153		+.148	.65	—		+.048		-.022
.95	-.054	.30	—		-.169	.25	+.173		—	.15	+.068	.40	-.043
	+.035		—	.70	-.182		+.182	.70	-.196		+.086		-.062
4227.00	+.136		—	.30	-.192		+.183	.30	-.193		+.121	.45	-.082
	+.283		—	.75	-.200		+.176	.75	-.180		+.156		-.101
.05	+.426		-.029	.80	-.200		+.174	.80	-.158	.25	+.182	.50	-.117
	+.511	4235.45	-.044		-.183	.35	+.175		-.134		+.195		-.130
.10	+.530		-.060	.85	-.153		+.181	.40	-.098	.30	+.192	.55	-.137
	+.510		-.071		-.131		+.176	.85	-.055		+.182		-.138
.15	+.471	.50	-.076		-.100	.45	+.164		-.007	.35	+.172	.60	-.133
	+.416		-.072	.90	-.138		+.133	.90	+.050		+.163		-.116
.20	+.361	.55	-.062		+.029	.50	+.102		+.119	.40	+.156	.65	-.097
	+.305		-.057	.95	+.130		+.066	.95	+.196		+.145		-.076
.25	+.250	.60	-.057		+.209	.55	+.036		+.288	.45	+.134	.70	-.059
	+.202		-.057	4238.00	+.282		-.001	4255.00	+.344		+.124		-.055
.30	+.161	.65	-.074		+.326	.60	-.029		+.368	.50	+.109	.75	-.065
	+.121		-.091	.05	+.340		-.054	.05	+.364		+.084		-.076
.35	+.082	.70	-.104		+.348	.65	-.076		+.342	.55	+.054	.80	-.082
	+.046		-.116	.10	+.340		-.085	.10	+.393		—		-.083
.40	+.012	.75	-.126		+.323	.70	-.090		+.262	.60	—	.85	-.082
	-.018		-.132	.15	+.307		-.083	.15	+.214		-.032		-.076
.45	-.047	.80	-.132		—	.75	-.077		+.170	.65	—	.90	-.065
	-.074		-.128	.85	—		-.090		+.127		-.086		-.050
.50	-.098	.85	-.116		—	.80	-.105		+.100	.70	—	.95	-.029
	-.122		-.104		—		-.123	.25	+.072		—		-.003
.55	-.143	.90	-.090		-.107	.85	-.144		+.047	.75	—	4273.00	+.019
	-.157		-.076	4244.50	-.127		-.162	.30	+.030		-.148		+.032
.60	—	.95	-.062		-.148	.90	-.169		+.014	.80	—	.05	+.037
	—		-.047	.55	-.169		-.162	.35	-.003		—		+.037
.65	-.184	4236.00	-.032		-.192	.60	-.192		-.013	.85	—	.10	+.032
	-.184		-.016	.60	-.214		-.097	.40	-.021		-.141		+.030
.70	-.190	.05	+.005	.65	-.228	4247.00	-.039		-.023	.90	-.134	.15	+.032
	-.191		+.037		-.235		+.048	.45	-.021		-.113		+.038
.75	-.186	.10	+.067		-.236	.05	+.156		-.025	.95	-.083	.20	—
	-.175		+.107	.70	-.228		+.293	.50	-.028		-.037		—
.80	-.156	.15	+.142		-.206	.75	-.169		-.029	4264.00	+.018	.25	—
	-.131		+.186	.75	-.199		-.126	.15	-.025		+.081		—
.85	-.103	.20	+.222		-.076	.80	-.076		-.024		+.281	.30	—
	-.072		+.243	.85	-.029	.20	+.575		-.019	.10	+.385	.35	—
.90	-.033	.25	+.241		+.013		—	.65	-.014		+.449		+.117
	+.015	.30	+.231		+.013	.90	+.058		-.020	.15	+.468	.40	+.127
.95	+.077		+.218		+.118	.70	+.175		-.026		+.450		+.129
	+.123	.35	+.206		+.175	.95	+.225	4253.40	-.034		—	.45	+.137
4228.00	+.166		+.198		+.225		+.268		-.039		—		+.141
	+.192	.40	+.189	4245.00	+.268		+.268		-.038		—	.50	+.137
.05	+.203		+.175		+.288	.45	+.288		-.025		—		+.119
	+.202	.45	+.150		—		—	.80	—		—		—

AI Velorum 1952

φ_0	$-\Delta m$	φ_0	$-\Delta m$	φ_0	$-\Delta m$	φ_0	$-\Delta m$	φ_0	$-\Delta m$	φ_0	$-\Delta m$	φ_0	$-\Delta m$
.55	+.089:		+.069		-.090				+.250		-.122		-.161
	+.054:	.90	+.114	.75	-.101			.15	+.227	.80	-.144	.65	-.182
.60	+.020:		+.160		-.105						-.159		-.195
	-.014:	.95	+.191	.80	-.101	4468.35	+.135			.85	-.182	.70	-.202
.65	-.043:		+.218		-.082		+.105				-.192		-.209
	-.068:	4415.00	+.236	.85	-.059	.40	+.059			.90	-.192	.75	-.211
.70	-.086:		+.237		-.033		+.025	4469.75	-.092:		-.184		-.209
	-.094:	.05	+.228	.90	-.014	.45	.000		-.068:	.95	-.166	.80	-.195
.75	-.101:		+.207		-.010		-.022	.80	-.041:		-.133		-.171
	-.103:	.10	+.191	.95	-.010	.50	-.047		-.014:	4478.00	-.083	.85	-.139
.80	-.105:		+.149		-.022		-.068	.85	+.004:		-.019		-.091
	-.100:	.15	+.119	4416.00	-.035	.55	-.089		+.020:	.05	+.053	.90	-.015
.85	-.098:		+.087		-.047	.60	-.111	.90	+.028:		+.129		+.066
	-.108:	.20	+.057	.05	-.050	.60	-.137			.10	+.231	.95	+.152
.90	-.115:		+.033		-.041		-.163				+.326		+.246
	-.118:	.25	+.014	.10	-.033	.65	-.189			.15	+.409	4479.00	+.324
.95	—		-.004		-.015		-.211				+.456		+.367
		.30	+.013	.15	+.012	.70	-.224	4477.35	+.215	.20	+.464	.05	+.381
			-.015		+.044		-.231		+.195		+.442		+.373
		.35	-.016	.20	+.090	.75	-.228	.40	+.173	.25	+.406	.10	+.351
			-.020		+.129		-.216		+.149		+.361		+.318
4414.55	—	.40	-.023	.25	+.163	.80	-.188	.45	+.121	.30	+.313	.15	+.292
	-.181		-.031		+.177		-.150		+.095		+.266		+.262
.60	-.209	.45	-.039	.30	+.184	.85	-.103	.50	+.069	.35	+.218	.20	+.222
	-.223		-.049		+.185		-.035		+.054		+.168		+.194:
.65	-.233	.50	-.054	.35	+.185	.90	+.036	.55	+.034	.40	+.126	.25	+.170:
	-.239		-.050		+.195		+.122		+.013		+.084		+.136:
.70	-.231	.55	-.040	.40	+.196	.95	+.203	.60	-.003	.45	+.051	.30	+.113:
	-.214		-.030		+.192		+.280		-.024		+.018		+.081:
.75	-.182	.60	-.026	.45	+.176	4469.00	+.317	.65	-.041	.50	-.014	.35	+.050:
	-.142		-.032		+.142		+.324		-.057		-.078		+.030:
.80	-.083	.65	-.044	.50	+.096		+.313	.70	-.065	.55	-.078	.40	+.011:
	-.026		-.058		+.062		+.292		-.078		-.106		-.017:
.85	+.022	.70	-.074			.10	+.272	.75	-.095	.60	-.137	.45	—

Table of observations. AI Velorum 1953

φ_0	$-\Delta m$	φ_0	$-\Delta m$	φ_0	$-\Delta m$	φ_0	$-\Delta m$	φ_0	$-\Delta m$	φ_0	$-\Delta m$	φ_0	$-\Delta m$
6460.00	—	.10	+.137		+.277		-.106	.75	-.111		+.032		-.034
	+.220		+.205	.35	+.231	.60	-.126		-.106	.35	+.010	6720.00	-.016
.05	+.321	.15	+.279		+.180		-.142	.80	-.098		-.011		+.002
	+.392		+.332	.40	+.123	.65	-.149		-.092	.40	-.027	.05	+.021
.10	+.432	.20	+.359		+.077		-.151	.85	—		-.042		+.046
	+.440			.45	+.038	.70	-.151		—	.45	-.058	.10	+.070
.15	+.422				-.001		-.156	.90	—		-.070		+.087
	+.385	.50	-.036	.50	-.036	.75	-.136		—	.50	-.083	.15	+.103
.20	+.346	6576.15	—		-.063		-.120	.95	—		—		+.114
	+.293		+.239:	.55	-.077	.80	-.095		—		—	.20	+.127
.25	+.243	.20	+.198:		-.091		-.072	6595.00	-.080		—	.20	+.143
	+.194		+.156:	.60	-.107	.85	-.053		-.035	6719.00	—	.25	+.163
.30	+.145	.25	+.120:		-.120		-.030	.05	+.022		+.315	.25	+.172
	+.102		+.086	.65	-.136	.90	-.009		+.092	.05	+.293	.30	+.171
.35	+.061	.30	+.059		-.151		+.015	.10	+.186		+.271		+.158
	+.026		+.031	.70	-.168	.95	+.036		+.284	.10	+.246	.35	+.133
.40	-.007	.35	+.005		-.184		+.053	.15	+.353		+.223		+.113
	-.034		-.020	.75	-.200	6587.00	+.067		+.399	.15	+.198	.40	+.101
.45	-.054	.40	-.037		-.214		+.083	.20	+.407		+.172		+.092
	-.080		-.048	.80	-.220	.05	+.098		+.399	.20	+.139	.45	+.080
.50	-.104	.45	-.055		-.221		+.114	.25	+.377		+.110		+.075
	-.125		-.060	.85	-.211		-.187		+.343	.25	+.090	.50	+.072
.55	-.142	.50	-.064		-.187		-.141		—		+.071		+.070
	-.157		-.068	.90	-.141		-.066	6594.10	—	.30	+.050	.55	+.064
.60	-.167	.55	-.072		-.066		+.062		-.206		+.031		+.048
	-.172		-.078	.95	+.012		+.046	6602.70	-.210	.35	+.011	.60	+.015
.65	-.172	.60	-.088		+.161	.15	+.039		-.214		-.003		-.012
	-.158		-.097	6586.00	+.325		+.037	.75	-.211	.40	-.009	.65	-.039
.70	-.132	.65	-.104		+.452	.20	+.037		-.201		-.016		-.063
	-.101		-.105	.05	+.513		+.049	.80	-.176	.45	-.024	.70	-.079
.75	-.075	.70	-.107		+.517	.25	+.064		-.144:		-.035		-.098
	-.056		-.112	.10	+.486		+.075	.85	—	.50	-.047	.75	-.119
.80	-.037	.75	-.112		+.444	.30	+.086		-.056:		-.062		-.141
	-.023:		-.107	.15	+.392		+.086	.90	+.014	.55	-.073	.80	-.158
.85	-.010:				+.338	.35	+.086		+.100		-.079		-.170
	+.011:	.20	+.285		+.226	.40	+.077	.95	+.197	.60	-.076	.85	-.175
.90	+.034:		+.226		+.179		+.075	6603.00	+.303	.65	-.071		-.175
	+.061:	6585.00	—	.25	+.134	.45	+.072		+.382		-.068	.90	-.174
.95	+.089:		+.015		+.096	.50	+.072		+.431	.70	-.067		-.131:
		.05	+.088	.30	+.063		—	.05	+.439		-.066	6721.00	-.041:
			+.177		+.029	.35	+.057	.10	+.410	.75	-.063		+.020:
6468.90	—	.10	+.367		-.003	.55	+.040		+.366		-.064	.05	+.081:
	-.137	.15	+.420	.40	-.027:		+.016	.15	+.317	.80	-.068		—
.95	-.112		+.432		-.040:	.60	-.017		+.266		-.070	.10	+.246:
	-.087	.20	+.424	.45	-.048		-.051	.20	+.213	.85	-.071		+.325:
6469.00	-.058		+.405		-.056	.65	-.075		+.164		-.070	.15	+.374:
	-.016	.25	—		-.063		-.094	.25	+.120	.90	-.066		+.391:
.05	+.032		+.349		-.073	.70	-.105		+.086		-.058	.20	+.374:
	+.085	.30	+.318	.55	-.089		—	.30	+.055	.95	-.047		—

AI Velorum 1953

Table with 14 columns: phi_0, -Delta m, phi_0, -Delta m, phi_0, -Delta m, phi_0, -Delta m, phi_0, -Delta m, phi_0, -Delta m, phi_0, -Delta m. It lists astronomical data for AI Velorum in 1953, showing variations in position and magnitude over time.

AI Velorum 1953

φ_0	$-\Delta m$	φ_0	$-\Delta m$	φ_0	$-\Delta m$	φ_0	$-\Delta m$	φ_0	$-\Delta m$	φ_0	$-\Delta m$	φ_0	$-\Delta m$
.60	.000	.40	-.027	.45	+.135	.85	-.109			.75	-.122		-.059
	-.029		-.042		+.109		-.039				-.094	.65	-.077
.65	-.057	.45	-.053	.50	+.085	.90	+.031			.80	-.070		-.089
	-.085		-.064		+.057		+.117				-.053	.70	-.102
.70	-.106	.50	-.081	.55	+.029	.95	+.212	6951.50	—	.85	-.036		-.109
	-.127		-.102		-.003		+.299		+.038		-.012	.75	-.111
.75	-.145	.55	-.118	.60	-.031	6916.00	+.333	.55	.000	.90	+.015		-.111
	-.157		-.129		-.047		+.349		-.031		+.042	.80	-.109
.80	-.167	.60	-.134	.65	-.067		+.443	.60	-.058	.95	+.064		-.109
	-.173		-.133		-.083		+.321		-.081		+.084	.85	-.113
.85	-.175	.65	-.125	.70	-.097		+.289	.65	-.105	6954.00	+.095		-.117
	-.175		—		-.112		+.249		-.120		+.106	.90	-.124
.90	-.169	.70	-.083	.75	-.128		+.218	.70	-.130		+.109		-.128
	-.156		-.069		-.142		+.192		-.133		+.111	.95	-.121
.95	-.136	.75	-.062	.80	-.152		+.161	.75	-.134		+.111		—
	-.105		-.057		-.163		+.126		-.135		+.107	6962.00	—
6891.00	-.068	.80	-.055	.85	-.173		+.101	.80	-.136		+.098		—
	-.028		-.050		-.175		+.075		-.141		+.091	.05	+.013
.05	+.024	.85	-.048	.90	-.175	.30	+.051	.85	-.146		+.082		—
	+.086		-.040		-.174		+.028		-.150		+.076	.10	+.141
.10	+.158	.90	-.031	.95	-.164	.35	+.007	.90	-.152		+.070		+.211
	+.249		-.021		-.136		-.013		-.149		+.068	.15	+.275
.15	+.340	.95	-.006		-.091	.40	—	.95	-.133		+.068		+.332
	+.404		+.014	6908.00	-.031		—		-.104		+.070	.20	+.361
.20	+.434	6900.00	+.031		+.057	.45	—	6952.00	-.063		+.068		+.367
	+.436		+.042	.05	+.159		—		-.015		+.059	.25	+.359
			+.051	.10	+.259	.50	—	.05	+.048		+.048		+.339
			+.055		+.366		—		+.114		+.033	.30	+.312
			+.059	.15	+.456	.55	—	.10	+.203		+.018		+.279
			+.061		+.499		—		+.285		+.006	.35	+.239
6897.80	-.200	.15	+.066	.20	+.499	.60	—	.15	+.351		-.002		+.200
	-.213		+.070	.25	+.477		—		+.395		-.010	.40	+.159
.85	-.219	.20	+.085	.30	+.437	.65	—	.20	+.413		-.011		+.121
	-.220		+.100		+.383		—		+.418		-.018	.45	+.085
.90	-.211	.25	+.122	.30	+.332	.70	—	.25	+.399		-.026		—
	-.187		+.147		+.280		-.092		+.368		-.040	.50	—
.95	-.151	.30	+.159	.35	+.228	.75	-.081	.30	+.335		-.058		—
	-.087		+.159		+.177		-.071		+.296		-.066	.55	-.060
6898.00	-.003	.35	+.146	.40	+.131	.80	-.058	.35	+.252		-.097		-.086
	+.099		+.129		+.088		-.043		+.207		—	.60	-.109
.05	+.233	.40	+.112	.45	+.049	.85	-.028	.40	+.161		—		-.133
	+.375		+.098		+.008		-.018		+.110		—	.65	-.149
.10	+.488	.45	+.092	.50	-.028	.90	-.005	.45	+.066		+.066		-.168
	+.545		+.087		-.059		-.006		+.028		+.028	.70	-.182
.15	+.543	.50	+.078	.55	-.074	.95	+.013	.50	-.021		-.021		-.197
	+.517		+.062		-.098		+.014		-.048	6960.40	-.050	.75	-.209
.20	+.467	.55	+.037	.60	-.120	6917.00	+.009	.55	-.076		-.055		-.217
	+.412		-.001		-.144		+.009		-.102		-.063	.80	-.219
.25	+.353	.60	-.035	.65	-.164	.05	+.011	.60	-.128		-.072		-.214
	+.295		-.064		-.185		+.016		-.105		-.086	.85	-.195
.30	+.236	.65	-.091	.70	-.191	.10	+.030	.65	-.166		-.108		-.154
	+.187		-.117		-.203		+.044		-.183		-.133	.90	-.090
.35	+.139	.70	-.136	.75	-.213	.15	+.062	.70	-.201		-.149		-.032
	+.094		-.153		-.217		+.078		-.213		-.164	.95	+.052
.40	+.059	.75	-.163	.80	-.214	.20	+.092	.75	-.172		-.172		+.142
	+.022		—		-.204		+.108		—		-.174	6963.00	—
.45	-.014	.80	-.159	.85	-.181	.25	+.126	.80	—		-.173		—
	-.039		-.157		-.136		+.149		-.226		-.168	.05	+.435
.50	-.060	.85	-.156	.90	-.058	.30	+.156	.85	-.197		-.156		+.481
	-.081		-.156		+.031		+.153		-.147		-.137	.10	+.481
.55	-.105	.90	—	.95	+.102	.35	+.140	.90	-.058		-.111		+.459
	-.132		—		+.192		+.120		+.041		-.082	.15	+.421
.60	-.157		—	6909.00	+.274	.40	+.103	.95	+.154		-.054		+.382
	-.179		—		+.340		+.090		+.277		-.024	.20	+.333
.65	-.200	.70	—	.05	+.363	.45	+.080	6953.00	+.382		+.009		+.281
	-.218		—		+.373		+.066		+.444		+.037	.25	+.232
.70	-.233	.75	-.119	.10	+.366	.50	+.054	.05	+.404		+.049		+.187
	-.240		-.117		+.348		+.037		+.460		+.058	.30	+.138
.75	-.237	.80	-.111	.15	+.324	.55	+.015	.10	+.442		+.062		+.093
	-.228		-.102		+.293		-.012		+.407	6961.00	+.060	.35	+.056
.80	-.212	.85	-.080	.20	—	.60	-.031	.15	+.366		+.053		+.019
	-.181		-.060		—		-.043		+.328		+.045	.40	-.016
.85	-.133	.90	-.050	.25	—	.65	-.059	.20	+.287		+.039		-.043
	-.069		-.039		—		-.073		+.246		+.037	.45	-.067
.90	+.007	.95	-.034	.30	—	.70	-.083	.25	+.205		+.041		-.086
	+.078		-.034		—		—		+.164		+.048	.50	-.096
.95	+.144	6907.00	-.034	.35	—	.75	—	.30	+.119		+.056		-.119
	+.210		-.034		—		—		+.086		+.064	.55	-.144
6899.00	+.270	.05	-.027	.40	—	.80	—	.35	+.049		+.075		-.160
	+.301		-.018		—		-.125		+.014		+.086	.60	-.170
.05	+.312	.10	-.002		—	.85	-.141	.40	-.016		+.107		-.177
	+.319		+.023		—		-.156		-.041		+.124	.65	-.183
.10	+.319	.15	+.048		—	.90	-.159	.45	-.059		+.132		-.189
	+.307		+.081	6915.60	-.164	.95	-.160		-.075		+.132	.70	—
.15	+.290	.20	+.114		-.172		-.145	.50	-.093		+.123		—
	—		+.151	.65	-.183	6918.00	-.113		-.112		+.107		—
.20	—	.25	+.176	.70	-.201		-.078	.55	-.135		+.089		—
	+.202		+.197		-.214		-.037		-.154		+.071		—
.25	—	.30	+.206	.75	-.218	.05	+.011	.60	-.165		+.054	6969.35	+.184
	—		+.201		-.219		+.072		-.170		+.042		+.142
.30	—	.35	+.189	.80	-.217	.10	+.132	.65	-.174		+.023	.40	+.105
	+.022		+.176		-.199		—		-.174		+.004		+.069
.35	—	.40	+.158		-.162	.15	—	.70	-.165		-.019	.45	+.023
	—		—		—		—		-.147		-.039		-.020

AI Velorum 1953

φ_0	$-\Delta m$	φ_0	$-\Delta m$	φ_0	$-\Delta m$	φ_0	$-\Delta m$	φ_0	$-\Delta m$	φ_0	$-\Delta m$	φ_0	$-\Delta m$
.50	-.047	.85	-.081	.90	-.190	6988.00	+.078	.35	+.122:		+.111	.40	+.226
	-.071		-.084		-.146		+.067		+.084:	.25	+.103		+.184
.55	-.093	.90	-.085	.95	-.066		+.055	.40	+.045		—	.45	+.138
	-.112:		-.084		+.043		+.044		+.008	.30	—		—
.60	-.133	.95	-.078	6980.00	+.156		+.039	.45	-.023		+.079:	.50	—
	-.147		-.066		+.264		+.045		-.048	.35	+.075		—
.65	-.156	6972.00	-.047	.05	+.369	.15	+.047	.50	-.074		+.072	.55	-.014:
	-.167		-.029		+.430		+.052		-.109	.40	+.069		-.044
.70	-.183	.05	-.001	.10	+.450	.20	+.062	.55	-.142		+.073:	.60	-.062
	-.195:		+.035		+.443		+.070		-.172	.45	—		-.075
.75	-.207	.10	+.075	.15	+.420	.25	+.081	.60	-.203:		—		—
	-.214		+.123		+.384		+.090		—		—		—
.80	-.213	.15	+.175	.20	+.345	.30	+.098		—		—		—
	-.201		+.232		+.301		+.105		—		—		—
.85	-.179	.20	+.282	.25	+.262	.35	+.108		—	7014.40	—	7023.35	—
	-.138		+.309		+.225		+.106	6996.25	+.346:		-.055:		+.195:
.90	-.071	.25	+.312	.30	+.195	.40	+.099		+.346:	.45	-.073	.40	+.163:
	+.009		+.301		+.162		+.090		+.334:		-.097		—
.95	+.109	.30	+.282:	.35	+.126	.45	+.078		+.309:	.50	-.126	.45	—
	+.215		+.259:		+.095		+.063		+.270:		-.147		—
6970.00	+.325	.35	+.223:	.40	+.069	.50	+.048		+.228:	.55	-.165	.50	—
	+.384		+.205		+.042		+.031		+.181:		-.175:		-.042:
.05	+.401:	.40	+.179	.45	+.011	.55	+.010	.40	+.132:	.60	-.182	.55	—
	+.395		+.146:		-.019		-.012		+.090:		-.187		—
.10	+.371	.45	+.113:	.50	-.043	.60	-.034	.45	+.040:	.65	-.190:	.60	—
	+.342		+.080		-.070		-.050		-.011:		-.186		—
.15	+.310	.50	+.045	.55	-.099:	.65	-.065	.50	-.050:	.70	-.174	.65	—
	+.275		+.005		-.131		-.073		-.085:		-.153		—
.20	+.239	.55	-.030	.60	-.156	.70	-.079	.55	-.113:	.75	-.124	.70	—
	+.206		-.055		-.174		-.076		-.136:		-.094		—
.25	+.176	.60	—	.65	-.188	.75	-.063	.60	-.154:	.80	-.066	.75	—
	+.145		—		-.199		-.065		-.162:		-.042		—
.30	+.119	.65	—	.70	-.204	.80	-.064	.65	-.169:	.85	-.018	.80	—
	+.087		—		-.200		-.068		-.175:		+.028		—
.35	+.060	.70	—	.75	-.188	.85	-.076	.70	-.186:	.90	+.073	.85	-.160:
	+.036	6978.40	+.086:		-.172		-.083		-.187:		+.108		-.136:
.40	+.011		+.078	.80	-.133	.90	-.096	.75	-.181	.95	+.138	.90	-.105:
	-.012		+.070		-.083		-.109		—		+.164		-.066:
.45	-.031	.45	+.061	.85	-.036	.95	-.117	.80	-.177:	7015.00	+.177	.95	-.019:
	-.053		+.049		+.012		-.117		-.169:		+.174		+.059:
.50	-.076	.50	+.028	.90	+.053	6989.00	-.107	.85	-.153:	.05	+.156	7024.00	+.117:
	-.102		+.005		+.083		-.087		-.114:		+.137		+.198:
.55	-.128	.55	-.019	.95	+.106	.05	-.058:	.90	-.058:	.10	+.122	.05	+.296:
	-.150		-.041		+.128		+.003		+.003		+.093		+.382:
.60	-.167	.60	-.063	.10	+.152:	.10	+.039	6997.00	+.069	.15	+.072	.10	+.437:
	-.178		-.079		+.163:		+.098		+.157		+.084		+.453:
.65	-.186	.65	-.090	.15	+.168:	.15	+.164		+.260	.20	+.072	.15	+.438:
	-.187		-.094		+.173:		+.231		+.355		+.061		+.402:
.70	-.186	.70	-.086:	.20	+.175:	.20	+.287	.05	+.399	.25	+.054	.20	+.371:
	-.176		-.075:		+.169:		+.332		+.416:		+.051		+.333:
.75	-.156	.75	-.063:	.25	+.159:	.25	+.352	.10	+.409	.30	+.048	.25	+.289:
	-.123		-.058:		+.144:		+.353		+.37		+.047		+.243:
.80	-.078	.80	-.063	.30	+.125:	.30	+.338	.15	+.359	.35	+.045	.30	+.200:
	-.035		-.073		+.108:		+.312		+.332		+.044		+.153
.85	+.010	.85	-.092	.40	+.091:	.40	+.278	.20	+.293	.40	+.039	.35	+.111
	+.054		-.112:		+.076:		+.245		+.252		+.020		+.075
.90	+.082	.90	-.129:	.25	+.062:	.25	+.210	.25	+.212	.45	+.005	.40	+.039
	+.103		-.133		+.051:		+.173		+.176:		-.011		+.005
.95	+.114	.95	-.124	.30	+.042:	.45	+.139:	.30	+.139:	.50	-.019	.45	-.023
	+.125	6979.00	-.108	.35	+.031:	.50	+.091	.35	+.100		-.027		-.045
6971.00	+.125		-.086		+.022:		+.060		+.067	.55	-.034	.50	-.067
	+.121		-.052		+.010:		+.029		+.030	.40	-.042		-.087
.05	+.119	.05	-.007	.40	—	.55	-.006	.40	-.003	.60	-.050	.55	-.105
	+.114		+.054		—		-.036		-.030		-.059		-.122
.10	+.111	.10	+.117	.45	—	.60	-.059	.45	-.047	.65	-.072	.60	-.140
	+.103		+.195		—		-.081		-.063		-.083		-.154
.15	+.098	.15	+.261	.65	—	.65	-.109	.50	-.079	.70	-.094:	.65	-.167
	+.093		+.318		—		-.136		-.097:		-.098:		-.174
.20	+.086	.20	+.352	.70	+.045:	.70	-.157	.55	-.116:	.75	-.098:	.70	-.175
	+.078		+.370		+.012:		-.176		-.141		-.085		-.160
.25	+.071	.25	+.373	.75	-.018:	.75	-.195	.60	-.165:	.80	-.065	.75	-.154
	+.070		+.359		-.042:		-.206		-.183:		-.046		-.130
.30	+.073	.30	+.328	.80	-.069:	.80	-.218	.65	-.188	.85	-.033	.80	-.099
	+.080		+.289		-.089:		-.223		-.188		-.031		-.064
.35	+.078	.35	+.233	.85	-.108:	.85	-.222	.70	-.185	.90	-.034	.85	-.021
	+.068		+.184		-.120:		-.210		-.175		-.042		+.036
.40	+.054	.40	+.137	.90	-.128:	.90	-.176	.75	-.157:	.95	-.055	.90	+.095
	+.039		+.091		-.134:		-.115		-.126:		-.066		+.162
.45	+.018	.45	+.054	.95	-.143:	.95	-.026	.80	-.089	7016.00	-.069	.95	+.211
	+.002		+.017		-.149:		+.068		-.040:		-.066		+.243
.50	-.014	.50	-.017	.65	-.152:	6990.00	+.173	.85	—	.05	-.055	7025.00	+.248
	-.017		-.039		-.150:		+.282		—		-.036:		+.246
.55	-.022	.55	-.058	.70	-.145:	.05	+.374	.90	+.060:	.10	-.009	.05	+.218
	-.026		-.075		-.136:		+.450		+.129		+.032		+.195
.60	-.029	.60	-.094:	.75	-.109:	.10	+.485	.95	+.147	.15	+.081	.10	+.174
	-.034		-.114:		-.090:		+.488		+.153		+.133		+.162
.65	-.042	.65	-.138	.80	-.071	.15	+.472	6998.00	+.149	.20	+.188	.15	+.148
	-.051		-.164		-.047		+.434		+.139		+.232		+.134:
.70	-.060	.70	-.181	.85	-.014	.20	+.384	.05	+.133:	.25	+.271	.20	+.122:
	-.067		-.198		+.025		+.338		+.131:		+.295		+.108:
.75	-.074	.75	-.211	.90	+.056	.25	+.296	.10	+.133:	.30	+.306	.25	+.095:
	-.078		-.219		+.077		+.249		+.131:		+.301		+.085:
.80	-.078	.80	-.220	.95	+.085	.30	+.202	.15	+.127	.35	+.282	.30	+.075:
	-.078		-.212		+.084		+.159		+.120		+.256		+.067:

AI Velorum 1953

φ_0	$-\Delta m$	φ_0	$-\Delta m$	φ_0	$-\Delta m$	φ_0	$-\Delta m$	φ_0	$-\Delta m$	φ_0	$-\Delta m$	φ_0	$-\Delta m$
.35	+ .060 :		+ .164 :		+ .139		-.140	7087.00	-.019	.70	-.159	.05	-.008
	+ .054 :		+ .187 :		+ .123		-.153		-.009		-.176		+ .044
.40	+ .051 :	.30		.40	+ .111	.65	-.164	.05	+ .005	.75	-.193	.10	+ .106
	+ .046 :			.45	+ .098	.70	-.173		+ .022		-.205		+ .179
.45	+ .031 :				+ .084		-.178	.10	+ .039	.80	-.211	.15	+ .253
	+ .013 :	7068.15	+ .504	.50	+ .054	.75	-.180		+ .056		-.203		+ .327
.50	-.001 :		+ .468		+ .029		-.177	.15	+ .072	.85	-.183	.20	+ .378
	-.019 :	.20	+ .410	.55	-.003	.80	-.163		+ .087		-.151		+ .390
.55	-.034 :		+ .349		-.031		-.130	.20	+ .107	.90	-.095 :	.25	+ .378
	-.047 :	.25	+ .288	.60	-.053	.85	-.075		+ .130		-.030		+ .353
.60	-.055 :		+ .232		-.072		-.003	.25	+ .153	.95	+ .045	.30	+ .321
.65	-.063 :	.30		.65	-.090	.90	+ .040		+ .165		+ .130		+ .285
	-.066 :				-.083 :		+ .097	.30	+ .164	7140.00	+ .223	.35	+ .247
.70	-.069 :	.35		.70	-.087 :	.95	+ .165		+ .152		+ .312		+ .212
	-.069 :				-.087 :		+ .226	.35	+ .137		+ .348	.40	+ .174
.75	-.065 :	.40		.75	-.089 :	7079.00	+ .270		+ .120	.05	+ .356		+ .138
	-.050 :	.45	-.036 :	.80	-.096 :		+ .303	.40	+ .105	.10	+ .346	.45	+ .103
.80	-.033 :		-.059 :		-.109 :	.05	+ .321		+ .093		+ .328		+ .076
	-.019 :	.50		.85	-.122 :	.10	+ .321	.45	+ .089	.15	+ .306	.50	+ .045
.85	-.010 :		-.109				+ .307		+ .088		+ .281		+ .009
	-.008 :	.55	-.139	.90			+ .288	.50	+ .081	.20	+ .252	.55	-.022 :
.90	-.010 :		-.159				+ .264		+ .063	.25	+ .220		-.043
	-.022 :	.60	-.175	.95	-.127 :	.20	+ .242	.55	+ .043	.30	+ .193	.60	-.069
.95	-.032 :		-.188		-.123 :	.25	+ .217		+ .020	.35	+ .163		-.092 :
		.65	-.201	7071.00	-.104 :	.30	+ .190	.60	-.008	.40	+ .130	.65	-.115 :
7026.00			-.213		-.037 :	.35	+ .161		-.029		+ .103		-.133 :
		.70	-.218	.05	+ .036 :		+ .131	.65	-.046	.35	+ .077	.70	-.144 :
			-.219		+ .123 :	.30	+ .101		-.061		+ .054		-.151 :
		.75	-.214	.10		.35	+ .075	.70	-.073	.40	+ .031	.75	-.154 :
			-.200				+ .048		-.078		+ .006		-.158 :
7051.10		.80	-.177	.15	+ .366 :	.40	+ .022	.75	-.086	.45	-.016	.80	
	+ .499 :		-.135				-.005		-.096		-.038		
.15	+ .498 :	.85	-.078			.45	-.026	.80	-.110	.50	-.060		
			-.022				-.039 :		-.128		-.081		
.20	+ .441	.90	+ .031			.50		.85	-.151	.55	-.106		
	+ .398 :		+ .082					.90	-.162		-.124	7148.55	-.017
.25	+ .343	.95	+ .146	7077.20	+ .131 :	.55			-.164	.60	-.138		-.024
			+ .206		+ .167 :				-.164	.65	-.148	.60	-.040
		7069.00	+ .246	.25	+ .188	.60	-.100 :	.95	-.154		-.154	.65	-.057
			+ .268		+ .195			7088.00	-.132	.70	-.144		-.071
		.05	+ .279	.30	+ .192	.65			-.095		-.127	.70	-.081
			+ .280		+ .184			.05	-.050	.75	-.104		-.081
7052.00		.10	+ .269	.35	+ .172	.70			+ .005		-.076	.75	-.077
	+ .242		+ .251		+ .155			.10	+ .074	.80	-.047		-.078
.05	+ .249	.15	+ .228	.40	+ .133				+ .187		-.024	.80	-.089
	+ .247		+ .201		+ .112			.15	+ .401	.85	-.010		-.105
.10	+ .242	.20	+ .170	.45	+ .095				+ .468		-.005	.85	-.127
	+ .231		+ .132		+ .081	7085.85		.20	+ .484	.90	-.002		-.148
.15	+ .215	.25	+ .092	.50	+ .061		-.031		+ .473		+ .004 :	.90	-.168
	+ .194		+ .062		+ .039	.90	+ .031	.25	+ .443	.95			-.177
.20	+ .169	.30	+ .033	.55	+ .007		+ .098		+ .398			.95	-.177
	+ .143		+ .005 :		-.027	.95	+ .153	.30	+ .343 :	7141.00	+ .025		-.167
.25	+ .117	.35	-.020	.60	-.043		+ .205		+ .285		+ .039	7149.00	-.147
	+ .092		-.037		-.064	7086.00	+ .237	.35	+ .230	.05	+ .057		-.110
.30	+ .067	.40	-.050	.65	-.079		+ .261 :		+ .176		+ .077	.05	-.060
	+ .039		-.063		-.095	.05	-.269 :	.40	+ .122	.10	+ .103		+ .009
.35	+ .016	.45	-.074	.70	-.110		+ .270 :		+ .078		+ .122	.10	+ .100
	-.005		-.085		-.128	.10	+ .261 :	.45	+ .037	.15	+ .131		+ .209
.40	-.024	.50	-.094	.75	-.146		+ .243		-.004		+ .132	.15	+ .319
	-.034		-.101		-.160	.15	+ .223	.50	-.036	.20	+ .125		+ .405
.45	-.044	.55	-.108 :	.80	-.172		+ .199		-.062	.25	+ .115	.20	+ .444
	-.050		-.112 :		-.182	.20	+ .174	.55	-.082		+ .103		+ .452
.50	-.057	.60	-.109 :	.85	-.188		+ .146		-.098	.30	+ .095	.25	+ .420
	-.066		-.103 :		-.190	.25	+ .114	.60	-.112		+ .093		+ .395
.55	-.079	.65	-.094 :	.90	-.187		+ .087		-.126	.35	+ .093	.30	+ .352
	-.091		-.084		-.174	.30	+ .062	.65	-.137		+ .086		+ .309
.60	-.097 :	.70	-.076	.95	-.148		+ .038		-.152	.40	+ .073	.35	+ .252
			-.070		-.093	.35	+ .009	.70	-.167		+ .055		+ .202
.65		.75	-.065	7078.00	-.031		-.010		-.180	.40	+ .039	.40	+ .154
			-.065		+ .046	.40	-.025	.75	-.193	.45	+ .021		+ .106
.70		.80	-.050	.05	+ .124		-.039		-.200		+ .009	.45	+ .067
			-.042		+ .229	.45	-.053 :	.80	-.198	.50	+ .007		+ .030
.75	-.089	.85	-.030	.10	+ .343		-.067 :		-.186		+ .006	.50	-.005
	-.082		-.023		+ .437	.50	-.082 :	.85	-.155 :	.55	+ .011		-.030
.80	-.071	.90	-.010	.15	+ .483		-.093 :		-.109		+ .023	.55	-.050
	-.058		-.002		+ .482	.55	-.098 :	.90	-.066	.60	+ .028		-.066
.85	-.042	.95	-.000	.20	+ .459		-.097 :		-.020	.65	+ .021	.60	-.084
	-.027		-.000		+ .413	.60	-.093	.95	+ .044		+ .009		-.106
.90	-.018 :	7070.00	-.002	.25	+ .359		-.079		+ .122		-.008	.65	-.128
	-.011 :		-.008		+ .306	.65	-.074	7089.00	+ .199	.70	-.029		-.153
.95	-.011 :	.05	-.015	.30	+ .250		-.070		+ .278		-.047	.70	-.174
	-.015 :		-.016		+ .202	.70	-.066	.05	+ .327 :	.75	-.066		-.195
7053.00	-.018 :	.10	-.015	.35	+ .157 :		-.060		+ .340 :		-.088 :	.75	-.214
	-.014 :		-.002			.75	-.058	.10	+ .339 :	.80	-.105		-.229
.05	-.011 :	.15	+ .020	.40	+ .070		-.058		+ .329 :		-.125	.80	-.242
	+ .002 :		+ .047		+ .036	.80	-.060	.15		.85	-.141		-.243
.10	+ .017 :	.20	+ .075	.45	+ .003		-.067				-.151	.85	-.234
	+ .036 :		+ .113		-.029	.85	-.072			.90	-.152		-.221
.15	+ .055 :	.25	+ .145	.50	-.054		-.066				-.152	.90	-.174
	+ .081 :		+ .164 :		-.073	.90	-.061	7139.60		.95	-.144		-.109
.20	+ .090 :	.30	+ .165	.55	-.090		-.053		-.111		-.122	.95	-.032
	+ .114 :		+ .164		-.107	.95	-.042	.65	-.128	7142.00	-.094		+ .067
.25		.35	+ .156	.60	-.125		-.030		-.144		-.055	7150.00	+ .171

AI Velorum 1953

φ_0	$-\Delta m$	φ_0	$-\Delta m$	φ_0	$-\Delta m$	φ_0	$-\Delta m$	φ_0	$-\Delta m$	φ_0	$-\Delta m$	φ_0	$-\Delta m$
.05	+.290	.90	-.006	.15	+.209	.40	-.043	.75	-.186	.60	-.032	7347.00	+.080
	+.399				+.201		-.052		-.190		-.027		+.207
	+.460	.95	+.037	.45	+.185	.45	-.062	.80	-.189	.60	-.030		+.326
.10	+.468		+.047	.20	+.165		-.069		-.176	.65	-.034	.05	+.426
	+.457	7158.00	+.052	.20	+.140	.50	-.076	.85	-.155		-.040		+.476
	+.431		+.058	.25	+.113		-.078		-.112	.70	-.050	.10	+.484
.15	+.387	.05	+.062	.30	+.087	.55	-.073	.90	-.065		-.059		+.461
	+.342		+.065	.30	+.063		-.061		-.006	.75	-.070	.15	+.425
.20	+.287	.10	+.067	.30	+.040	.60	-.043	.95	+.062		-.086		+.375
	+.239		+.073	.35	+.017		-.030		+.137	.80	-.104	.20	+.324
.25	+.195	.15	+.075	.40	-.008	.65	-.020	7259.00	+.218		-.117		+.268
	+.150		+.075	.40	-.029		-.017		+.296	.85	-.124	.25	+.217
.30	+.109	.20	+.077	.45	-.042	.70	-.020	.05	+.351		-.130		+.171
	+.067		+.077	.45	-.052		-.026		+.372	.90	-.134	.30	+.129
.35	+.031	.25	+.078	.50	-.064	.75	-.034	.10	—		-.136		+.106
	-.008		+.082	.50	-.073		-.044		—	.95	-.137	.35	+.067
.40	-.036	.30	+.086	.55	-.080	.80	-.055		—		-.112		+.038
	-.061		+.093	.55	-.085		-.058		—	7339.00	-.091	.40	+.005
.45	-.083	.35	+.100	.60	-.085	.85	-.063		—		-.064		-.021
	-.105		+.096	.60	-.084		-.064	7336.70	-.165	.05	-.027	.45	-.038
.50	-.128	.40	+.084	.65	-.077	.90	-.063		-.176		+.015		-.057
	-.147		+.077	.65	-.068		-.056	.75	-.187	.10	+.074	.50	-.080
.55	-.163	.45	+.070	.70	-.055	.95	-.050		-.200		+.136		-.105
.60	-.173		+.051	.70	-.042		-.047	.80	-.211	.15	+.199	.55	-.136
	-.181	.50	+.025		-.030	7257.00	-.042		-.214	.20	+.254		-.159
.65	-.185	.55	+.005	.75	-.022		-.033	.85	-.203	.20	+.202	.60	-.175
	-.182		-.012	.80	-.016	.05	-.020		-.179		+.305	.65	-.186
.70	-.175	.60	-.028	.80	-.012		+.002	.90	-.128	.25	+.301		-.191
	-.154		-.042	.85	-.012	.10	+.031		-.056		+.278	.70	-.192
.75	-.123	.65	-.058	.85	-.016	.15	+.062	.95	+.011	.30	+.243		-.190
	-.089		-.069	.90	-.023	.15	+.089		+.093		+.214	.75	-.181
.80	-.059	.70	-.073	.90	-.035		+.123	7337.00	+.199	.35	+.190		-.165
	-.042		-.073	.95	-.047	.20	+.166		+.304		+.165	.75	-.142
.85	-.033	.75	-.073	.95	-.054	.25	+.191	.05	+.375	.40	+.132	.80	-.112
	-.031		-.074		-.061	.25	+.213		+.400		+.112		-.081
.90	-.025	.80	-.081	7240.00	-.063		+.225	.10	+.396	.45	+.088	.85	-.058
	-.014		-.089		-.062	.30	+.223		+.370		+.061		-.034
.95	+.001	.85	-.102	.05	-.053	.15	+.210		+.339			.90	-.011
	+.022		-.120	.35	-.039	.35	+.190		+.300				+.026
7151.00	+.047	.90	-.136	.10	-.012	.20	+.171		+.252			.95	+.059
	+.077		-.144	.40	+.024	.40	+.153		+.208				+.089
.05	+.110	.15	—	.15	+.062	.25	+.131	.25	+.169	7345.65	—	7348.00	+.122
	+.149	.95	—	.45	+.105	.45	+.119		+.131		-.063		+.148
.10	+.179	.20	—	.20	+.153	.50	+.099	.30	+.094	.70	-.069	.05	+.168
	+.192		—	.50	—	.50	+.078		+.065		-.072		+.176
.15	+.194	7159.00	-.120	.25	+.225	.35	+.054	.35	+.034	.75	-.073	.10	+.176
	+.172	.05	-.031	.30	+.242	.55	+.027	.40	+.008		-.073	.15	+.171
.20	+.151		-.047	.30	+.247	.60	.000	.40	-.020	.80	-.078	.15	+.157
	+.125	.10	+.123	.35	+.238	.60	-.018	.45	-.042		-.091	.20	+.134
.25	+.098	.15	+.220	.35	+.222	.65	+.222	.45	-.059	.85	-.109	.20	+.101
	+.078		—	.40	+.197	.65	+.197	.45	-.073		-.129	.25	+.075
.30	+.065		—	.40	+.168	.70	-.055	.50	-.090	.90	-.090	.25	+.059
	+.053		—	.45	+.135	.70	-.056		-.114		-.164		
.35	+.038		—	.45	+.107	.70	-.058	.55	-.137	.95	-.167		
	+.021		—	.75	+.081	.75	-.066		-.162		-.161		
.40	+.009	7238.15	—	.50	+.054	.80	-.080	.60	-.181	7346.00	-.181		
	-.002		+.475	.80	+.027	.80	-.103		-.191		-.103	7381.85	—
.45	-.019	.20	+.419	.55	+.005	.65	-.126	.65	-.197	.05	-.055		-.013
	-.031		+.390	.55	-.019	.85	-.147		-.195		-.005	.90	+.030
.50	-.039	.25	+.297	.60	-.024		-.164	.70	-.187	.10	+.075		+.074
	-.038		+.234	.60	-.036	.90	-.177		-.168		+.155	.95	+.106
.55	-.034	.30	+.175	.65	-.042		-.177	.75	-.144	.15	+.241		+.136
	-.017		+.125	.70	-.046	.95	-.168		-.112		+.317	7382.00	+.159
.60	.000	.35	+.076	.70	-.050		-.147	.80	-.074	.20	+.363		+.153
	+.003		+.039	.75	-.063	7258.00	-.063		-.048		+.371	.05	—
.65	-.003	.40	+.002	.75	-.082		-.060	.85	-.019	.25	+.385		—
	-.012		-.028	.80	-.105	.05	+.013		+.006		+.370	.10	+.134
.70	-.024	.45	-.047	.80	-.125	.10	+.115	.90	+.027	.30	+.340		+.127
	-.038		-.066	.10	-.146	.10	+.255		+.047		+.299	.15	+.117
.75	-.056	.50	-.086	.85	-.163	.15	+.398	.95	+.066	.35	+.254		+.104
	-.075		-.106	.90	-.176	.15	+.500		+.084		+.209	.20	+.089
.80	-.090	.55	-.120	.90	-.185	.20	+.544	7338.00	+.096	.40	+.157		+.073
	-.096		-.134	.20	-.180	.20	+.546		+.103		+.112	.25	+.062
.85	-.095	.60	-.147	.95	-.169	.25	+.522	.05	+.110	.45	+.073		+.061
	—		-.151	.25	-.140	.25	+.476		+.116		+.041	.30	—
	—	.65	-.156	7241.00	-.086		+.421	.10	+.117	.50	+.009		—
	—		-.155		-.024	.30	+.356	.15	+.113	.35	-.020	.35	+.036
7157.50	-.142	.70	-.151	.05	+.048		+.293	.15	+.106	.55	-.042	.40	+.032
	-.136		-.145		—	.35	+.228		+.093		-.061		+.020
.55	-.130	.75	-.137	.35	+.277	.40	+.172	.20	+.082	.60	-.076	.45	+.013
	-.128	.80	-.121	.40	+.273		+.123		+.067		-.093		—
.60	-.127		-.105	.45	+.256	.25	+.078	.25	+.052	.65	-.114		—
	-.125	.85	-.080	7256.10	+.279	.45	+.044		+.039		-.137	.50	-.030
.65	-.120		-.048		+.273		+.003	.30	+.030	.70	-.159		—
	-.117	.90	-.016	.15	+.250	.50	-.032		+.026		-.183	.55	—
.70	-.114		+.012	.20	+.229	.35	-.050		+.023	.75	-.204		-.055
	-.112	.95	+.046	.20	+.192	.55	-.064		+.016		-.222	.60	-.065
.75	-.107		+.086	.25	+.156	.60	-.073	.40	+.004	.80	-.237		-.070
	-.097	7239.00	+.126	.25	+.116	.60	-.089		-.011		-.237	.65	-.073
.80	-.086		+.163	.30	+.082	.45	-.105		-.024	.85	-.230		-.078
	-.073	.05	+.188	.30	+.045	.65	-.126		-.032		-.211	.70	-.081
.85	-.055		+.204	.35	+.013	.70	-.148	.50	-.035	.90	-.174		-.073
	-.031	.10	+.211		-.013		-.164		-.034		-.100	.75	-.066
			+.214		-.032		-.174	.55	-.034	.95	-.016		-.065

AI Velorum 1953

ϕ_0	$-\Delta m$	ϕ_0	$-\Delta m$	ϕ_0	$-\Delta m$	ϕ_0	$-\Delta m$	ϕ_0	$-\Delta m$	ϕ_0	$-\Delta m$	ϕ_0	$-\Delta m$
.80	-.063	.80	-.150	.25	+.106:	.50	-.065			.75	-.036:	.65	—
.85	-.059	.85	-.172		+.089:		-.087				-.037:		—
	-.058		-.191		+.074:	.55	-.112	7605.35	—	.80	-.037:	.70	-.181:
	-.059:		-.199	.30	+.059:		-.136		+.086:		-.034:		—
.90	-.062		-.195		+.044:	.60	-.157	.40	+.057:	.85	-.025:	.75	—
	-.064	.90	-.178	.35	+.030:		-.173		+.029:		-.016:		—
.95	-.068		-.146		+.020:	.65	-.186	.45	+.005:	.90	-.009:	.80	—
	-.069	.95	-.097	.40	+.010:		-.196		-.018:		-.008:		—
7383.00	-.066		-.039		-.003:	.70	-.206	.50	-.034:	.95	-.010:	.85	—
	-.050	7391.00	+.043	.45	-.015:		-.206		-.051:		-.011:		—
.05	-.028		+.152		-.028:	.75	-.197	.55	-.078:	7607.00	-.012:	.90	-.060
	.000	.05	+.288	.50	-.042:		-.181		-.112:		-.011:		-.005
.10	+.038		+.405		-.059:	.80	-.155	.60	-.131:	.05	-.009:	.95	+.067
	+.067	.10	+.479	.55	-.073:		-.113		-.147:		-.001:		+.151
.15	+.103		+.494		-.078:	.85	-.070	.65	-.167:	.10	+.012:	7660.00	+.251
	+.147	.15	+.480	.60	-.081:		-.027		-.177:		+.036:		+.333
.20	+.184		+.441		-.076:	.90	+.030	.70	-.179:	.15	+.064:	.05	+.373
	+.212	.20	+.390	.65	-.070:		+.075		-.181:		+.089:		+.385:
.25	+.234		+.366		-.063:	.95	+.114	.75	-.177:	.20	+.117:	.10	+.369:
	+.239:	.25	+.279	.70	-.058:		+.155		-.165:		+.148:		—
.30	+.237		+.227		-.055:	7562.00	+.183	.80	-.150:	.25	+.181:		—
	+.226	.30	+.179	.75	-.054:		+.188		-.119:		+.206:		—
.35	+.209		+.132		-.055:	.05	+.192	.85	-.079:	.30	+.218:		—
	+.191	.35	+.090	.80	-.055:		+.193:		-.038:		+.218:	7704.20	+.278
.40	+.169		+.058		-.055:	.10	+.191:	.90	+.009:	.35	+.210:		+.245
	+.148	.40	+.028	.85	-.054:		+.186:		+.060:		+.192:	.25	+.219
.45	+.109		-.002		-.051:	.15	+.170:	.95	+.117:	.40	+.176:		+.192
	+.082	.45	-.023	.90	-.049:		+.149:		+.172:		+.161:	.30	+.164
.50	+.053		-.040			.20	+.131:	7606.00	+.213:	.45	+.138:		+.133
	+.027	.50	-.057				+.110:		+.243:		+.116:	.35	+.104
.55	.000		-.070			.25	+.091:		+.254:	.50	—		+.075
	-.027	.55	-.088				+.071:	.05	+.254:		—	.40	+.049
.60	-.049		-.109	7560.85	-.220	.30	+.053:	.10	+.247:	.55	—		+.018
	-.069	.60	-.134		-.220		+.036:		+.234:		—	.45	-.011
.65	—		-.155	.90	-.203	.35	+.018:	.15	+.221:		—		-.040
	—	.65	-.169		-.170		+.012:		+.204:		—	.50	-.069
.70	—		-.183	.95	-.108	.40	+.005:	.20	+.181:		—		-.103:
	—	.70	-.188		-.044		-.004:		+.153:		—	.55	-.132:
.75	-.167:		-.190	7561.00	+.055	.45	-.016:	.25	+.125:	7659.15	+.396		-.159
	-.185:	.75	-.185		+.171		-.034:		+.099:		+.403	.60	-.175
.80	-.198:		-.175	.05	+.304	.50	-.041:	.30	+.072:		+.395		-.185
	—	.80	-.152		+.420		-.042:		+.046:		+.370	.65	—
.85	—		-.115	.10	+.468	.55	-.043:	.35	+.020:	.25	+.342		-.190
	—	.85	-.073		+.473		-.040:		+.004:		+.309	.70	-.183
.90	-.183:		-.031	.15	+.449	.60	—	.40	-.011:	.30	+.270		-.165
	-.151:	.90	+.028		+.410		-.043:		-.026:		+.232	.75	-.137
.95	-.094:		—	.20	+.363	.65	-.040:	.45	-.039:	.35	+.196		-.091
	-.019:	.95	+.146		+.316		-.039:		-.050:		+.155	.80	-.045
7384.00	+.087:		+.193	.25	+.256	.70	-.042:	.50	-.058:	.40	+.116		.000:
	+.223:	7392.00	+.220		+.217		-.047:		-.064:		+.081	.85	+.042
.05	+.348:		+.232:	.30	+.175	.75	-.055:	.55	-.066:	.45	+.051		+.075
	+.465:	.05	+.232:		+.136		-.062:		-.065:		—	.90	+.104
.10	+.539:		+.223:	.35	+.102	.80	-.066:	.60	-.063:	.50	—		+.129:
	—	.10	+.207:		+.070		-.073:		-.056:		—	.95	+.155:
	—	.15	+.191:	.40	+.036	.85	-.074:	.65	-.052:	.55	—		+.166:
	—		+.171:		+.009		-.071:		-.048:		—	7705.00	+.180:
7390.75	-.121		+.148:	.45	-.020		—	.70	-.044:	.60	—		—
	—	.20	+.122:		-.042		—		-.039:		—	.05	—

Table of observations. SX Phoenicis

ϕ_0	$-\Delta m$	ϕ_0	$-\Delta m$	ϕ_0	$-\Delta m$	ϕ_0	$-\Delta m$	ϕ_0	$-\Delta m$	ϕ_0	$-\Delta m$	ϕ_0	$-\Delta m$
442.90	—		+.289	.20	+.258	.40	+.301	.80	-.100	.90	-.135	.10	+.335
	-.100	.10	+.397		+.269		+.184		-.106		-.098		+.469
443.00	-.016		+.405	.30	+.247	.50	+.095	.90	-.103	499.00	-.013		+.478
	+.175	.20	+.355		+.203		+.017		-.097		+.138	.20	+.431
.10	+.531		+.307	.40	+.154	.60	-.037	.90	-.068	.10	+.464		+.346
	—	.30	+.215		+.091		-.072		-.027		—	.30	+.253
.20	—		+.150	.50	+.041	.70	-.100	498.00	+.034	.20	—		+.171
	+.516	.40	—		-.008		—		+.139		+.548	.40	+.185
.30	+.352		—	.60	-.052		—	.10	+.254	.30	+.408		+.027
	+.234	.50	-.012		-.082		—		+.339		+.272	.50	-.021
.40	+.133		-.047	.70	-.103		—	.20	+.369	.40	+.157		-.055
	+.056	.60	-.077		-.120		—		+.346		+.062	.60	-.083
.50	-.024		-.095	.80	-.132	497.20	+.311	.30	+.286	.50	-.011		-.100
	-.069	.70	-.111		-.135		+.282	.40	+.208		-.063	.70	-.109
.60	-.112		-.117	.90	-.130	.30	+.235		+.137	.60	-.102		-.112
	-.131	.80	-.111		-.109		+.156	.50	+.058		-.130	.80	-.107
.70	-.141		-.106	446.00	-.077	.40	+.116		+.006	.70	-.152		-.097
	-.147	.90	-.089		+.060		+.059	.60	-.045		-.159	.90	-.074
.80	-.138		-.054	.10	+.323	.50	+.018		-.086	.80	-.152		-.050
	-.116	445.00	-.007		+.518		-.022	.70	-.111		-.130	501.00	+.009
.90	-.074		+.062	.20	+.574	.60	-.051		-.135	.90	-.083		+.078
	-.007	.10	+.145		+.540		-.076	.80	-.151		-.004	.10	+.169
444.00	+.116		+.213	.30	+.430	.70	-.090		—	500.00	+.127		+.233

SX Phoenixis

φ_0	$-\Delta m$	φ_0	$-\Delta m$	φ_0	$-\Delta m$	φ_0	$-\Delta m$	φ_0	$-\Delta m$	φ_0	$-\Delta m$	φ_0	$-\Delta m$
.20	+.264		+.141		-.149		-.040	.60	-.074	592.00	+.028	.70	-.103
	+.263	.40	+.091	.90	-.108	570.00	+.086		-.092		+.115	.80	-.108
.30	+.248		+.031		-.040		+.351	.70	-.107	.10	+.194		-.093
	+.196	.50	-.005	535.00	+.098	.10	+.556			.20	+.239	.90	-.074
.40	+.142		-.040		—		+.540			.30	+.244		-.043
	+.087	.60	-.066	.10	+.502	.20	+.465			.40	+.220	645.00	-.043
.50	+.034		-.086		+.500		+.338			.50	+.182		+.006
	-.008	.70	-.100	.20	+.433	.30	+.228	587.70	—	.60	+.137		+.070
.60	-.047		-.110		+.327		+.139		-.154	.70	+.091	.10	+.160
	-.076	.80	-.112	.30	+.215	.40	+.071	.80	-.141	.80	+.045	.20	+.237
.70	-.102		-.111		+.131	.50	+.013		-.118	.90	+.005	.30	+.285
	-.118	.90	-.102	.40	+.053	.60	-.030		-.075		-.030	.40	+.283
.80	-.130		-.083		-.002		-.066		-.066	.60	-.061	.50	+.264
	-.136	519.00	-.036	.50	-.048	.60	-.095	588.00	-.004	.70	-.088	.60	+.214
.90	-.130		+.042		-.084		-.115		+.103	.80	-.110	.70	+.153
	-.107	.10	+.144	.60	-.110	.70	-.126		+.262	.90	-.126	.80	+.099
502.00	-.051		+.244		-.131		-.133	.10	+.344		-.137	.90	+.046
	+.040	.20	+.322	.70	-.140	.80	-.125		+.351	.20	-.138		-.006
.10	+.210		+.337		-.141		-.106	.20	+.321	.30	-.125	.60	-.033
	+.427	.30	+.319	.80	-.138	.90	-.082		+.265	.40	-.102	.70	-.070
.20	+.521		+.265		-.122		-.040	.30	+.197	593.00	-.051	.80	-.098
	+.519	.40	+.190	.90	-.101	571.00	+.021	.40	+.086		+.028	.90	-.121
.30	+.436		+.114		-.066		+.101		+.045	.10	+.158	.80	-.128
	+.314	.50	+.052	536.00	-.011	.10	+.181		+.045	.20	+.323	.90	-.130
.40	+.219		-.007		+.073		+.229	.50	-.010	.30	+.420		-.122
	+.109	.60	-.052	.10	+.165	.20	+.238		-.044	.40	+.418	.60	-.091
.50	+.028		-.087		+.226		+.225	.60	-.070	.50	+.363	646.00	-.033
		.70	-.110	.20	+.245	.30	+.193		-.090	.60	+.275		+.071
		.80	-.132		+.239		+.142	.70	-.106	.70	+.175	.10	+.285
		.90	-.147	.30	+.214	.40	+.093		-.118	.80	+.090	.20	+.513
515.20	—		-.166		+.164		+.044	.80	-.125	.90	+.014	.30	+.570
	+.254	.90	-.137	.40	+.110	.50	+.002		-.118		-.035	.40	+.538
.30	+.227		-.008		+.057		-.035	.90	-.103		-.077	.50	+.424
	+.183	520.00	-.031	.50	+.007	.60	-.066		-.077	.60	+.033	.60	+.293
.40	+.135		+.127		-.035		-.094	589.00	-.033		+.038	.70	+.185
	+.091	.10	+.423	.60	-.070	.70	-.116		+.038	.10	+.126	.80	+.088
.50	+.034		+.635		-.100		-.130	.20	+.214	641.80	—	.90	+.019
	-.012	.20	+.647	.70	-.130	.80	-.131		+.275		-.101	.90	-.030
.60	-.047		+.552		-.150		-.128	.30	+.285	.90	-.086		-.072
	-.082	.30	+.415	.80	-.158	.90	-.119		+.266		-.060	.60	-.107
.70	-.107		+.291		-.158		-.095	.30	+.266	642.00	-.022	.70	-.131
	-.120	.40	+.165	.90	-.142	572.00	-.058		+.221		+.032	.80	-.146
.80	-.152		+.065		-.112		+.024	.40	+.166	.10	+.146	.90	-.148
	-.137	.50	-.003	537.00	-.064	.10	+.164		+.108	.20	+.265		-.135
.90	-.128		-.054		+.025		+.353	.50	—	.30	+.368	.60	-.100
	-.107	.60	-.097	.10	+.175	.20	+.451		-.046	.40	+.391	.70	-.032
516.00	-.064		-.129		+.388		+.448	.60	-.086	.90	+.368	647.00	+.081
	+.033	.70	-.155	.20	+.489	.30	+.374		+.296		+.360		+.347
.10	+.197		-.166		+.483		+.276	.70	-.117	.40	+.208	.10	+.582
	+.415	.80	-.160	.30	+.415	.40	+.179		-.138	.50	+.130	.20	+.604
.20	+.516		-.145		+.298		+.081	.80	-.153	.60	+.062	.30	+.528
	+.515	.90	—	.40	+.193	.50	+.018		-.153	.70	+.009	.40	+.417
.30	+.423		—		+.081		—	.90	-.146	.80	-.040	.50	+.293
	+.303	.50	—		+.002	.60	—		-.118	.90	-.088	.60	+.189
.40	+.193		—		-.051		—	590.00	-.062	.70	-.112	.70	+.099
	+.095	.60	—		-.092	.70	—		+.065	.80	-.133	.80	+.030
.50	+.013		-.047		-.130		—	.10	+.304	.90	-.147	.90	-.020
	-.049	533.00	+.014	.70	-.165	.80	—		+.566		-.147	.60	-.060
.60	-.091		+.115		-.177		—	.20	+.596	.90	-.129	.70	-.089
	-.121	.10	+.229	.80	-.182	.90	—		+.531		-.088	.80	-.107
.70	-.153		+.305		-.178		—	.30	+.400	643.00	+.006	.90	-.120
	-.166	.20	+.329	.90	-.151	573.00	—		+.268		+.192		-.126
.80	-.170		+.305		-.091		+.229	.40	+.152	.10	+.553	.80	-.118
	-.161	.30	+.242	538.00	+.012	.10	+.615		+.055	.20	+.674	.90	-.093
.90	-.128		+.167		+.235		+.682	.50	-.011	.30	+.642		-.054
	-.071	.40	+.096	.10	+.586	.20	+.587		-.057	.40	+.513		—
517.00	+.045		+.023		+.653		+.444	.60	-.097	.50	+.360	.60	+.347
	+.272	.50	-.030	.20	+.681	.30	+.311		-.133	.70	+.238	.70	+.582
.10	+.628		-.072		+.462		+.191	.70	-.159	.80	+.131	.80	+.604
	—	.60	-.106	.30	+.327	.40	+.090		-.173	.90	+.043	.90	+.528
.20	+.576		—		+.223		+.014	.80	-.174		-.015		+.417
	+.438	.70	—	.40	+.118		-.039	.90	-.163	.10	-.061	.30	+.293
.30	+.307		—		+.025	.50	-.078		-.126	.20	-.096	.40	+.189
	+.183	.80	—		-.042	.60	-.111		-.045	.30	-.133	.50	+.099
.40	+.087		—		-.085		-.139	591.00	+.093	.40	-.140	.60	+.030
	+.006	.90	—		-.125	.60	-.151		+.367	.70	-.143	.70	-.135
.50	-.050		-.114		-.158	.70	-.148	.10	—	.80	-.130	.80	-.148
	-.087	534.00	-.058		-.174		-.135		—	.90	-.103	.90	-.146
.60	-.111		+.058	.70	-.173	.80	-.115	.20	+.464		-.063		-.119
	-.131	.10	+.389		-.162		-.073	.30	+.343	.90	+.004	.60	-.086
.70	-.144		+.614	.80	-.130	.90	-.014		+.236		+.103	.70	-.036
	-.137	.20	+.516		—		+.085	.40	+.141	644.00	+.275	.80	+.037
.80	-.120		+.366	.90	—	574.00	+.064		+.400		+.415	.90	+.139
	-.096	.30	+.228		—	.10	+.231		+.003	.10	+.376		+.228
.90	-.065		+.120		—	.20	+.355		-.080	.20	+.312	.10	+.266
	-.006	.40	+.025		—		+.323	.60	-.109	.30	+.233	.20	+.236
518.00	+.081		-.046	569.60	-.073		+.265		-.127	.40	+.156	.30	+.193
	+.196	.50	-.089		-.111	.30	+.201		-.133	.50	+.091	.40	+.146
.10	+.285		-.121		-.140		+.133	.70	-.133	.60	+.035	.50	+.093
	+.315	.60	-.147	.70	-.155	.40	+.077	.80	-.127	.70	-.006	.60	+.049
.20	+.295		-.170	.80	-.160		+.031		-.111	.80	-.039	.70	+.007
	+.257	.70	-.177		-.139	.50	-.017	.90	-.078	.90	-.071	.80	-.030
.30	+.197		-.169	.90	-.102		-.051		-.034		-.090	.90	-.064

SX Phoenicis

φ_0	$-\Delta m$	φ_0	$-\Delta m$	φ_0	$-\Delta m$	φ_0	$-\Delta m$	φ_0	$-\Delta m$	φ_0	$-\Delta m$	φ_0	$-\Delta m$
	-.095		-.085	.90	-.156	.70	-.126		-.151	1424.00	-.039	.20	+.380
.70	-.117	.70	-.117		-.124		-.129		-.153		+.028		+.303
	-.128		-.142	734.00	-.038	.80	-.128		-.138	.10	+.112	.30	+.226
.80	-.133	.80	-.155		+.102		-.112	.90	-.105		+.208		+.155
	-.128		-.156	.10	+.395	.90	-.083		-.028	.20	+.271	.40	+.082
.90	-.114	.90	-.131		+.628		-.044		-.044		+.290		+.026
	-.084		-.091	.20	+.627	936.00	+.004		+.102	.30	+.342	.50	-.019
663.00	-.031	699.00	-.019		+.541		—	.10	+.527		+.249		-.059
	+.041		+.134	.30	+.393	.10	—		+.531	.40	+.181	.60	-.083
.10	+.136	.10	+.486		+.265		—	.20	+.457		+.111		-.100
	+.265		+.667	.40	+.148	.20	—		+.361	.50	+.048	.70	-.110
.20	+.367	.20	+.633		+.050		+.237	.30	+.259		-.007		-.115
	+.386		+.524	.50	-.019	.30	+.206		+.138	.60	-.055	.80	-.116
.30	+.358	.30	—		-.063		—	.40	+.088		-.096		-.107
	+.291		+.249	.60	-.097		—	.50	+.023	.70	-.122	.90	-.096
.40	+.200	.40	+.143		-.126		—		-.017	.80	-.144		-.069
	+.115		+.048	.70	-.149		—	.60	-.053		—	1515.00	-.022
.50	+.042	.50	-.014		-.102	986.90	—		-.084	.90	—		+.043
	-.014		-.056	.80	-.160		-.082		-.115		-.154	.10	+.136
.60	-.057	.60	-.088		-.147	987.00	+.038	.70	-.128		-.119		+.221
	-.095		-.118	.90	-.107		+.277		-.132	1425.00	-.047	.20	+.273
.70	-.126	.70	-.141		-.022	.10	+.627	.80	-.130		+.068		+.272
	-.147		-.150	735.00	+.115		+.662		-.107	.10	+.311	.30	+.245
.80	-.161	.80	-.147		—	.20	+.585	.90	-.075		+.593		+.193
	-.161		-.129	.10	+.491		+.458		-.026	.20	+.627	.40	+.141
.90	-.148	.90	-.090		+.492	.30	+.322	992.00	+.030		+.568		+.081
	-.105		-.015	.20	+.432		+.209		+.116	.30	+.433	.50	+.028
664.00	-.026	700.00	+.111		+.338	.40	+.105		+.198		+.292		-.013
	+.138		+.310	.30	+.242		+.022	.10	+.250	.40	+.194	.60	-.048
.10	+.510	.10	+.475		+.151	.50	-.027	.20	+.259		+.076		-.081
	+.668		+.473	.40	+.078		-.068	.50	+.251	.50	+.000	.70	-.108
.20	+.638	.20	+.413		+.020	.60	-.104	.30	+.216		-.062		-.131
	+.599		+.330	.50	-.028		-.132	.60	+.164	.60	-.103	.80	-.145
.30	+.368	.30	+.245		-.064	.70	-.149	.40	+.111		-.136		-.150
	+.229		+.159	.60	-.088		-.152	.70	+.061	.70	-.162	.90	-.135
.40	+.110	.40	+.089		-.103	.80	-.136	.50	+.024		-.180		-.103
	+.024		+.030	.70	-.111		-.113	.80	-.009	.80	-.179	1516.00	-.047
.50	-.034	.50	-.012		-.116	.90	-.070	.60	-.039		-.160		+.050
	-.079		—	.80	-.112		-.031		-.067	.90	-.122	.10	+.144
.60	-.118	.60	—		-.097	988.00	+.084	.70	-.088		-.045		+.482
	-.144		—	.90	-.074		+.215		-.106	1426.00	+.080	.20	+.546
.70	-.160	.70	-.100		-.035	.10	+.316	.80	-.117		+.307		—
	-.165		-.108	736.00	+.013		+.341		-.126	.10	+.529	.30	—
.80	-.158	.80	-.106		+.083	.20	+.327	.90	-.127		+.350		+.293
	-.128		-.094	.10	+.162		+.263		-.112	.20	+.500	.40	+.186
.90	-.088	.90	-.077		+.229	.30	+.200	993.00	-.059		+.393		+.084
	-.014		-.043	.20	+.253		+.134		+.003	.30	+.276	.50	+.012
665.00	+.110	701.00	+.008		+.247	.40	+.081		+.142	.10	+.174		—
	+.299		+.084	.30	+.220		+.035		—	.40	+.087	.60	—
.10	+.424	.10	+.168		+.173	.50	—	.20	+.450		+.015		-.119
	+.429		+.246	.40	+.124		-.039	.50	+.457		-.038	.70	-.147
.20	+.381	.20	+.274		+.077	.60	-.068	.30	+.411		-.079		-.169
	+.303		+.278	.50	+.030		-.091	.60	+.310		-.106	.80	-.174
.30	+.216	.30	+.260		-.009	.70	-.104	.40	+.209		-.126		-.165
	+.136		+.221	.60	-.040		-.113	.70	+.117		-.139	.90	-.136
.40	+.071	.40	+.162		-.068	.80	-.115	.50	+.044		-.135		-.171
	-.015		+.092	.70	-.091		-.107	.80	—		-.126	1517.00	+.055
.50	-.021	.50	+.036		-.109	.90	-.092		-.059	.90	-.104		+.232
	-.052		-.007	.80	-.121		-.016		-.016		-.069	.10	+.625
.60	-.078	.60	-.041		-.127	989.00	—		+.042	1427.00	+.026		+.654
	-.099		-.069	.90	-.123		+.042		—		+.024	.20	+.551
.70	-.109	.70	-.095		-.100	.10	+.134		+.223		+.116		+.416
	-.112		-.116	737.00	-.051		+.224	.40	+.128	.10	+.193	.30	+.290
.80	-.109	.80	-.125		+.037	.20	+.285		+.030		+.240		+.183
	-.099		-.127		—	.30	+.300	.50	-.042	.20	+.247	.40	+.092
.90	-.080	.90	-.120		—	.40	+.280		—		+.231		+.022
	-.049		-.093	.30	+.233	.60	+.167		—	.30	+.203	.50	-.031
666.00	-.005	702.00	-.038		+.127	.40	+.097	.70	—		+.163		-.069
	+.063		+.050	934.40	+.037	.50	+.039		—	.40	+.118	.60	-.100
.10	+.138	.10	+.225		-.025		-.002	.80	—	.50	+.072		-.126
	+.214		+.459	.50	-.071	.60	-.039		-.128		-.014	.70	-.143
.20	+.257	.20	+.533		-.112		-.077	.90	-.090	.60	-.051	.80	-.127
	+.268		+.512	.60	-.140	.70	-.107		-.019		-.076		-.104
.30	+.244	.30	+.419		-.156		-.133		+.071		+.071	.90	-.065
	+.202		+.305	.70	-.162	.80	-.152		+.224		+.224		-.008
			+.109	.80	-.161		-.154	.10	+.338		+.338	1518.00	+.065
			+.099		-.129	.90	-.146		+.378		+.378		+.156
			—	.90	-.089		-.122		+.362	1513.40	—	.10	+.243
697.90	-.106		-.014		-.014	990.00	-.048		+.303		+.035		+.267
	-.088		+.126	935.00	+.126		+.076	.30	+.232	.50	-.020	.20	+.259
698.00	-.049	733.30	+.315		+.337	.10	+.377		+.148		-.069		+.229
	+.018		+.473	.10	+.473		+.631	.40	+.069	.60	-.107	.30	+.192
.10	+.123		+.255		+.463	.20	+.639		+.017		-.141		+.148
	+.249		+.187	.20	+.416		+.556	.50	-.027	.70	-.160	.40	+.099
.20	+.333	.40	+.108		+.330	.30	+.407		-.066		-.167		+.045
	+.354		+.051	.30	+.224		+.276	.60	-.094	.80	-.163	.50	-.003
.30	+.331	.50	-.001		+.139	.40	+.159		-.115		-.138		-.042
	+.257		-.049	.40	+.064		+.062	.70	-.132	.90	-.092	.60	—
.40	+.176	.60	-.092		+.005	.50	-.004		-.137		-.009		
	+.108		-.123	.50	-.034		-.045	.80	-.135	1514.00	+.127		
.50	+.042	.70	-.148		-.064	.60	-.082		-.127		+.310		
	-.003		-.163	.60	-.095		-.114	.90	-.113		+.427		
.60	-.046	.80	-.168		-.116	.70	-.138		-.088	.10	+.432		

SX Phoenicis

φ_0	$-\Delta m$	φ_0	$-\Delta m$	φ_0	$-\Delta m$	φ_0	$-\Delta m$	φ_0	$-\Delta m$	φ_0	$-\Delta m$	φ_0	$-\Delta m$
1696.40	—	.40	+ .190	1714.50	—	.50	+ .012	.50	+ .002		—		— .118
	— .005		+ .111		— .059		— .049		— .038	.70	—	.70	— .125
.50	— .057	.50	+ .029	.60	— .092	.60	— .091	.60	— .071		—		— .127
	— .096		— .031		— .112		— .122		— .094	.80	—	.80	— .126
.60	— .127	.60	— .086	.70	— .123	.70	— .145	.70	— .111		— .164		— .118
	— .143		— .120		— .131		— .162		— .123	.90	— .147	.90	— .097
.70	— .148	.70	— .148	.80	— .130	.80	— .169	.80	— .124		— .110		— .064
	— .146		— .172		— .124		— .150		— .127	1734.00	— .044	1736.00	— .010
.80	— .137	.80	— .184	.90	— .106	.90	— .112	.90	— .105		+ .117		+ .059
	— .119		— .183		— .077		— .046				+ .449	.10	+ .135
.90	— .089	.90	— .163	1715.00	— .044	1717.00	+ .077				+ .665		+ .204
	— .046		— .113		+ .052		+ .335				+ .631	.20	+ .243
1697.00	+ .029	1699.00	— .030	.10	+ .151	.10	+ .609				+ .511		+ .238
	+ .124		+ .151		+ .229		+ .632	1732.30	+ .192	.30	+ .346	.30	+ .210
.10	+ .216	.10	+ .506	.20	+ .264	.20	+ .553		+ .138		+ .218		+ .173
	+ .257		+ .667		+ .266		+ .428		+ .083	.40	+ .107	.40	—
.20	+ .257	.20	+ .644	.30	+ .241	.30	+ .287		+ .028		+ .024		—
	+ .234		+ .530		+ .198		+ .183		— .012	.50	— .044	.50	—
.30	+ .190	.30	+ .369	.40	+ .143	.40	+ .080		— .046		— .084		—
	+ .137		+ .238		+ .082		+ .003		— .081	.60	— .118	.60	—
.40	+ .082	.40	+ .122	.50	+ .029	.50	— .049		— .104		— .141		—
	+ .037		+ .018		— .020		— .082		— .122	.70	— .158	.70	—
.50	— .005	.50	— .051	.60	— .058	.60	— .106		— .137		— .165		—
	— .047		— .093		— .093		— .122		— .144	.80	— .155	.80	—
.60	— .079	.60	— .126	.70	— .121	.70	— .134		— .142		— .133		—
	— .109		— .150		— .140		— .140		— .129	.90	— .092	.90	—
.70	— .134	.70	— .165	.80	— .151	.80	— .131		— .106		— .033		—
	—		— .166		— .151		—	1733.00	— .058	1735.00	+ .081	1737.00	— .068
.80	—	.80	— .154	.90	— .135	.90	—		+ .013		+ .273		+ .038
	—		— .127		— .111		— .030		+ .116	.10	+ .417	.10	+ .221
.90	—	.90	—	1716.00	— .061	1718.00	+ .044		+ .235		+ .434		+ .463
	— .098		—		+ .033		+ .136		+ .323	.20	+ .390	.20	+ .557
1698.00	— .043	1700.00	+ .126	.10	+ .212	.10	+ .231		+ .332		+ .308		+ .538
	+ .032		+ .306		+ .454		+ .274		+ .305	.30	+ .211	.30	+ .430
.10	+ .140	.10	+ .429	.20	+ .564	.20	+ .279		+ .245		+ .126		—
	+ .283		+ .441		+ .555		+ .253		+ .169	.40	+ .056		—
.20	+ .370	.20	+ .403	.30	+ .449	.30	+ .200		+ .085		— .001		—
	+ .382		—		+ .307		+ .140		+ .031	.50	— .043		—
.30	+ .352		—	.40	+ .191	.40	+ .089		— .029		— .076		—
	+ .278		—		+ .084		+ .041		— .080	.60	— .105		—